

RESPONSIVE POLYMER PARTICLES FOR FOULING REMOVAL
DURING MEMBRANE FILTRATIONS

A THESIS SUBMITTED TO
THE GRADUATE SCHOOL OF NATURAL AND APPLIED SCIENCES
OF
MIDDLE EAST TECHNICAL UNIVERSITY

BY

CANAN AKSOY

IN PARTIAL FULLFILMENT OF REQUIREMENTS
FOR
THE DEGREE OF MASTER OF SCIENCE
IN
CHEMICAL ENGINEERING

AUGUST 2018

Approval of the thesis:

**RESPONSIVE POLYMER PARTICLES FOR FOULING REMOVAL
DURING MEMBRANE FILTRATIONS**

submitted by **CANAN AKSOY** in partial fulfillment of the requirements for the degree of **Master of Science in Chemical Engineering Department, Middle East Technical University** by,

Prof. Dr. Halil Kalıpçılar
Dean, Graduate School of **Natural and Applied Sciences** _____

Prof. Dr. Pınar Çalık
Head of Department, **Chemical Engineering** _____

Assoc. Prof. Dr. Zeynep Çulfaz Emecen
Supervisor, **Chemical Engineering Dept., METU** _____

Asst. Prof. Dr. Ayşe Asatekin
Co-Supervisor, **Chemical and Biological Eng. Dept., Tufts University** _____

Examining Committee Members:

Prof. Dr. Nihal Aydoğan
Chemical Engineering Dept., Hacettepe University _____

Assoc. Prof. Dr. P. Zeynep Çulfaz Emecen
Chemical Engineering Dept., METU _____

Prof. Dr. Levent Yılmaz
Chemical Engineering Dept., METU _____

Assoc. Prof. Dr. İrem Erel-Göktepe
Chemistry Department, METU _____

Asst. Prof. Dr. Emre Büküşoğlu
Chemical Engineering Dept., METU _____

Date: 17.08.2018

I hereby declare that all information in this document has been obtained and presented in accordance with academic rules and ethical conduct. I also declare that, as required by these rules and conduct, I have fully cited and referenced all material and results that are not original to this work.

Name, Last Name: Canan Aksoy

Signature:

ABSTRACT

RESPONSIVE POLYMER PARTICLES FOR FOULING REMOVAL DURING MEMBRANE FILTRATIONS

Aksoy, Canan

M.S., Department of Chemical Engineering

Supervisor: Assoc. Prof. Dr. Zeynep Çulfaz Emecen

Co-Supervisor: Asst. Prof. Dr. Ayşe Asatekin

August 2018, 111 Pages

In this study, temperature and ionic-strength responsive polymeric microgels are used for fouling removal in membrane filtrations by adding them into feed solutions such that they deposit on the membrane surface together with the foulants during filtration. For removal of the fouling layer, the microgels in collapsed form are brought into swollen phase or vice versa by applying temperature change. Recently, in literature, there are several studies that stimuli-responsive surfaces have been shown to be effective in removing the fouling by “shaking off” the foulants from the membrane surface in response to appropriate stimuli.

In the filtrations, PES (polyethersulfone) and PES/PVP (polyvinylpyrrolidone) blend membranes were used. It was observed that flux declined less with PVP addition than PES membrane owing to its hydrophilicity. Poly(N-isopropylacrylamide), p(NIPAm), and poly(N-isopropylacrylamide-co-sulfobetainemethacrylate), p(NIPAm-co-SBMA), microgels were synthesized by precipitation polymerization and used in the filtrations as responsive microgels. Pure water permeances (PWP) of clean membranes, filtration permeances and PWP of the used membranes after cleaning were compared in terms of flux recovery and fouling resistances. Bovine serum albumin (BSA) and humic acid (HA) were used as foulants in the presence and

absence of microgels. For fouling removal, cleaning was done by stirring and simultaneously heating or cooling the filtration cell above or below lower critical solution temperature (LCST) depending on filtration condition, e.g. cleaning was done above LCST for the filtration performed below LCST in order to change size of the responsive microparticles.

Thermo-responsive p(NIPAm) and p(NIPAm-co-SBMA) microgels used had swelling ratios of 2.9 and 2.1, and LCST of 32 and 29°C, respectively. Addition of p(NIPAm-co-SBMA) microgel enabled less fouling resistance and more efficient cleaning compared to microgel-free cases for HA filtrations where the microgels were hydrophilic during filtration. In consequent filtrations, flux was almost completely recovered after HA filtrations for both PES and PES/PVP membranes either in pure water and in 0.5 M NaCl while flux recovery was around 60, 92 and 80% for PES membrane in pure water, PES/PVP blend one in pure water and 0.5 M NaCl, respectively. However, P(NIPAm) microgels did not provide better cleaning efficiency in neither BSA nor HA fouling for the filtrations above LCST where the microgels were hydrophobic.

Keywords: Membrane fouling, thermo-responsive polymeric microgels, zwitterionic microgels, P(NIPAm), P(NIPAm-co-SBMA)

ÖZ

MEMBRAN KİRLİLİĞİNİN TEMİZLENMESİNE YÖNELİK UYARANA DUYARLI POLİMERLERİN SENTEZİ VE KULLANIMI

Aksoy, Canan
Yüksek Lisans, Kimya Mühendisliği Bölümü
Tez Yöneticileri: Doç. Dr. Zeynep Çulfaz Emecen
Dr. Öğr. Üyesi Ayşe Asatekin

Ağustos 2018, 111 Sayfa

Bu çalışmada, membran kirliliğinin temizlenmesi için sıcaklığa ve iyonik güce duyarlı polimerik mikrojel kullanılmıştır. Söz konusu mikrojel besleme çözeltisine katılarak kirleticilerle birlikte membran yüzeyinde oluşan kirlilik tabakasının içinde biriktirilmiştir. Kirliliğin temizlenmesi amacıyla uyarın şiddeti değiştirilerek mikrojel boyut değiştirmesi sağlanmış temizleme işlemi çökmüşten şişmiş ya da tersi yönde denenmiştir. Yakın zamanda, literatürde uyarana duyarlı yüzeylerle alakalı çeşitli çalışmalar uygun bir uyarın eşliğinde kirliliğin membran yüzeyinden “silkenmesi” ile etkili temizleme sağlandığını göstermektedir.

Filtrasyonlar esnasında PES (polietersülfon) ve PES/PVP (polivinilprolidon) karışımı membranlar ile poli(n-izopropilakrilamid), p(NIPAm), and poli(n-izopropilakrilamid-co-sulfobetainmetakrilat), p(NIPAm-co-SBMA), mikrojel kullarılmıştır. İlki sıcaklığa, ikincisi hem sıcaklığa hem iyonik güce duyarlı bu mikrojel çöktürme polimerizasyonu ile sentezlenmiştir. PVP eklenmiş olan membranlarda daha hidrofilik olmaları dolayısı ile akı düşüşünün daha az olduğu saptanmıştır.

Performans testlerinde membranların saf su geçirgenliği, filtrasyon esnasındaki geçirgenliği ve ilkiyle kıyaslamak üzere tekrar membran temizlendikten sonraki saf su geçirgenliği ölçülmüş, bu veriler akının geri kazanımı ile tersinmez kirlilik direnci bakımından incelenmiştir. Bovin serum albümin (BSA) ve hümik asit (HA) çözeltileri mikrojel eklenerek ve eklenmeden besleme çözeltisi olarak kullanılmış, oda sıcaklığında filtrasyon için düşük kritik çözelti sıcaklığının (DKÇS) üzerinde, DKÇS sıcaklığı üzerinde filtrasyon için DKÇS altında karıştırılarak temizlik yapılmıştır. Dolayısı ile mikrojeller şişmiş halde kirlilik tabakasında biriktirildikten sonra çökmüş hale getirilerek ya da çökmüş halde filtrasyon sonunda şişmiş hale getirilerek boyut değişikliği ile temizlik sağlanmıştır.

Filtrasyonlarda kullanılan sıcaklık uyarana duyarlı p(NIPAm) ve p(NIPAm-co-SBMA) mikrojelleri sırasıyla 3 ve 1.4 şişme oranlarına ve 32 ve 29°C DKÇS değerlerine sahiptir. P(NIPAm-co-SBMA) mikrojellerinin besleme çözeltisine eklenmesi ile hümik asit filtrasyonlarında daha etkili temizlik elde edilmiştir. Bu deneyler esnasında mikrojeller hidrofilik durumdadırlar. Aynı membranla tekrarlanan seri filtrasyonlarda hem saf suda hem de 0.5 M NaCl ortamında PES ve PES/PVP karışımı membranların ikisi için de başlangıçtaki membran akısı neredeyse tamamen geri kazanılmıştır. Diğer yandan, mikrojel eklenmemiş durumdaki akının geri kazanımı değerleri PES membran için, saf suda ve 0.5 M NaCl ortamında PES/PVP membran için sırasıyla %60, 92 ve 80'dir. Aynı sonuçlar BSA ve HA filtrasyonlarında p(NIPAm) mikrojelleri için söz konusu değildir. Sonuç olarak, p(NIPAm-co-SBMA) mikrojelleri HA kirlenmesini kullanılmadığı duruma ve p(NIPAm) kullandığı duruma kıyasla daha iyi temizlenebilir hale getirmiştir.

Anahtar kelimeler: Membran kirliliği, sıcaklığa duyarlı polimerik mikrojeller, zwitteriyonik mikrojeller, P(NIPAm), P(NIPAm-co-SBMA)

To My Beloved Family

ACKNOWLEDGEMENTS

I would like to thank Zeynep ulfaz-Emecen to give me an opportunity to work with her and for her guidance and support. I am very grateful to be a part of ulfaz-Emecen Research group. I would like to thank every old “*Tüslemeyen*” and new member of the group: Elif, Faqih, Kaan, Hazal, Kübra, Begüm, Zeynep, Fatma, and Ecem for their support and friendship. I would like to express my very great appreciation to my co-advisor Ayşe Asatekin for her guidance and to give me the chance to work in her laboratory. It was a great pleasure for me. I also thank Ayşe Asatekin’s students: Ilin Sadeghi, Meg Saksiriwatekul, Grace J. Aro and especially Papatya Kaner for all their help. I would also like to thank all other Professors and their students who allowed me to use their lab and helped me in Tufts University.

I would like to thank “*bi’ buçuk pide*” Elif Nur Durmaz, Irmak Sel, Müge Öztürk and Özge Arman for being my second family. I am very grateful to know that you will always be there for me wherever we will be in the world. I am sure about that we will added new exiting memories to our unforgettable dinner and dance nights, movie events or holidays.

My beloved family, I owe you my deepest gratitude. My father Mehmet, my mother Şerife, my brother Onur and my little sister Dilan, you never hesitated about me in the way that I preferred to go forward even when I did so. I thank you my parents for not being like the others and for teaching me to hope and dream. My brother and sister, you are my biggest and most colorful wealth that my mom and dad gave me as a gift. I feel very lucky to have you as friends, and confidants.

My aunt Hüsna Aksoy, my twin, thank you for being friend and for being a model with your upright personality. My uncle İbrahim Aksoy, thank you to broaden my horizon and to give me the chance to breath the smell of that much book at one time. Special thanks to my old roomies Dilan “*diya*” and Sevcan “*cecan*” for all scientific and funny sharing in our “Chemical Engineering Chamber”.

I would like to thank Elif Ayar to touch my life for 21 years. I am very thankful to her for encouragement and support to participate in EUROMembrane 2018 Conference. I would like to thank Eray Demir for every moment we spent together to be so enjoyable even when we could see each other once for a year. I thank Dilan Dibek for speaking the same language about troubles in our lives every time even if we have very irrelevant jobs.

I would like to thank Sarper Demir for unintentionally helping me to finding my own motivations while he tries to create new meaningful alternatives for his life. I am also very thankful to Selda Odabaşı for being a good colleague, and for sharing our stresses, at the same time laughing at them and supporting each other. Thank you Meryem Öztürk for being the best roomie ever.

Ömer, thank you for always being there for me whenever I need your hug in every sad, boring, exciting or happy moment. Thank you for your encouragement, friendship and love. I am so glad to have you in my life. Thanks to *DKSK* for giving us the chance to get know each other.

I would like to acknowledge the financial support provided by the Scientific and Technological Research Council of Turkey (TUBITAK MAG116M047), Research Coordination Office of Middle East Technical University (METU BAP 03-04-2014-001 Project) and National Science Foundation of the United States (NSF CBET-1437772 Project).

TABLE OF CONTENTS

ABSTRACT	v
ÖZ	vii
ACKNOWLEDGEMENTS	x
TABLE OF CONTENTS	xiii
LIST OF FIGURES.....	xvi
LIST OF TABLES	xxi
NOMENCLATURE.....	xxiv
CHAPTERS	
1 INTRODUCTION.....	1
1.1 Membrane fouling.....	3
1.2 Stimuli Responsive Polymeric Microgels.....	6
1.2.1 P(n-isopropylacrylamide), P(NIPAm)	6
1.2.2 P(n-isopropylacrylamide-co-sulfobetainemethacrylate), P(NIPAm-co-SBMA)	9
1.3 Membrane materials: Polyethersulfone and Polyvinylpyrrolidone.....	10
1.4 Foulants: Bovine Serum Albumin and Humic Acid	13
Aim of the study.....	15
2 EXPERIMENTAL METHOD	17

2.1	Materials	17
2.2	Membrane Preparation	17
2.3	Microgel Synthesis and Characterization.....	18
2.4	Dynamic Light Scattering	20
2.5	Light Transmission.....	20
2.6	Scanning Electron Microscopy (SEM).....	21
2.7	Filtration and Cleaning Procedures	21
2.8	Filtration Analysis	25
2.9	Adsorption Tests.....	26
3	RESULTS AND DISCUSSION.....	27
3.1	PES and PES/PVP Blend Membranes.....	27
3.2	Characterization of Microgels	29
3.2.1	P(NIPAM) Microgels	29
3.2.2	P(NIPAM-co-SBMA) Microgels	32
3.3	Performance Tests	36
3.3.1	Effect of P(NIPAm) Microgels Addition into BSA Solution on Fouling Removal from PES Membrane.....	36
3.3.2	Effect of P(NIPAm) Microgels Addition into Humic Acid Solution on Fouling Removal from PES Membrane	42
3.3.3	Effect of P(NIPAm-co-SBMA) Microgels Addition into Humic Acid Solution on Fouling Removal from PES membrane	45

3.3.4	Effect of P(NIPAm) Microgels Addition into Humic Acid Solution on Fouling Removal from PES/PVP Blend Membrane.....	51
3.3.5	Effect of P(NIPAm-co-SBMA) Microgels Addition into Humic Acid Solution on Fouling Removal from PES/PVP Membrane.....	58
3.3.6	Effect of P(NIPAm-co-SBMA) Microgels Addition into Humic Acid Solution on Fouling Removal from PES/PVP Membrane in 0.5 M NaCl Solution.....	63
3.3.7	Cleaning of similar fouling resistances.....	66
3.3.8	SEM Results of microgel depositions.....	68
3.4	Adsorption Tests.....	70
4	CONCLUSION.....	75
	REFERENCES.....	77
	APPENDICES.....	85
	APPENDIX A ADSORPTION TESTS.....	85
	APPENDIX B CALIBRATIONS.....	92
	B.1 Bovine Serum Albumin (BSA) Calibration.....	92
	B.2 Humic Acid Calibration.....	93
	B.3 P(NIPAm) Microgels Calibration.....	94
	APPENDIX C FILTRATION DATA.....	95
	APPENDIX D ADDITIONAL FILTRATION.....	108
	APPENDIX E MICROGEL RECOVERY.....	109

LIST OF FIGURES

FIGURES

Figure 1.1 Flow diagram of a typical membrane filtration process	1
Figure 1.2 Cross-flow and dead-end modes of membrane filtration.....	2
Figure 1.3 Chemical structures of (a) P(NIPAm) and (b) P(NIPAm-co-SBMA) polymers	7
Figure 1.4 The places where H-bonds form with temperature stimulus below LCST (intermolecular H-bonds) where microgels are swollen	8
Figure 1.5 Polyethersulfone (a) and polyvinylpyrrolidone (b) chemical structures.	10
Figure 2.1 Light Transmission Experimental Set-up	20
Figure 2.2 Experimental set-up for the filtrations with Amicon stirred cell (50 ml)	22
Figure 2.3 Presumed cleaning mechanism for Procedure 1 (<i>cooling</i>)	24
Figure 2.4 Presumed cleaning mechanism for Procedure 2 (<i>heating</i>)	24
Figure 2.5 Presumed cleaning mechanism for extra cleaning (<i>cyclic</i>).....	24
Figure 3.1 SEM images of the membrane cross-sections of PES-20 (top left), PES- 25 (top middle) and PES/PVP (top right) and membrane surfaces of PES-20 (bottom left), PES/PVP (bottom right).....	28
Figure 3.2 Hydrodynamic diameters of four different batches against temperature (°C) according to DLS analysis.....	30
Figure 3.3 Light transmission and DLS results of P(NIPAm) microgels against temperature (°C).....	31
Figure 3.4 Hydrodynamic diameters and LCST analysis of P(NIPAm-co-SBMA) microgels with respect to temperature via DLS in pure water and 0.5 M NaCl	33
Figure 3.5 Light transmission and DLS results of P(NIPAm-co-SBMA) microgels in pure water with respect to temperature	34

Figure 3.6 SEM images of (a) P(NIPAm) and (b) P(NIPAm-co-SBMA) microgels deposited on PES membrane.....	35
Figure 3.7 Normalized flux graphs of three BSA filtrations at 35 °C with PES membranes and their average flux recoveries after cleaning via cooling below LCST (procedure 1)	37
Figure 3.8 Normalized flux graphs of three BSA and 0.1 g/L P(NIPAm) microgels filtrations at 35°C with PES membranes and their average flux recoveries after cleaning via cooling below LCST (procedure 1)	38
Figure 3.9 Resistances of (1) BSA and (2) BSA + 0.1 g/L P(NIPAm) microgels filtrations at 35 °C with PES membranes cleaning via cooling below LCST (procedure 1)	39
Figure 3.10 Normalized flux graph of BSA filtrations at room temperature with PES membranes and flux recovery after cleaning via heating above LCST (procedure 2)	39
Figure 3.11 Normalized flux graphs of two BSA + 0.1 g/L P(NIPAm) microgels filtrations at room temperature with PES membranes and average flux recovery after cleaning via heating above LCST (procedure 2)	40
Figure 3.12 Resistances of (1) BSA and (2) BSA + 0.1 g/L P(NIPAm) microgels filtrations at room temperature with PES membranes cleaning via heating above LCST (procedure 2)	41
Figure 3.13 Normalized flux graphs of two HA filtrations at 35 °C with PES membranes and average flux recovery after cleaning via cooling below LCST (procedure 1)	42
Figure 3.14 Normalized flux graph of HA and 0.1 g/L P(NIPAm) microgels filtrations at 35 °C with PES membranes and cleaning via cooling below LCST (procedure 1)	43

Figure 3.15 Resistances of (1) HA and (2) HA + 0.1 g/L P(NIPAm) microgels filtrations at room temperature with PES membranes cleaning via cooling below LCST (procedure 1).....	44
Figure 3.16 Normalized flux graphs of HA (A) and HA + 0.01 g/L P(NIPAm-co-SBMA) (B) series filtrations with PES membrane at room temperature and cleaning via heating above LCST (procedure 2).....	47
Figure 3.17 Resistance graphs of HA (A) and HA + 0.01 g/L P(NIPAm-co-SBMA) (B) series filtrations with PES membrane at room temperature and cleaning via heating above LCST (procedure 2)	48
Figure 3.18 PES membrane photographs after 1 st and extra cleaning of HA and HA + 0.01 g/L P(NIPAm-co-SBMA) microgels series filtrations with PES membrane at room temperature and cleaning via heating above LCST (procedure 2)	50
Figure 3.19 Normalized flux graphs of three HA filtrations with PES/PVP blend membranes at room temperature and their average flux recoveries after cleaning via heating above LCST (procedure 2)	52
Figure 3.20 Resistances of HA filtrations at room temperature with PES/PVP blend membrane and cleaning via heating above LCST (procedure 2)	53
Figure 3.21 Normalized flux graphs of three HA and 0.01 g/L p(NIPAm) filtrations with PES/PVP blend membranes at room temperature and their average flux recoveries after cleaning via heating above LCST (procedure 2).....	54
Figure 3.22 Resistances of HA and 0.01 g/L P(NIPAm) filtrations at room temperature with PES/PVP blend membrane and cleaning via heating above LCST (procedure 2).....	55
Figure 3.23 Normalized flux graphs of two HA and 0.1 g/L p(NIPAm) filtrations with PES/PVP blend membranes at room temperature and average flux recovery after cleaning via heating above LCST (procedure 2).....	55

Figure 3.24 Resistances of HA and 0.1 g/L P(NIPAm) filtrations at room temperature with PES/PVP blend membrane and cleaning via heating above LCST (procedure 2)	56
Figure 3.25 Normalized flux (a) and resistance (b) graphs of HA filtration with PES/PVP blend membrane at room temperature and cleaning at room temperature.....	57
Figure 3.26 Normalized flux graphs of the series filtrations with PES/PVP blend membranes from top to bottom: HA filtration at room T and cleaning via heating above LCST (procedure 2), HA and 0.01 g/L p(NIPAm) microgels filtration at room T and cleaning via heating above LCST (procedure 2), and HA and 0.01 g/L p(NIPAm) microgels filtration at room T and cleaning at room T	59
Figure 3.27 Fouling resistances of filtrations in pure water with PES/PVP membrane: HA solution and cleaning with temperature stimulus (top); HA and P(NIPAm-co-SBMA) microgels solution and cleaning with temperature stimulus (middle); HA and P(NIPAm-co-SBMA) microgels solution and cleaning without response (bottom).....	60
Figure 3.28 PES/PVP membrane photographs after 1 st and extra cleaning of HA solution filtration with and without 0.01 g/L P(NIPAm-co-SBMA) microgels, cleaning via heating above LCST (procedure 2) and cleaning at room T	62
Figure 3.29 Normalized flux graphs of HA (top) and HA with P(NIPAm-co-SBMA) microgels (bottom) filtrations in 0.5 M NaCl with PES/PVP blend membranes at room T and cleaning via heating above LCST (procedure 2)	64
Figure 3.30 Fouling and irreversible fouling resistances of HA with P(NIPAm-co-SBMA) microgels (left) and HA (right) filtrations in 0.5 M NaCl with PES/PVP blend membranes at room T and cleaning via heating above LCST (procedure 2)	65
Figure 3.31 Comparison of fouling and irreversible fouling resistances graphs of (a) standard (std) HA + P(NIPAm-co-SBMA) microgels filtration and low R	

filtration of HA filtrations and (b) std HA filtration and high R HA + P(NIPAm-co-SBMA) microgels filtrations with procedure 2.....	67
Figure 3.32 SEM images of PES and PES/PVP blend membranes with the microgels after deposition, cleaning via heating above LCST and cleaning at room temperature.....	69
Figure 3.33 Humic acid filtrations with (a) PES and (b) PES/PVP membrane	71
Figure 3.34 BSA filtration with (a) PES and (b) PVP- PES membrane	72
Figure B.1 BSA calibration in UV/Visible Spectroscopy at 280 nm.....	92
Figure B.2 Humic acid calibration in UV/Visible Spectroscopy at 254 nm.....	93
Figure B.3 P(NIPAm) microgels calibration in UV/Visible Spectroscopy at 239 nm	94
Figure E.1 Schematic representation of microgel recovery	92
Figure E.2 Iron decorated P(SBMA) microgels.....	93

LIST OF TABLES

TABLES

Table 2.1 Monomer (NIPAm and SBMA), cross-linker (BA), and initiator (KPS) mass per 100 mL DI water used in synthesis.....	19
Table 2.2 Different monomer (NIPAm), cross-linker (BA), and initiator (KPS) mass per 100 mL DI water for different synthesis to improve swelling ratio.....	19
Table 3.1 Hydrodynamic diameters (D_h) of microgels in pure water and 0.5 M NaCl according to DLS analysis	32
Table 3.2 Filtration flux ratios and flux recoveries of BSA and BSA + 0.1 g/L P(NIPAm) microgels filtrations at 35 °C with PES membranes cleaning via cooling below LCST (procedure 1).....	38
Table 3.3 Filtration flux ratios and flux recoveries of BSA and BSA + 0.1 g/L P(NIPAm) microgels filtrations at room temperature with PES membranes cleaning via heating above LCST (procedure 2).....	41
Table 3.4 Filtration flux ratios and flux recoveries of HA and HA + 0.1 g/L P(NIPAm) microgels filtrations at room temperature with PES membranes cleaning via heating	44
Table 3.5 Filtration flux ratios and flux recoveries of HA and HA + 0.01 g/L P(NIPAm-co-SBMA) series filtrations with PES membrane at room temperature and cleaning via heating above LCST (procedure 2).....	49
Table 3.6 Filtration flux ratios and flux recoveries of HA filtrations with PES/PVP blend membrane at room temperature and cleaning via heating above LCST (procedure 2)	52
Table 3.7 Filtration flux ratio and flux recovery of HA and 0.01 g/L P(NIPAm) microgels filtration with PES/PVP blend membrane at room temperature and cleaning via heating above LCST (procedure 2).....	54

Table 3.8 Filtration flux ratio and flux recovery of HA and 0.1 g/L P(NIPAm) microgels filtration with PES/PVP blend membrane at room temperature and cleaning via heating above LCST (procedure 2).....	56
Table 3.9 Filtration flux ratio and flux recovery of HA filtration with PES/PVP blend membrane at room temperature and cleaning at room temperature	57
Table 3.10 Filtration flux ratios and flux recoveries of HA with and without 0.01 g/L P(NIPAm-co-SBMA) microgels filtration at room T with PES/PVP blend membrane and cleaning via heating above LCST (procedure 2) and cleaning at room T	61
Table 3.11 Filtration flux ratios and flux recoveries of HA and HA with P(NIPAm-co-SBMA) microgels filtrations in 0.5 M NaCl with PES/PVP blend membranes at room T and cleaning via heating above LCST (procedure 2)	65
Table 3.12 Adsorption of Humic Acid on PES and PES/PVP blend membranes....	71
Table 3.13 Adsorption of BSA on PES membrane with and without P(NIPAM) microgels, and on PES/PVP membrane	72
Table 3.14 Adsorption of P(NIPAm) on PES and PES/PVP blend membranes.....	73
Table A.1 Adsorption of HA on PES membrane	85
Table A.2 Adsorption of HA on PES/PVP blend membrane.....	86
Table A.3 Adsorption of BSA on PES membrane	87
Table A.4 Adsorption of BSA on PES membrane with presence of P(NIPAm) microgels in the solution	88
Table A.5 Adsorption of BSA on P(NIPAm) microgels deposited PES membrane	89
Table A.6 Adsorption of BSA on PES/PVP blend membrane.....	90
Table A.7 Adsorption of P(NIPAm) microgels on PES membrane.....	91
Table A.8 Adsorption of P(NIPAm) microgels on PES/PVP blend membrane	91
Table C.1 Yeast filtrations by stirring feed solutions for 40 ml permeate volume at given pressures and temperatures using PES membrane	96

Table C.2 BSA and HA filtrations using P(NIPAm) microgels with PES membrane	98
Table C.3 HA filtrations using P(NIPAm) microgels with PES/PVP blend membrane	100
Table C.4 Series filtrations of HA using P(NIPAm-co-SBMA) microgels with PES/PVP blend membrane.....	102
Table C.5 Series filtrations of HA using P(NIPAm-co-SBMA) microgels with PES membrane.....	104
Table C.6 Series filtrations of HA using P(NIPAm-co-SBMA) microgels with PES/PVP blend membrane in 0.5 M NaCl	106
Table C.7 HA filtrations for <i>low resistance</i> and <i>high resistance</i> analysis using P(NIPAm-co-SBMA) microgels with PES/PVP blend membrane.....	107

NOMENCLATURE

BA	N, N-methylene-bis-acrylamide
BSA	Bovine serum albumin
C, SC	Cooling, slow cooling
CL	Cleaning condition
DI	Dionized
DLS	Dynamic light scattering
DMSO	Dimethyl sulfoxide
FFR & FR	Filtration flux ratio & Flux Recovery
FP	Filtration permeance, LMH/bar
H, SH	Heating, slow heating
HA	Humic acid + CaCl ₂ feed
D _h	Hydrodynamic diameter
J	Permeate flux, LMH
KPS	Potassium per sulfate
LCST	Lower critical solution temperature
LMH	Liter per meter square per hour (L/m ² h)
NIPAM	N-isopropyl acrylamide
PES	Poly(ethersulfone)
PEG400	Polyethylene glycol with molecular weight of 400 Da
PVP	Poly(vinylpyrrolidinone)

PWP	Pure water permeance, LMH/bar
RO	Reverse osmosis
R_i	Resistance due to I where i can represent membrane (mem), fouling (foul), and irreversible fouling (irr) respectively, $m^{-1} \times 10^{12}$
SEM	Scanning electron microscope
SBMA	Sulfobetaine methacrylate
T	Temperature, °C
t	Time, seconds or hours
TMP	Trans membrane Pressure
UP	Ultra purified
V	Permeate volume, ml or lt
Y	1 g/L Yeast
η	Viscosity, Pa.s or bar.h
$R_i\%$	Retention of species i
*	means after 1 st cleaning
**	means after 2 nd cleaning
0.01 PN	0.01 g/L P(NIPAm) microgels
0.01 PNcS	0.01 g/L P(NIPAm-co-SBMA) microgels
0.1 PN	0.1 g/L P(NIPAm) microgels
$c_{i,p}$ and $c_{i,f}$	concentration of species i in the permeate and feed side which is composed of fresh feed and retentate, respectively

CHAPTER 1

INTRODUCTION

Membrane is a thin selective barrier which controls the permeation rate of species which contacts with it (Baker, 2004). In a typical filtration process, the stream which is fed to membrane system to separate is feed and the one which can pass to the other side of the membrane is permeate while the remaining stream containing rejected species after the filtration is called as retentate (Figure 1.1). Filtration processes can be operated in two modes: cross-flow and dead-end (Figure 1.2). In the former, also called tangential flow filtration, the feed flows over the membrane surface and sweeps it (Fröhlich 2012). Besides that, the retentate stream, which contains the rejected solutes, leaves the unit from the same side with the feed. In the latter, on the other hand, the feed side is also the retentate itself during filtration and rejected species accumulates on the membrane.

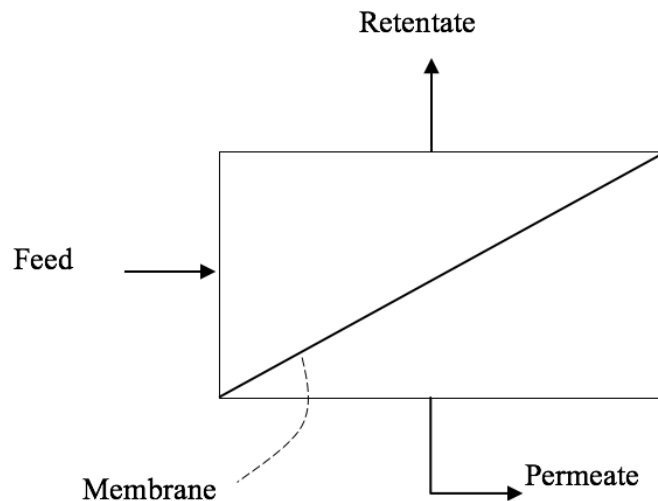


Figure 1.1 Flow diagram of a typical membrane filtration process

Membranes are recently used in many separation process applications in water purification systems, bio-processes, wastewater treatment, food and pharmaceutical industries. Especially, water scarcity is one of the most urgent topics all around the world. To obtain sufficient and clean water with a sustainable technique has become a necessity. Producing drinking water from sea and ground water and removing contamination in fresh water sources are the main applications of membrane technology (Goosen et al., 2004, Werber et al., 2016). In biotechnology, membranes are increasingly preferred for especially downstream processing (e.g. protein concentration, desalting, and separation of DNA from cell culture) due to its controllable retention and accordingly quality of product. Also, capacity to achieve high efficiency in separation of microbial pollutants and viruses during water treatments makes it popular during other separation techniques (Reis, 2007, & Fröhlich 2012).

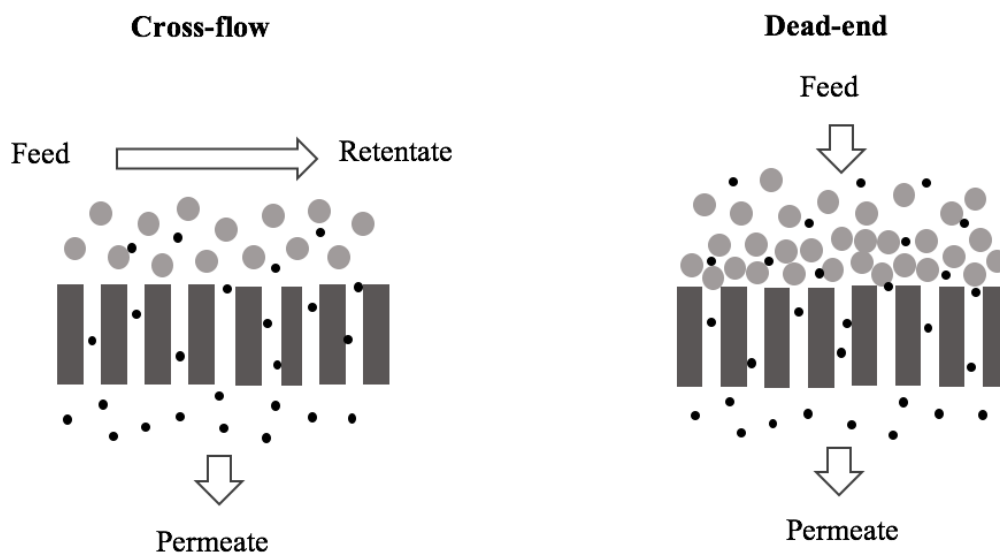


Figure 1.2 Cross-flow and dead-end modes of membrane filtration

Membranes may be made of different materials such as ceramics, polymers, or metals. In this study, however, only polymeric membranes were used. They can be classified with respect to their structure or average pore-size. Their structures may be symmetric (isotropic) or asymmetric (anisotropic). Isotropic membranes have uniform pore size through the membrane cross-section whereas anisotropic ones have a thin selective layer at the top and supportive micro-pores at the bottom. They are named as reverse osmosis (RO), nanofiltration (NF), ultrafiltration (UF) and microfiltration membranes (MF) where RO membranes are nonporous and the nominal pore sizes of the others are roughly in between 1 – 2 nm, 2 – 100 nm and more than 100 nm, respectively (Baker, 2004). They are used in a very wide range of applications from separation of an aqueous salt solution to purification of a hormone from bio-reactor product.

Membranes can practically be used in well-designed packed units called as modules since industrial applications need to use membranes with very large areas to achieve mass production. They are generally spiral-wound modules that are used for flat sheet membranes and hollow-fiber membrane modules. In small scale, plate and frame modules can also be used (Baker, 2004). In membrane separation, driving force can be a pressure, partial pressure, concentration or electrical potential difference between the feed and the permeate sides. Separation can be carried out by size exclusion, charge exclusion or solution-diffusion.

1.1 Membrane fouling

In membrane processes, fouling is among the most crucial troubles since it causes permeate flux to decline and accordingly it increases operating cost and decreases lifetime of the membrane. Membrane fouling may most generally be due to adsorption of feed components, pore blockage, gel or cake formation and bacterial growth (Baker, 2004 & Goosen et al., 2004 & Marselina et al., 2007). Quality and

property of fouling is determined by the chemical interactions between different foulants and between foulants and membranes. Concentration polarization is another phenomenon which is the concentration difference of solutes (i.e. rejected species) between the bulk and the membrane surface in pressure driven filtrations (Fröhlich 2012). It causes filtration flux to be lower than the flux of pure solvent, it is a reversible decline but it may evolve into cake or gel layer on membrane surface.

In order to deal with fouling, significant amount of research is devoted to finding ways to prevent membrane fouling and to render membrane fouling easily cleanable. Fouling removal may be performed in two ways: physical and chemical cleaning. Fouling is called as reversible when it can be removed by physical cleaning such as flushing (applying shear force), back-washing, vibration, or relaxation (Wang et al. 2014 & Chen et al. 2003). It is generally originated from loose cake formation on membrane surface. If it cannot be removed by those cleaning techniques, then it may be removed by chemical cleaning (Chede et al., 2015). Although chemical cleaning is more efficient and initial flux can be recovered totally in many cases, it is limited for membranes that are not tolerant to oxidants and/or extreme pH levels, it may damage membrane, change membrane properties and reduce membrane lifetime since highly active and/or hazardous chemicals are used in cleaning processes such as acids, bases, oxidizing agents, enzymes, and detergents and alkaline are used in order to clean membrane (Baker, 2004 & Madaeni et al., 2001 & Zondervan et al., 2007 & Arkhangelsky et al., 2007). It is not an environmental friendly method as much as physical cleaning and it is more expensive way than it to apply. Therefore, there are several methods in order to prevent and/or reduce fouling or to make it removable. Membrane materials can be chosen or modified in order to lower the tendency to absorb the foulants such as using more hydrophilic materials to increase hydration on membrane surface (Wavhal et al., 2002), or flow hydrodynamics near the membrane surface can be improved in order to reduce concentration polarization and accordingly back diffusion such as increasing flow rate and making patterned membrane surface to promote the turbulence (Gençal et al. 2014). Pretreatment of

feed solution to separate different foulants may also be applied but it brings an additional separation step at the expense of a more complicated process scheme.

Fouling analysis of the membranes is commonly done by Darcy's Law (eqn.1). It is a model equation which is used in order to express the pressure-driven convective flow in porous media (Baker, 2004).

$$R = \frac{\text{TMP}}{\eta J} \quad (1)$$

Here, η is the permeate viscosity, TMP is transmembrane pressure, J is the permeate flux, R is the resistance. Resistances in series model (eqn.2) is used by defining fouling as sum of reversible and irreversible fouling (eqn.3).

$$R_{\text{filtration}} = R_{\text{membrane}} + R_{\text{fouling}} \quad (2)$$

$$R_{\text{fouling}} = R_{\text{reversible fouling}} + R_{\text{irreversible fouling}} \quad (3)$$

Permeate flux is calculated as given in eqn.4 where V is the permeate volume, t is the time to collect the permeate volume V, and A is the active membrane area.

$$J = \frac{V}{A \times t} \quad (4)$$

In this study, viscosity of water was calculated and used as permeate, which was nearly pure water, by using the following correlation (eqn.5) as a function of temperature (van de Ven, 2008).

$$\eta = 0.497 [T (\text{°C}) + 42.5]^{-1.5} \quad (5)$$

Rejection (\mathbb{R}_i) of a species I in the feed is defined as follows:

$$\mathbb{R}_i \% = \left(1 - \frac{c_{i,p}}{c_{i,f}}\right) \times 100 \quad (6)$$

where $c_{i,p}$ and $c_{i,f}$ are the concentration of species i in the permeate and feed side.

1.2 Stimuli Responsive Polymeric Microgels

Polymers which give response to changing external stimuli by changing their size or shape, solubility, hydrophilicity, or phase are called as stimuli responsive polymers (Byeongmoon et al., 2002). Recently, there is a great interest in these polymers and they have an increasing research area day-by-day.

They can be affected by a physical or chemical stimulus such as temperature and magnetic field or pH and ionic strength, respectively. Their dimensional changes or molecular arrangements with changing environmental conditions enable to use them in several application field, such as sensors, biosensors and controlled drug delivery.

1.2.1 P(n-isopropylacrylamide), P(NIPAm)

P(NIPAm) is the most commonly used thermo-responsive (or thermo-sensitive) nonionic polymer. P(NIPAm) microgels were synthesized and used in filtration experiments in this study since it is the most widely used responsive polymer in research related to membrane fouling in literature (Yu et al., 2011, Gorey et al., 2011

and Chede et al., 2015). The structure of the polymer is given in Figure 1.3 (a). It has hydrocarbon backbone and pendant isopropyl group which is hydrophobic, and amide group which is hydrophilic.

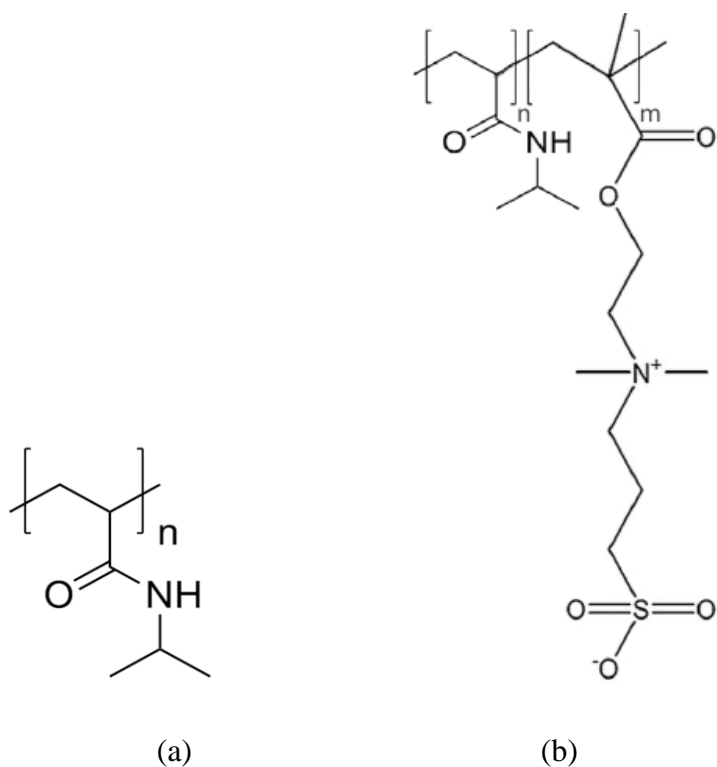


Figure 1.3 Chemical structures of (a) P(NIPAm) and (b) P(NIPAm-co-SBMA) polymers

The main property of thermo-responsive microgels is that reversible and sharp phase change occurs with changing temperature. These kinds of responsive gels have lower critical solution temperature, LCST, or upper critical solution temperature, UCST, which are the temperatures that polymer precipitates or dissolves upon heating, respectively. P(NIPAm) has LCST and it was reported to be around 32°C in literature (Pelton, 2000, Qui et al., 2012 & Chen et al., 2010). Its LCST makes P(NIPAm) convenient to use in membrane processes since it is close to room temperature. This was another reason to use P(NIPAm) in performance tests. For the polymeric

microgels, swelling behavior can be explained by the domination of intermolecular and intramolecular forces over each other. H-bonds between amide groups of the polymer chains and water molecules are stronger than intermolecular interactions below LCST; on the other hand, hydrophobic polymer–polymer interactions dominate over water-polymer interactions above LCST (Figure 1.4). Then, polymeric microgels which have LCST are soluble (swollen) and insoluble (collapsed) below and above that temperature, respectively (Chen et al., 2010 & Li et al., 2011).

There are other thermo-responsive polymers known in literature with different application areas. For example, poly(methylvinylether) (PMVE) has LCST around 37°C which is highly suitable temperature for drug release (Gandhi et al., 2015 & Arndt et al., 2001 & Schmaljohann 2006). Another example is the study on the application of Poly(N,N-diethylacrylamide) (PDEAM) in nanomechanical cantilever sensors (Roy et al., 2013).

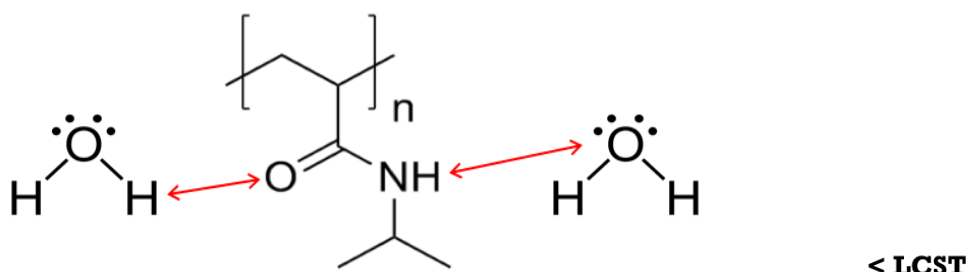


Figure 1.4 The places where H-bonds form with temperature stimulus below LCST (intermolecular H-bonds) where microgels are swollen

1.2.2 P(n-isopropylacrylamide-co-sulfobetainemethacrylate), P(NIPAm-co-SBMA)

P(NIPAm-co-SBMA) is a thermo-responsive polymer and known as it has both LCST and UCST due to NIPAm and SBMA parts, respectively (Zhao et al., 2015). It shows also ionic strength-responsive behavior where it is swollen in water with increasing ionic strength due to zwitterionic structure originated from the presence of SBMA which can be seen in Figure 1.3 (b). Zwitterions in polymer chain interact with each other in pure water and polymer is collapsed; however, their interaction is interrupted by free ions in existence of salt, and polymer is swollen. Alternately, carboxybetaine methacrylate (CBMA) is also a very common nonfouling zwitterionic monomer that can be used in copolymerization. They, SBMA and CBMA, both were observed to have good antifouling abilities since they are highly resistant to protein adsorption owing to self-assembly of opposite charges together.

Zhao et al. (2015) and Obiweluozor et al. (2014) observed that SBMA addition shifted LCST of polymeric microgels to higher temperatures. Also, Zhao et al. (2015) reported that increase in molar ratio of NIPAm to SBMA lowered the swelling ratio. They showed that increasing SBMA content resulted in increasing LCST. Li et al. (2008) and Burmistrova et al. (2011) also observed higher LCST for zwitterionic poly(N-isopropylacrylamide)-block-poly(lysine-co-glutamic acid) and acrylic acid addition as co-monomer than LCST of P(NIPAm).

1.3 Membrane materials: Polyethersulfone and Polyvinylpyrrolidone

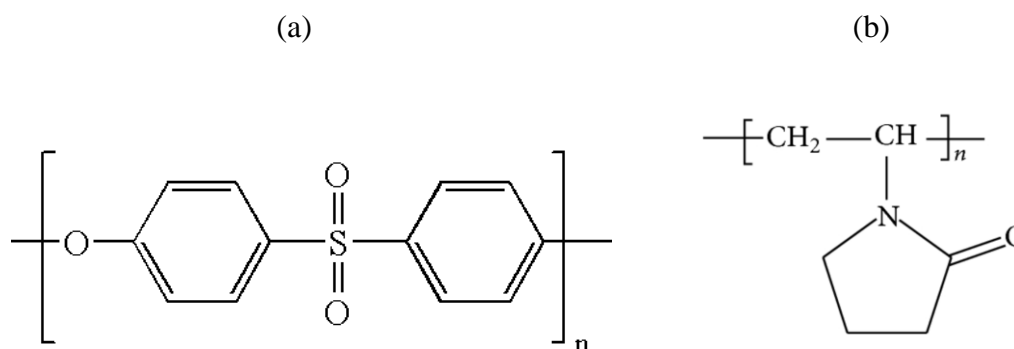


Figure 1.5 Polyethersulfone (a) and polyvinylpyrrolidone (b) chemical structures

Polyethersulfone (PES) and polyvinylpyrrolidone (PVP) were used as membrane material and hydrophilic additive in this study (Figure 1.5). PES membrane is among the most commonly used polymeric membranes despite the fact that it is prone to adsorption of most solutes and suspended materials in water due to its hydrophobic nature. It is preferred in membrane processes due to high chemical resistance, mechanical strength, thermal stability, durability and easily producing asymmetric membrane structure. Also, its morphology is easily controllable in terms of pore size and permeance of membrane (Jönsson et al., 1995, Dal-Cin et al., 1995, Wang et al., 2008 & Fröhlich et al., 2012). From this point of view, it gains more importance to make these kinds of membranes more cleanable.

Recently, producing non-fouling membranes with high stability has been an urgent topic for membrane separation. Membrane surface and solute interaction plays a crucial role for membrane fouling. For this purpose, blending other hydrophilic materials with PES was applied in order to make it more hydrophilic and accordingly more anti-fouling by decreasing the interaction since it may cause serious flux decline during filtration. PVP is among these hydrophilic materials that are used to improve membrane flux and rejection and the fouling-resistance properties of PES

membranes. (Wienk et al., 1996, Basri et al., 2011 & Wang et al., 2008). PVP cannot leave the polymeric membrane solution in coagulation step owing to its high molecular weight. Other additives for hydrophobic membrane to increase hydrophilicity can be illustrated as zwitterion containing polymers (Kaner et al., 2017 & Razi et al., 2012) and polyethylene glycol (PEG) (Yuan et al., 2008).

Stimuli responsive polymers have also started to be used in membrane applications recently. Most of them are based on blending them into membrane or grafting them on membranes. Gorey et al. (2011) modified the surface of cellulose acetate membranes by grafting with thermo-responsive P(NIPAm) on them with the claim that changing hydrophilicity – hydrophobicity of the membrane surface would provide more efficient cleaning. They followed two procedures: polymerizing of NIPAm onto membrane surface by creating radicals and terminating P(NIPAm) polymers with radicals onto membrane surface by putting membrane into reaction media. They performed filtrations in cold and hot conditions and also with a cyclic exposure to high and low temperature stimuli during filtrations. Then, they obtained lower flux decline with modified membranes compared to unmodified CA membranes. Chede et al. (2015) made thermally responsive-membranes that are composed of cellulose acetate (CA) and thermo-sensitive P(NIPAm) by casting them together via phase inversion. They reported that the CA-P(NIPAm) membranes display higher initial flux values, higher flux recoveries, and, therefore, lower irreversible fouling than CA membranes with the help of dynamic temperature stimulus; using lipase, bovine serum albumin (BSA) and humic acid as foulant. Also, Yu et al. (2010) deposited poly(n-isopropyl acrylamide-co-acrylamide), P(NIPAm-co-Aam), on thin film composite aromatic polyamide reverse osmosis (RO) membrane surface. Modified membranes showed higher permeance with higher rejection and better flux recovery for the experiments that were performed with different concentrations of BSA at different pressure and pH in cross-flow system than non-modified membranes. Yu et al. (2011) also suggested a model in order to clean a fouled membrane by the help of thermo-responsive polymers in another study. They used BSA as foulant with polyamide thin-film composite RO membrane and

poly(N-isopropylacrylamide) (P(NIPAm)), poly(N-isopropylacrylamide-co-acrylic acid) (P(NIPAm-co-AAc)) and poly(N-isopropylacrylamide-co-acrylamide) (P(NIPAm-co-Am)) as thermos-responsive polymers by applying the following fouling-cleaning mechanism: Membranes were fouled by BSA, then at a certain pressure, responsive polymers were deposited into the fouling layer at the soluble phase, and then cleaning was performed by changing the phase and accordingly the size by changing the temperature. Parameters were soaking time with water containing polymers and their concentration. As a result, they obtained higher cleaning efficiency by using responsive polymers as compared to the cleaning with only de-ionized water.

Han et al. (2014) studied pH-responsive composite membranes. They used polyethersulfone (PES) as membrane and poly(methyl methacrylate-co-acrylic acid) (P(MMA-AA)) and poly(methyl methacrylate-co-4vinyl pyridine) (P(MMA-4VPy)) as model pH-responsive copolymers. They added copolymers into PES solution and obtained membrane via phase inversion. Contact angle, membrane morphology, pH sensitivity and reversibility, protein anti-fouling property and Cu^{2+} adsorption capacity were analyzed in the research for composite and PES membranes for comparison. Foulant used in the experiments was BSA. Permeance of phosphate buffered saline (PBS) solution was measured before fouling test; then, filtration of BSA solution was done; afterwards, PBS permeance was measured again. Flux recoveries and percentages of fouling resistances and irreversibility were analyzed. It was seen that antifouling behavior improves with the addition of thermo-responsive polymer to PES by comparing regular PES membrane. Meanwhile, contact angle decreases, i.e., better hydrophilicity can be obtained.

Chen et al. (2013) wanted to control membrane pore sizes and accordingly permeance value by using polymers response to stimuli such as temperature, pH and ionic concentration. In other words, they tried to obtain multi-stimuli-responsive gates in membrane. Nylon-6 (N6) membrane was used in their study with poly(isopropylacrylamide)-block-poly(methacrylic acid) which has both a thermally

and pH response owing to P(NIPAm) and P(MAAc), respectively. They grafted membranes with the responsive polymers via surface-initiated atom transfer radical polymerization technique. At the end, they obtained open pores (“gates” as they named) when temperature was above LCST of P(NIPAm) with increasing pH and increasing salt concentration in P(NIPAm)-dominant segments and closed pores in the opposite case. Meng et al. (2014) and Zhu et al. (2016) produced ionic strength and electrolyte responsive membranes. They all reported higher permeance and higher flux recovery.

1.4 Foulants: Bovine Serum Albumin and Humic Acid

Bovine serum albumin (BSA) alone and humic acid (HA) with the presence of calcium chloride salt were used as foulant in aqueous feed solutions in filtrations. In literature, these are two very common model foulants for proteins, which compose an important part of fouling in downstream processing of bio-products with membranes, and natural organic matters, which are the main cause of the fouling during the filtration of surface or ground water, respectively (Lee et al. 2004 & Yuan et al., 2000 & Zularisam et al., 2006).

Serum albumins are the most common proteins in blood plasma (Salgın et al., 2005 & Majorek et al., 2012). They are responsible for carrying fatty acids, metals, drugs (Du et al., 2013 & Roche et al., 2008) and they are main supplier of colloid osmotic (oncotic) pressure in blood (Majorek et al., 2012). As, it was mentioned before, foulant-membrane interaction is one of the major reason in membrane flux decline. And, proteins (here BSA) tend to cause adsorptive fouling with hydrophobic membrane surfaces. Huisman et al. (2000) mentioned that adsorption of BSA on polysulphone dominated the fouling at the beginning of the filtration while the interaction between proteins themselves was the major mechanism of the fouling.

On the other hand, HA is the dark brown substance in soil which is formed with degradation of dead plant or animals by microorganisms. It is highly polydisperse in size (Sutton et al., 2005). Its binding capacity for metals and other contaminants in water makes it crucial to remove HA from water (Paolis et al., 1997). Its hydrophobic nature and gelation in the presence of calcium ions poses a major problem due to cake/gel layer formation on membrane surface in terms of membrane lifetime and energy consumption (Zularisam et al., 2006). Forming gel on the surface and high fouling behaviors are because HA is prone to bind multivalent ions (Nyström et al., 1996). Calcium and HA forms a complex and increasing calcium concentration in the feed causes increasing flux decline, i.e. more calcium brings lower filtration flux (Na et al., 2011).

Aim of the study

In this study, it was aimed to remove membrane fouling via addition of stimuli-responsive polymeric microgels into feed solution. This constitutes a more practical approach both due to the possibility of integrating it into any process from microfiltration to reverse osmosis and any module type (spiral wound, hollow fiber, submerged membrane bioreactor) and due to its action on high amount of cake or gel formation. The latter is quite common in MBRs and drinking water treatment systems and typically combatted using optimized backwash or forward flush operation. The proposed approach while be an alternative to such physical cleaning procedures. In detail, the proposed technique is to deposit them into cake or gel layer during filtration and they will be free instead of attaching the membrane; then, cleaning of the fouling layer was performed by changing the intensity of the stimuli, i.e. decreasing temperature to swell collapsed microgels or increasing it to collapse swollen microgels, and accordingly changing hydrophilicity and size of particles. It is hypothesized that adding these microgels into the feed will help break down the fouling layer more easily by changing their dimensions inside the fouling layer. Another effect of the microgels can originate from changing interactions within the fouling layer due to their relatively hydrophilic character, which can decrease the extent of fouling and/or render it more easily cleanable. Temperature and ionic strength were used as stimuli in the study. Poly(n-isopropylacrylamide) and poly(n-isopropylacrylamide-co-sulfobetainemethacrylate) microgels were both used in cleaning experiments that were performed with temperature stimulus. Latter one was also used with ionic strength response.

CHAPTER 2

EXPERIMENTAL METHOD

2.1 Materials

N-Isopropylacrylamide (97%), N, N'-Methylenebis(acrylamide) (Bis- acrylamide, 99%), 2-(Methacryloyloxy)ethyl]dimethyl-(3-sulfopropyl)ammonium hydroxide (sulfobetaine methacrylate) (97%), potassium persulfate ($\geq 99\%$), hexane ($\geq 95\%$), toluene ($\geq 99.5\%$), polyethylene glycol 400 (PEG400, MW = 400 Da), polyvinylpyrrolidone K90 and K30, humic acid sodium salt, calcium chloride dehydrate ($\geq 99\%$), and bovine serum albumin (BSA, MW = 66 kDa) were purchased from Sigma Aldrich. Polyethersulfone was supplied by BASF. Dimethyl sulfoxide ($\geq 99.5\%$) was purchased from Sigma Aldrich or Merck. Technical ethanol (99.5%) was bought from Sigma Aldrich or Gurup Deltalar. Dr. Oetker brand instant yeast was purchased from supermarket.

Ultra-pure (UP) water was used in filtration experiments for preparing the feed solutions and in physical cleaning whereas reverse-osmosis (RO) water was used as non-solvent in order to coagulate polymer solutions for membrane fabrication.

2.2 Membrane Preparation

Two types of membranes were prepared via phase inversion: PES and PES/PVP blend membranes. Here, the former is hydrophobic and the latter is more hydrophilic owing to addition of PVP into polymer solution. They were cast at 250 μm thickness from polymer solutions with three different concentrations: 20% PES, 20% PEG400, 60% DMSO; 25% PES, 20% PEG400, 55% DMSO; and 15% PES, 5% PVP K90,

5% PVP K30 and 75% DMSO solutions. Membranes were named as PES-20, PES-25 and PES/PVP, respectively. Polymer solutions were coagulated in pure water for 10 minutes and washed with fresh water for 1 hour and then for 24 hours. Membranes were stored in 20% ethanol-80% water solution until use.

2.3 Microgel Synthesis and Characterization

P(NIPAm) and P(NIPAm-co-SBMA) microgels were synthesized by precipitation polymerization where monomer and initiator are soluble in water but polymers precipitate when polymerization starts since they are insoluble in it. Reaction mechanism was radical polymerization. In Table 2.1, amounts of monomers, n-isopropyl acrylamide and n-isopropylacrylamide-co-sulfobetainemethacrylate (NIPAm and SBMA), cross-linker, methylene bis-acrylamide (BA), and initiator, potassium persulfate (KPS) are given. Here, molar ratio of NIPAm to SBMA is 10.

P(NIPAm) microgels were obtained by using different monomer, cross-linker and initiator amounts and ratios (Table 2.2). The amounts in the first batch were directly taken from the study of Das et. al. (2008). The other batches were decided by ourselves with the aim of increasing swelling ratio which was calculated as the ratio of the highest and lowest diameter with changing stimuli. It was thought that higher size difference between two phases of the microgel might improve the mechanical cleaning effect on the fouling layer.

Before the synthesis, firstly, monomer purification was performed to remove inhibitors. It was dissolved in toluene, precipitated in hexane, and then filtered and dried at room temperature. In microgel synthesis, firstly, NIPAm and BA were added into DI water in given amounts at 70°C. Pure nitrogen was passed through the mixture to get rid of dissolved oxygen in water for 20 minutes. By addition of KPS, polymerization was started. After 5 h, polymerization was completed. For P(NIPAm-co-SBMA) synthesis, SBMA monomers were added 15 minutes after polymerization

started. After that, polymeric microgels were separated from the mixture by centrifugation at 8000 rpm for 30 minutes by running 4 times at 45°C where polymers are collapsed, and dried at room temperature.

Table 2.1 Monomer (NIPAm and SBMA), cross-linker (BA), and initiator (KPS) mass per 100 mL DI water used in synthesis

Microgel	Reaction Mixture (g)			
	NIPAm	SBMA	BA	KPS
P(NIPAm)	0.89	–	0.05	0.06
P(NIPAm-co-SBMA)	0.89	0.23	0.05	0.06

Table 2.2 Different monomer (NIPAm), cross-linker (BA), and initiator (KPS) mass per 100 mL DI water for different synthesis to improve swelling ratio

Batch	NIPAM	BA	KPS	% BA	% KPS
1	0.89	0.05	0.06	5.6	6.7
2	0.89	0.05	0.03	5.6	3.4
3	1.78	0.10	0.12	5.6	6.7
4	0.89	0.02	0.06	2.2	6.7

Synthesized particles were characterized in terms of particle size and lower critical solution temperature. Two methods were used to determine particle size: dynamic light scattering (DLS) and scanning electron microscopy (SEM). Two methods were also used for analysis of lower critical solution temperature: light transmission and DLS.

2.4 Dynamic Light Scattering

Dynamic light scattering (DLS) analyses were performed in METU Central Laboratory (Malvern CGS-3). Microgel solutions were analyzed by increasing temperature gradually from room temperature to 45°C. At each temperature, more than one measurement (between 2 – 5) was done.

2.5 Light Transmission

In light transmission experiments, light intensities of the microgel solution for each temperature were measured by taking advantage of changing opacity of aqueous polymer solution with temperature change. Here, the solution was heated above LCST; and then, it was let to cool down to room temperature spontaneously by contact with the ambient air for the analysis by collecting light intensity and temperature data simultaneously (Figure 2.1).

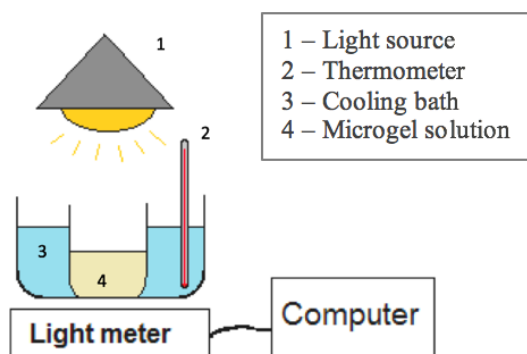


Figure 2.1 Light Transmission Experimental Set-up

2.6 Scanning Electron Microscopy (SEM)

Microgels and membrane surfaces were observed by SEM analysis (QUANTA 400F Field Emission SEM) in METU Central Laboratory. Membrane cross-sections were analyzed with Phenom Pure Desktop SEM in Tufts University. For cross-section images, membranes were broken after freezing with liquefied nitrogen. Membranes were dried under vacuum at least overnight. After that, they were sputter-coated with Au/Pd particles.

2.7 Filtration and Cleaning Procedures

Filtrations were performed in 50 mL Amicon cells at 2 bar TMP in dead-end mode without stirring to deposit all foulants in the same amount on membrane surface at each time, to reduce variables during filtrations and accordingly to enhance reproducibility (Figure 2.2). Effective membrane area was 13.4 cm². During filtrations, 10 ml permeate was collected from a starting feed volume of 40 ml. Two feeds were used as 1 g/L bovine serum albumin (BSA) and 1 g/L humic acid with 2 mM CaCl₂ solutions (HA). Concentrations of polymeric microgels were 0.1 and 0.01 g/L for P(NIPAm) and 0.01 g/L for P(NIPAm-co-SBMA) in filtration experiments. Starting concentration was adjusted to 0.1 g/L to understand their effect on fouling removal; then, it was lowered to 0.01 g/L since high amount of microgel usage was not practical. Cleaning was performed in both directions: from swollen to collapsed state and collapsed to swollen state. Also, some of experiments had an additional cleaning step named as “extra cleaning” by applying heating and cooling consecutively more than once.

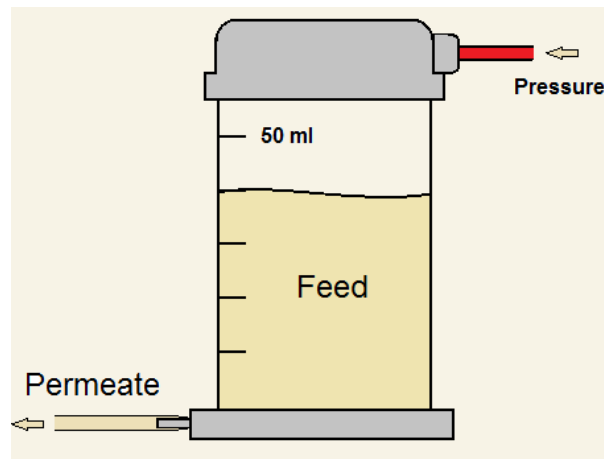


Figure 2.2 Experimental set-up for the filtrations with Amicon stirred cell (50 ml)

Firstly, pure water permeance (PWP) of membrane was measured at room temperature for all the cases. After that, following two procedures were performed.

Procedure 1 – cooling below LCST for cleaning

- ✓ Filtration was done above LCST (35°C in BSA experiments).
- ✓ After filtration, retentate was cooled below LCST rapidly by adding water at 0°C (below LCST) in the same quantity (30 ml) with it to bring the temperature to around 20 °C.
- ✓ Stirring at 400 rpm was applied for 5 minutes to remove fouling.

Procedure 2 – heating above LCST for cleaning

- ✓ Filtration was done at room temperature (below LCST), where microgels are swollen and hydrophilic.

- ✓ After the filtration, retentate was heated to above LCST (35 and 38 °C in BSA and HA experiments, respectively), rapidly by adding hot water in the same quantity (30 ml) with it.
- ✓ Stirring at 400 rpm was applied for 5 minutes to remove fouling.

Pure water permeance after cleaning (PWP*) of membrane was measured again at room temperature in order to compare it to its initial value.

Extra cleaning (cyclic)

After some of filtrations done with procedure 1, an additional cleaning was applied to investigate the effect of applying cyclic temperature change on fouling removal. The cleaning procedure followed was as follows:

- ✓ Stirring at 600 rpm for 10 minutes above LCST (38°C),
- ✓ Stirring at 600 rpm for 10 minutes below LCST (room T),
- ✓ Stirring at 600 rpm for 10 minutes above LCST (38°C).
- ✓ PWP after extra cleaning (PWP**) measurement at room temperature in order to compare it to its initial and second (PWP*) values.

Schematic views of the presumed deposition and cleaning mechanisms of the procedure 1, procedure 2 and extra cleaning are given in Figure 2.3 –Figure 2.5.

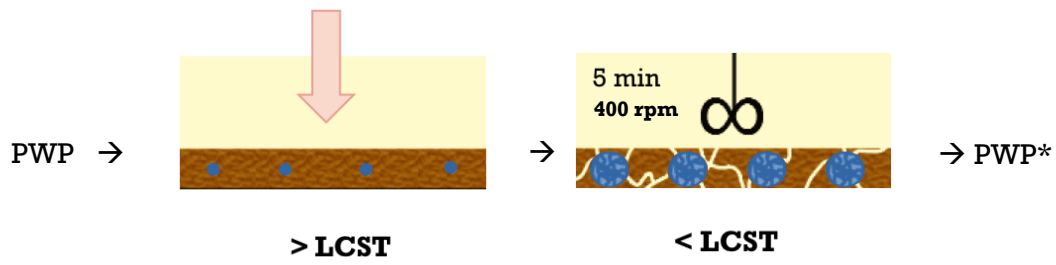


Figure 2.3 Presumed cleaning mechanism for Procedure 1 (*cooling*)

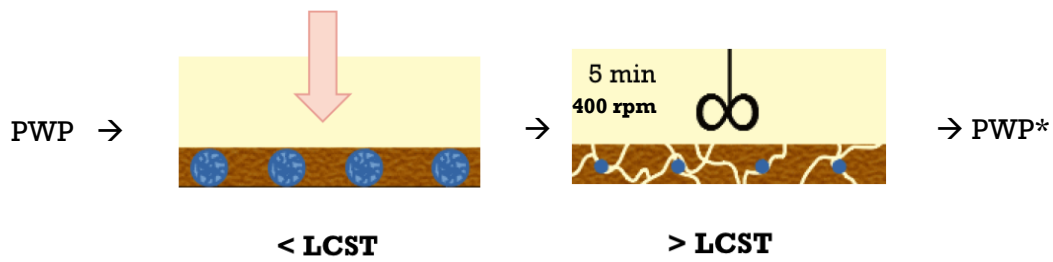


Figure 2.4 Presumed cleaning mechanism for Procedure 2 (*heating*)

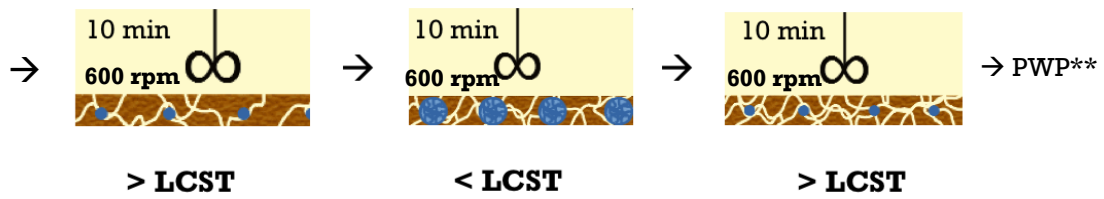


Figure 2.5 Presumed cleaning mechanism for extra cleaning (*cyclic*)

2.8 Filtration Analysis

Irreversibility in fouling was calculated as the percentage of remaining fouling resistance after physical cleaning to total fouling resistance at the end of filtration (eqn.6).

$$\% \text{ Irreversibility} = \frac{R_{\text{irreversible}}}{R_{\text{fouling}}} \times 100 \% \quad (6)$$

Filtration flux ratio (FFR) at the end of filtration and flux recovery (FR) after cleaning were defined for each filtration as follows:

$$\text{FFR \%} = \frac{J_{\text{filtration}}}{J_0} \times 100 \% \quad (7)$$

$$\text{FR \%} = \frac{J_{\text{final}}}{J_0} \times 100 \% \quad (8)$$

Here $J_{\text{filtration}}$, J_0 and J_{final} represent flux at the end of filtration, pure water flux at the beginning and pure water flux after cleaning. They were normalized in order to eliminate the temperature effect.

UV/Visible Spectroscopy (Schimadzu UV-1601) was used in order to measure retention of foulants. Analysis of BSA and HA concentrations were performed at 280 and 254 nm, respectively. Calibration plots of BSA and HA solutions are given in Appendix B. Also, retentions of all filtrations are given in Appendix C.

2.9 Adsorption Tests

Adsorption tests were performed in order to assess the extent of adsorptive fouling on membranes and understand the interactions between foulant, membrane and microgels. Membranes with known area were put into BSA, humic acid and/or microgel solutions for 24 hours. Initial and final concentrations in these solutions were measured using UV/Visible Spectroscopy (Schimadzu UV-1601) at 280, 254 and 239 nm wavelengths for BSA, humic acid and P(NIPAm) microgel solution, respectively. Using the membrane area and the concentration difference at the beginning and at the end, adsorbed amounts were calculated in $\mu\text{g}/\text{cm}^2$. Used membrane areas varied from one to another test and they are given in Appendix A.

CHAPTER 3

RESULTS AND DISCUSSION

3.1 PES and PES/PVP Blend Membranes

PES was chosen since it is a common membrane material but is hydrophobic and easily fouled nature whereas PVP addition was done in order to make PES membranes more hydrophilic and accordingly to reduce adsorptive fouling effect (Basri et al., 2011 & Wang et al., 2008). Hydrophilic contribution was preferred because the target fouling type was the cake or gel formation on membrane surface in order to see the effect of responsive polymeric microgels on the fouling removal.

SEM images of membranes which were used in filtrations can be seen in Figure 3.1. PES-20 membranes were used in BSA filtrations since their BSA retention was around 100% while PES-25 membranes were preferred in HA filtrations to get higher rejection values after some filtrations performed with PES-20 and obtained low rejections.

From the SEM images of PES-20, PES-25 and PES/PVP membranes, it was seen that all are asymmetric with a thin skin layer and microvoids. Also, it was observed a thicker selective layer of PES membrane for higher polymer concentration. However, there was not an obvious difference between cross-sectional structures of these membranes. (Figure 3.1).

PWP values of PES-20 and PES-25 membranes were found as 51 ± 19 and 36 ± 3 LHM/bar, respectively, whereas the ones PES/PVP blend membranes were around 3.2 ± 1.1 LHM/bar.

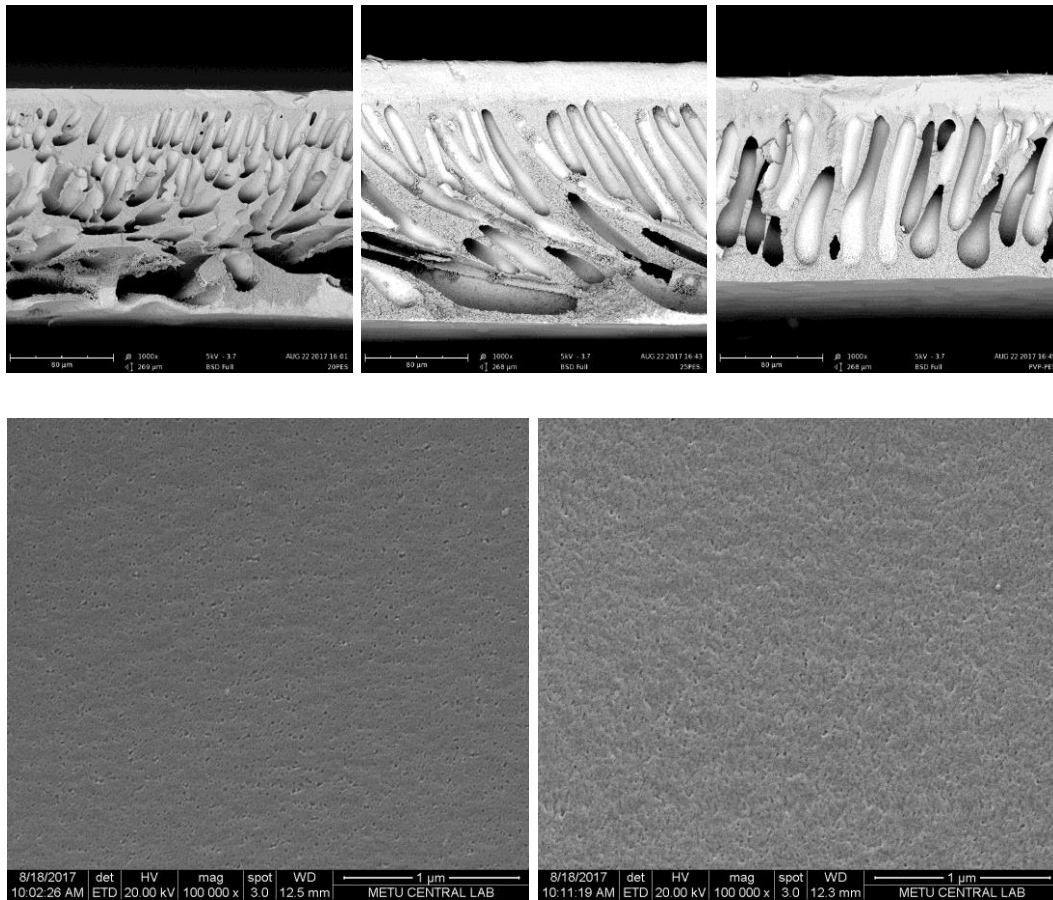


Figure 3.1 SEM images of the membrane cross-sections of PES-20 (top left), PES-25 (top middle) and PES/PVP (top right) and membrane surfaces of PES-20 (bottom left), PES/PVP (bottom right)

Pore sizes measured at membrane surfaces were 21 ± 5 and 17 ± 6 nm for PES-20 and PES/PVP blend membranes, respectively, using SEM images shown in Figure 3.1. They did not have much different pores sizes but PES-20 membrane had higher pore density than PES/PVP blend membrane.

3.2 Characterization of Microgels

Synthesized microgel particles were characterized in terms of particle size and lower critical solution temperature.

3.2.1 P(NIPAM) Microgels

Hydrodynamic diameters were measured by DLS analysis for all syntheses performed with the given amounts in Section 2.3, Table 2.2. Their LCST and hydrodynamic diameters (D_h) against temperature are shown in Figure 3.2. Then, as described in Section 1.2, swelling ratios were calculated as the ratio of the highest and lowest diameter values of microgels in swollen and shrunk states, respectively.

Swelling ratios were similar for the first, second and fourth batches but almost no swelling was observed for the third batch which had the monomer, cross-linker and initiator in double amount of the first batch. From Figure 3.2, it seemed D_h of swollen state for the first and second were the same while the fourth batch had a slightly higher D_h in collapsed state. The first and second batches also had the same in D_h in both states whereas phase transition was observed to be sharper in the first batch than in the second batch where the former had higher cross-linker concentration than the latter. In literature, Burmistrova et al. (2011) reported that increasing cross-linker concentration in reaction media lowers swelling ratio and effect the sharpness of the phase change. Also, it can be said that the change in the monomer to cross-linker ratio did not make a significant difference in the microgel swelling properties, except the third case.

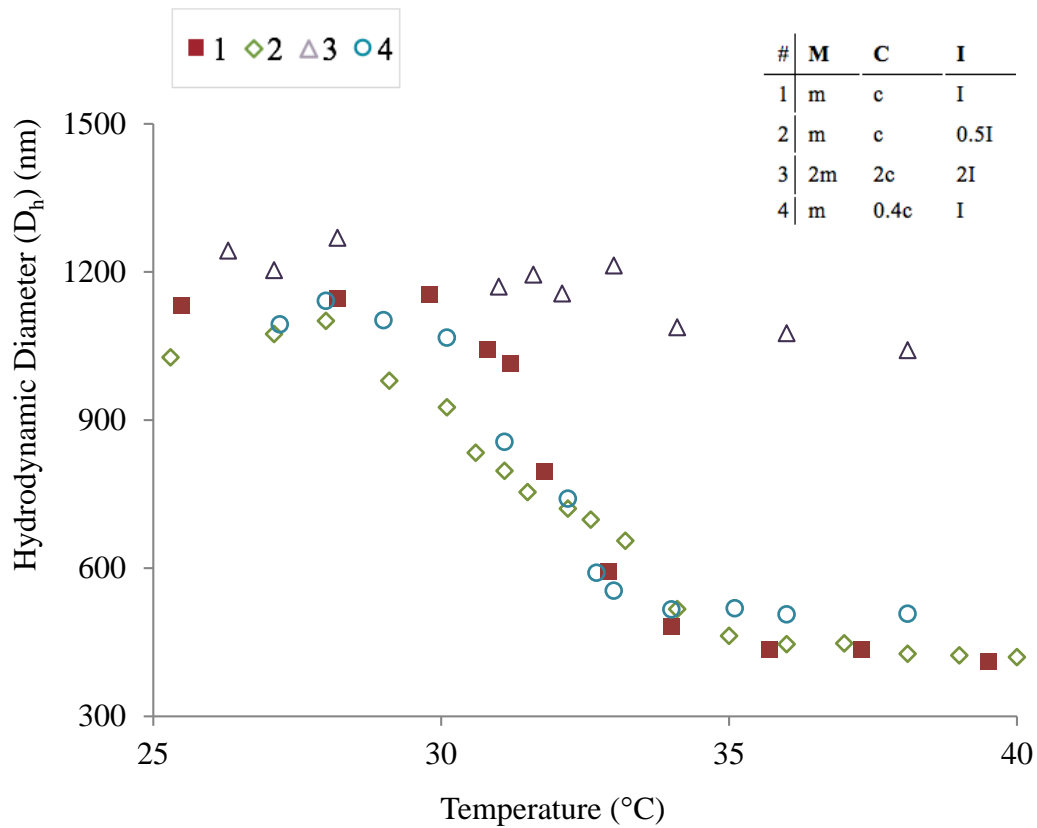


Figure 3.2 Hydrodynamic diameters of four different batches against temperature (°C) according to DLS analysis

In addition, lower critical solution temperature (LCST) values are seen as similar around 32°C for all. However, the sharpness of the phase change is different. Then, it is decided to use the first batch in performance tests due to its highest swelling ratio and relatively sharp phase change. For the first batch, swelling ratio found as 2.9 by using D_h values of swollen and collapsed phases so it means that the volumetric ratio was approximately 24.

In light transmission experiments, light intensity values of the solution for each temperature were measured by taking advantage of changing opacity of aqueous polymer solution with the given stimulus. Here, the solution was heated above LCST;

and then, it was let to cool down to room temperature spontaneously for the analysis. Light intensity versus temperature graph is plotted in Figure 3.3.

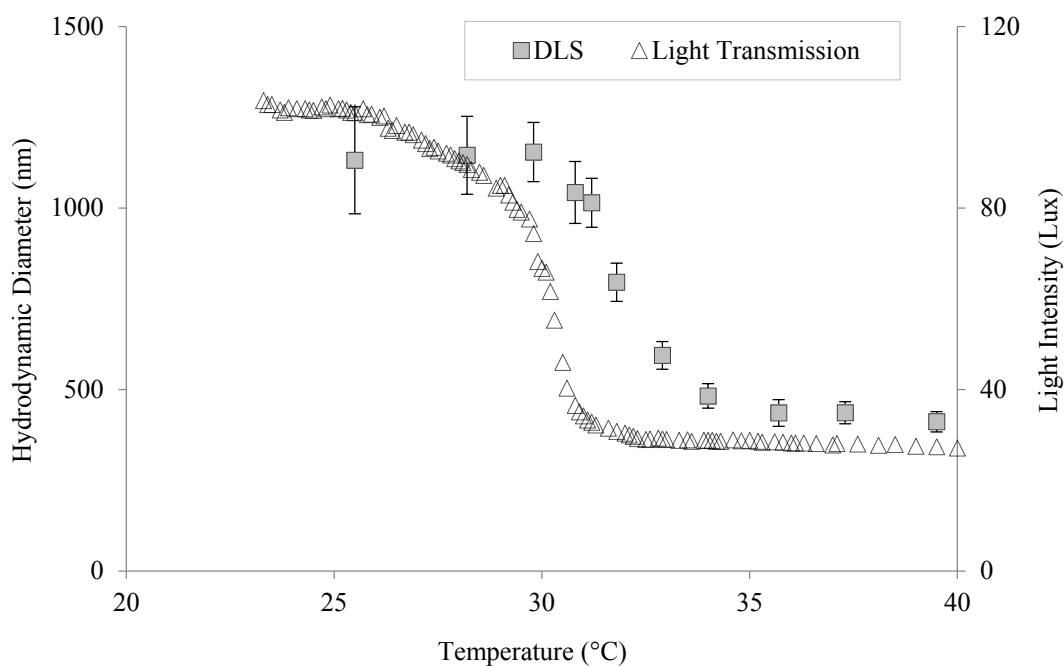


Figure 3.3 Light transmission and DLS results of P(NIPAm) microgels against temperature (°C)

There is approximately 2°C difference between LCST values found from DLS and light transmission plots. Hysteresis may be the reason of this delay due to formation of additional H-bonding in collapsed state. Then, giving response in two directions separately may bring a shift in microgels LCST analysis.

Table 3.1 Hydrodynamic diameters (D_h) of microgels in pure water and 0.5 M NaCl according to DLS analysis

Microgel	Medium	D_h at 22 °C (nm)	D_h at 45 °C (nm)	Swelling Ratio
P(NIPAm)	Pure Water	1146 ± 74	411 ± 14	2.9 ± 0.6
P(NIPAm-co-SBMA)	Pure Water	751 ± 26	357 ± 3	2.1 ± 0.1
	0.5 M NaCl	864 ± 7	226 ± 0	3.8 ± 0

3.2.2 P(NIPAM-co-SBMA) Microgels

P(NIPAM-co-SBMA) microgels were also obtained by precipitation polymerization. NIPAM to SBMA monomers molar ratio were taken as 10:1 (Rubio-Retama et al., 2010) while the other quantities were kept the same as in the P(NIPAm) microgel synthesis.

Hydrodynamic diameters of microgels were measured via DLS for different temperatures in both pure water and in 0.5 M NaCl solution to see temperature response and LCST in both conditions. Highest and lowest hydrodynamic diameters are found as 864 and 226 nm, respectively, at room temperature in 0.5 M NaCl while swollen and collapsed diameters in pure water are 751 and 357 nm, respectively. After that, swelling ratios were calculated as the ratio of the highest and lowest diameter values of microgels with and without salt and found as 2.1 and 3.8, respectively (Table 3.1 and Figure 3.4). Swelling ratio was lower than P(NIPAm) in pure water. It was reported in literature that increasing co-monomer acrylic acid addition into P(NIPAm) lowered the swelling ratio (Burmistrova et al., 2011). It is seen that microgels swell 80% more in 0.5 M NaCl media than in pure water. However, volume expanded 9 and 55 times from collapsed to swollen state in pure

water and 0.5 M NaCl solution, respectively. Therefore, volume ratio difference was found as 6 times larger in the presence of salt.

LCST value was found around 29 °C (Figure 3.4). Filtrations with P(NIPAm-co-SBMA) microgels were performed both in pure water and in the presence of salt to understand the effect of ionic strength.

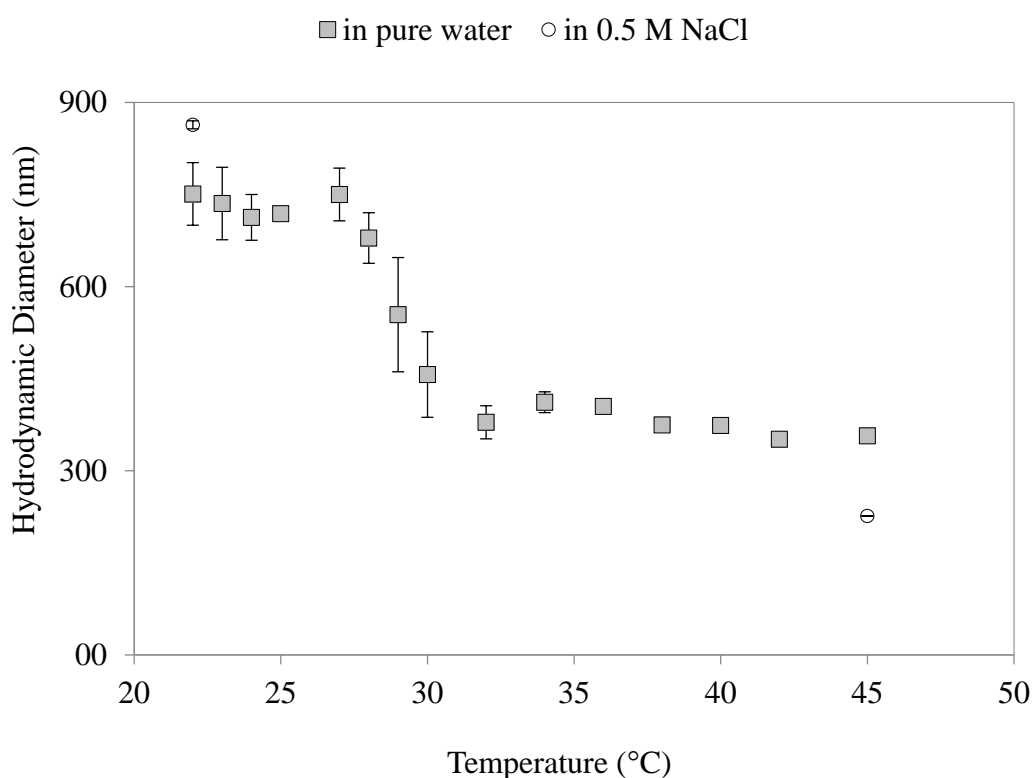


Figure 3.4 Hydrodynamic diameters and LCST analysis of P(NIPAm-co-SBMA) microgels with respect to temperature via DLS in pure water and 0.5 M NaCl

DLS and light transmission plots gave very similar LCST around 29°C (Figure 3.5). Hysteresis was not observed here. The light transmission graph was seen as broader than DLS. This shape difference may be related to cooling and heating rate. In DLS analysis temperature was gradually increased and stopped at each temperature to

measure hydrodynamic diameter. In light transmission, hot polymeric microgel solution was let to cool down to room temperature slowly.

Contrary to expectations, LCST of P(NIPAm-co-SBMA) was found lower than P(NIPAm). In literature, it was seen that addition of more hydrophilic SBMA as comonomer into P(NIPAm) microgels resulted in higher LCST since it brought stronger interaction with water (Zhao et al., 2015 & Obiweluozor et al., 2014).

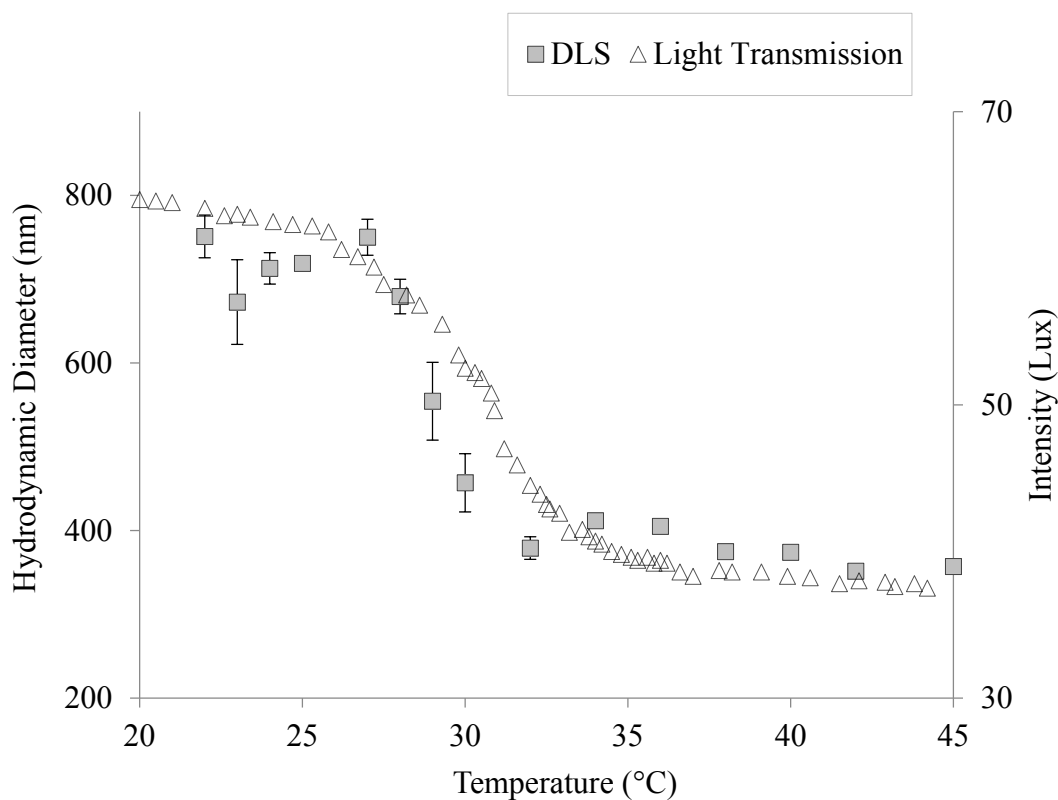


Figure 3.5 Light transmission and DLS results of P(NIPAm-co-SBMA) microgels in pure water with respect to temperature

Diameters of dry microgels were read from SEM images of the microgels deposited on PES membrane surfaces in Figure 3.6. as around 500 and 350 nm for P(NIPAm) and P(NIPAm-co-SBMA) microgels, respectively. They were in collapsed state in the images since they were taken under vacuum conditions. SEM image of P(NIPAm-co-SBMA) gave similar result to DLS while dry diameter of P(NIPAm) was found approximately 20% higher than D_h .

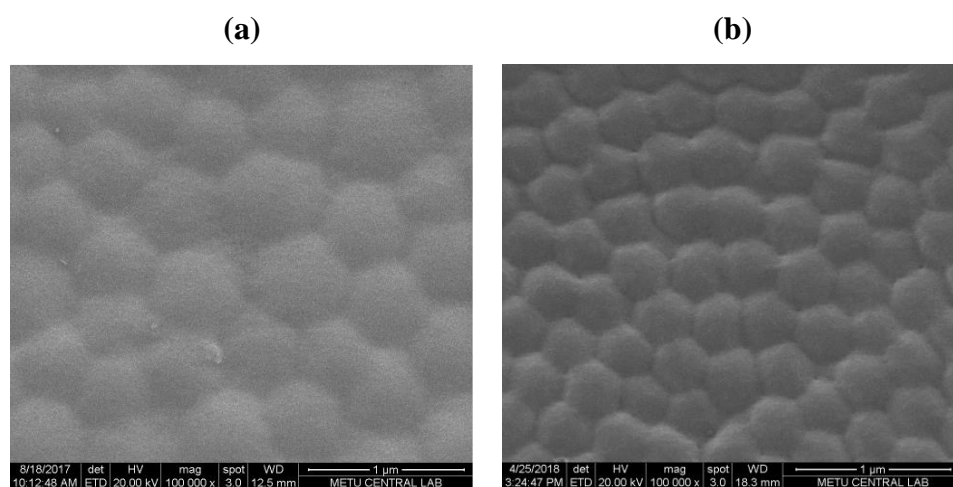


Figure 3.6 SEM images of (a) P(NIPAm) and (b) P(NIPAm-co-SBMA) microgels deposited on PES membrane

3.3 Performance Tests

Performance tests were done in several conditions with different membranes, foulants and microgels. Membranes were PES and PES/PVP blend membranes, foulants were BSA and humic acid, microgels were P(NIPAm) and P(NIPAm-co-SBMA) polymeric microgels as mentioned before.

3.3.1 Effect of P(NIPAm) Microgels Addition into BSA Solution on Fouling Removal from PES Membrane

Experiments of BSA with PES-20 membrane were performed with both procedure 1, i.e. *cooling below LCST*, and procedure 2, i.e. *heating above LCST*. Former had cleaning direction from collapsed to swollen state while latter occurred in the opposite direction. Rejections of all BSA filtrations were found above 99% (Appendix C). In Figure 3.7 and

Figure 3.8, BSA filtrations were done at 35°C without and with 0.1 g/L P(NIPAm) microgels, respectively. Plots given in those figures belong the repetition of the same procedure and the same feed. Higher temperatures were not applied to the filtrations of BSA in order to avoid denaturation. After filtration, retentate was cooled to room temperature with the addition of 0°C water and stirring at 400 rpm for 5 minutes as described in procedure 1 in Section 2.7.

It can be seen that fluxes rapidly declined to around 20% of the initial pure water flux at the beginning of the filtration for both feeds (Figure 3.7 and 3.8). This can be explained by adsorptive fouling of BSA onto PES membrane and accordingly it brings additional resistance to aqueous solution permeance due to its highly hydrophobic nature. At the end, filtration flux ratios (FFR) and flux recoveries (FR) were slightly higher in presence of P(NIPAm). Flux increased to 25% of the initial flux compared to 17% when there was no microgels (Table 3.2). However, average fouling and irreversible fouling resistances were seen as the same (Figure 3.9). The

slight difference in the results of the flux recovery and resistance analysis originated from the initial PWP values of the membranes.

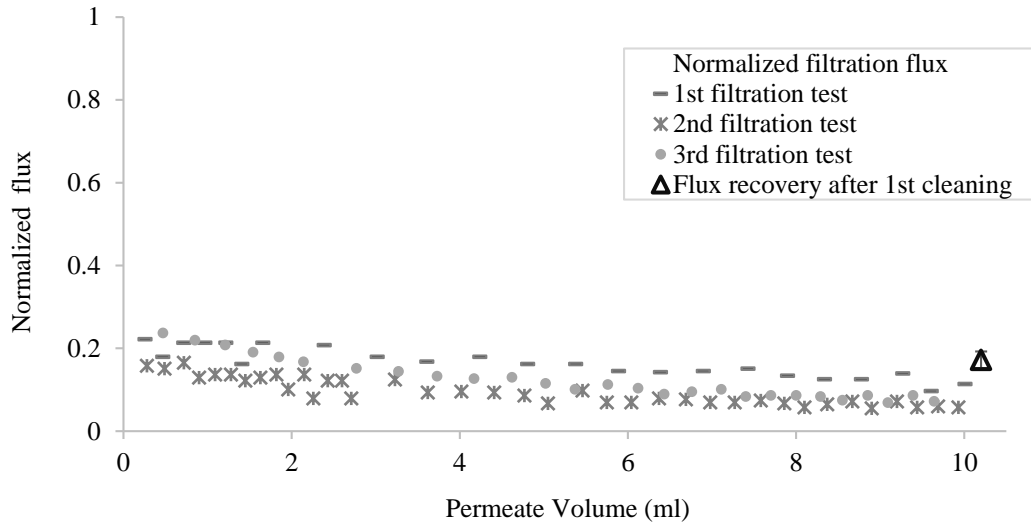


Figure 3.7 Normalized flux graphs of three separate BSA filtrations at 35 °C with PES membranes and their average flux recoveries after cleaning via cooling below LCST (procedure 1)

Besides that, experiments were also performed at room temperature where microgels were swollen and hydrophilic, with cleaning by bringing them into collapsed phase via heating, i.e. procedure 2 was applied (Figure.10 and 3.11).

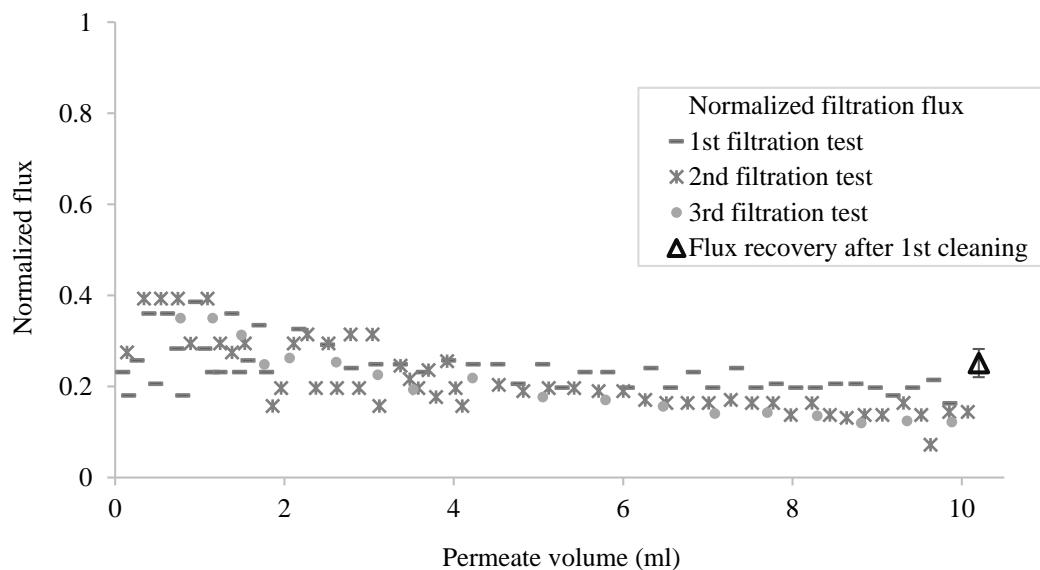


Figure 3.8 Normalized flux graphs of three separate BSA and 0.1 g/L P(NIPAm) microgels filtrations at 35°C with PES membranes and their average flux recoveries after cleaning via cooling below LCST (procedure 1)

Table 3.2 Filtration flux ratios and flux recoveries of BSA and BSA + 0.1 g/L P(NIPAm) microgels filtrations at 35 °C with PES membranes cleaning via cooling below LCST (procedure 1)

Filt.	BSA		BSA + P(NIPAm)	
	FFR %	FR %	FFR %	FR %
1	11.5	17.4	14.5	28.7
2	5.9	14.7	8.6	25.0
3	7.2	19.1	8.3	20.9
Avg	8.2 ± 2.4	17.1 ± 1.8	10.5 ± 2.9	24.9 ± 3.2

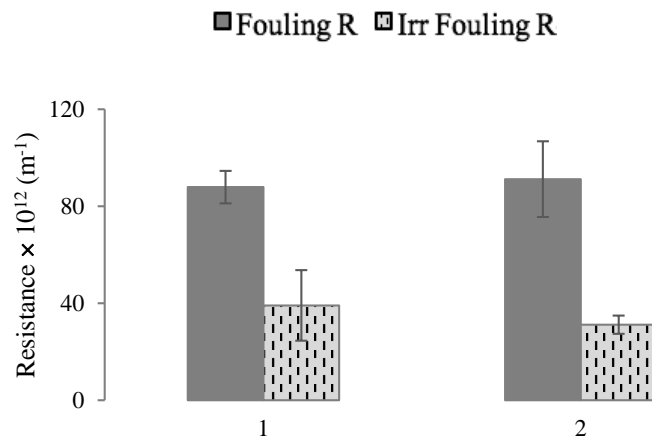


Figure 3.9 Resistances of (1) BSA and (2) BSA + 0.1 g/L P(NIPAm) microgels filtrations at 35 °C with PES membranes cleaning via cooling below LCST (procedure 1)

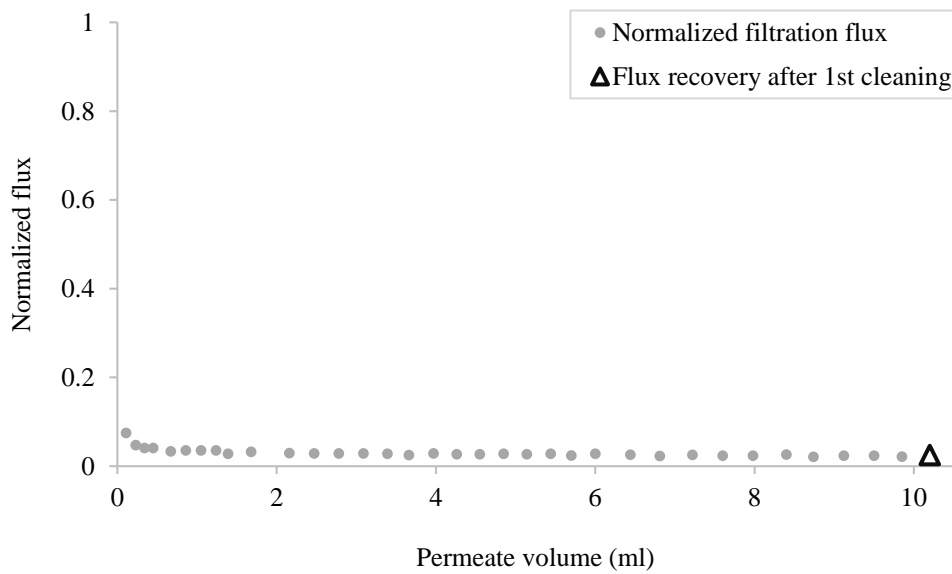


Figure 3.10 Normalized flux graph of BSA filtrations at room temperature with PES membranes and flux recovery after cleaning via heating above LCST (procedure 2)

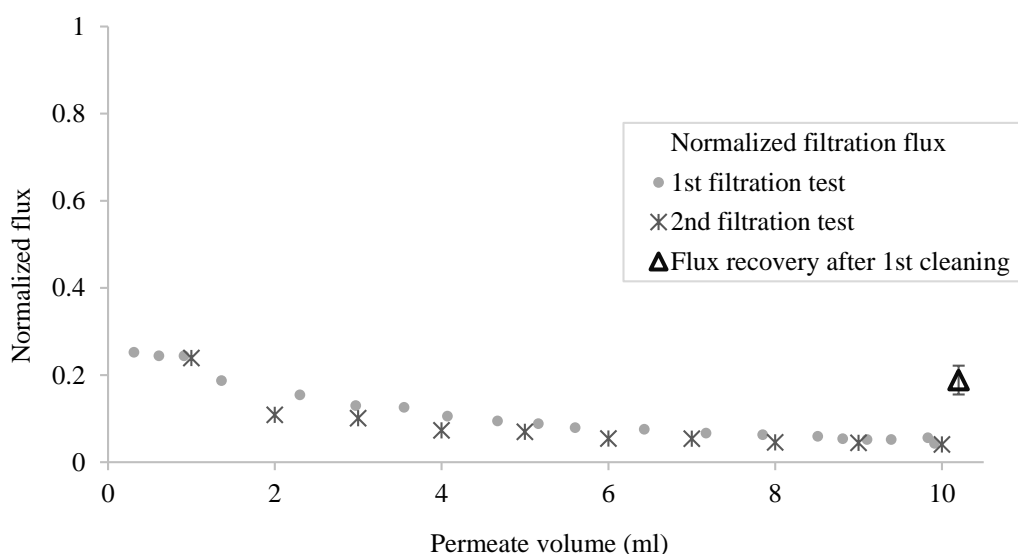


Figure 3.11 Normalized flux graphs of two separate BSA + 0.1 g/L P(NIPAm) microgels filtrations at room temperature with PES membranes and average flux recovery after cleaning via heating above LCST (procedure 2)

Initial sudden flux declines were similar, around 20% for both procedures. Filtration flux ratio reached the lowest values at room temperature (procedure 2) with microgel addition among all BSA filtration with PES via procedure 1 and 2 (Table 3.2 and 3.3). In BSA filtrations, there was not an obvious difference between procedure 1 and 2 in terms of filtration flux ratio and flux recovery. However, fouling with P(NIPAm) gave similar results with BSA experiments in terms of flux recoveries while the microgel addition brought a better result in procedure 1. Also, higher fouling and irreversible fouling resistances were obtained with P(NIPAm) in procedure 2 (Figure 3.12). During the series experiments of procedure 2, microgels have around 24 times larger volume compared to procedure 1 although they were hydrophilic. This might be the reason behind higher amount of fouling during filtrations with procedure 2 than 1.

When we look at the results of BSA and P(NIPAm) with PES membranes as a whole, it can be said that using P(NIPAm) microgels does not bring a better fouling removal performance. In general, fouling could just be cleaned until where filtration flux ratios

were dropped rapidly at the beginning of the filtrations. Those sharp decreases were due to adsorption of BSA on PES membrane. As a result, it was difficult to clean BSA from PES membrane with volume change of microgels after it was adsorbed once.

Table 3.3 Filtration flux ratios and flux recoveries of BSA and BSA + 0.1 g/L P(NIPAm) microgels filtrations at room temperature with PES membranes cleaning via heating above LCST (procedure 2)

Filt.	BSA		BSA + P(NIPAm)	
	FFR %	FR %	FFR %	FR %
1	6.5	20	4.1	15.5
2			4.5	22.1
Avg			4.3 ± 0.2	18.8 ± 3.3

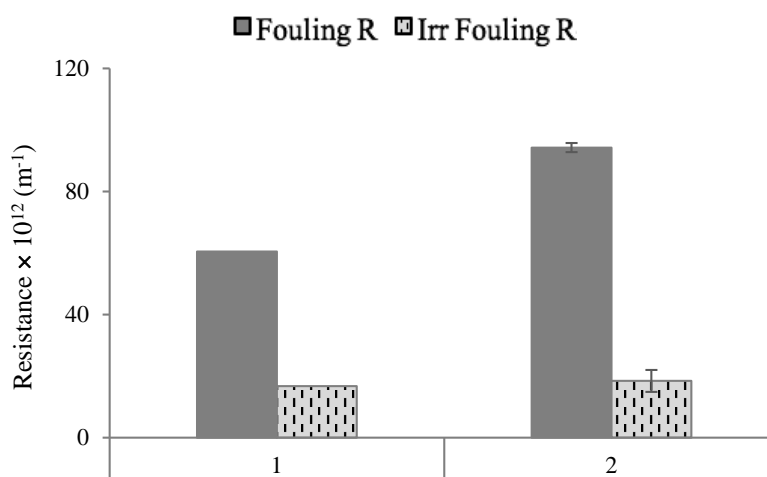


Figure 3.12 Resistances of (1) BSA and (2) BSA + 0.1 g/L P(NIPAm) microgels filtrations at room temperature with PES membranes cleaning via heating above LCST (procedure 2)

BSA filtration with PES/PVP blend membrane was also performed. This foulant-membrane couple was not used for further experiments since BSA was cleaned from the PES/PVP membrane easily. Its normalized flux graph is given in Appendix D.

3.3.2 Effect of P(NIPAm) Microgels Addition into Humic Acid Solution on Fouling Removal from PES Membrane

Experiments of HA to see the effect of P(NIPAm) in filtrations with PES-20 were only performed with procedure 1 (*cooling below LCST*). Rejections of HA with PES membrane were obtained to be in between 72 – 74 and around 77 % for microgel-free and microgel-added filtrations, respectively (Appendix C). P(NIPAm) microgels were used in 0.1 g/L concentration.

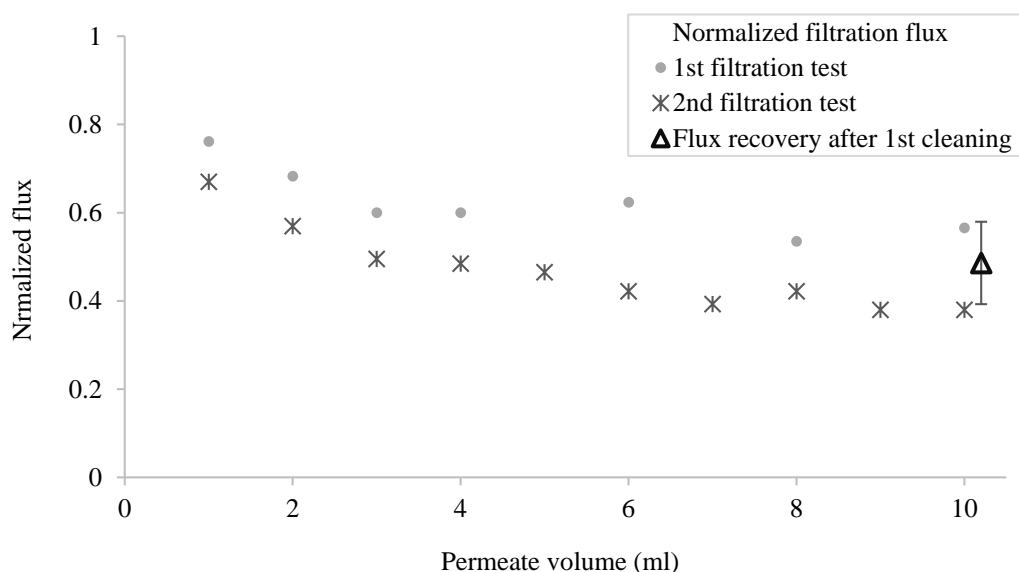


Figure 3.13 Normalized flux graphs of two HA filtrations at 35 °C with PES membranes and average flux recovery after cleaning via cooling below LCST (procedure 1)

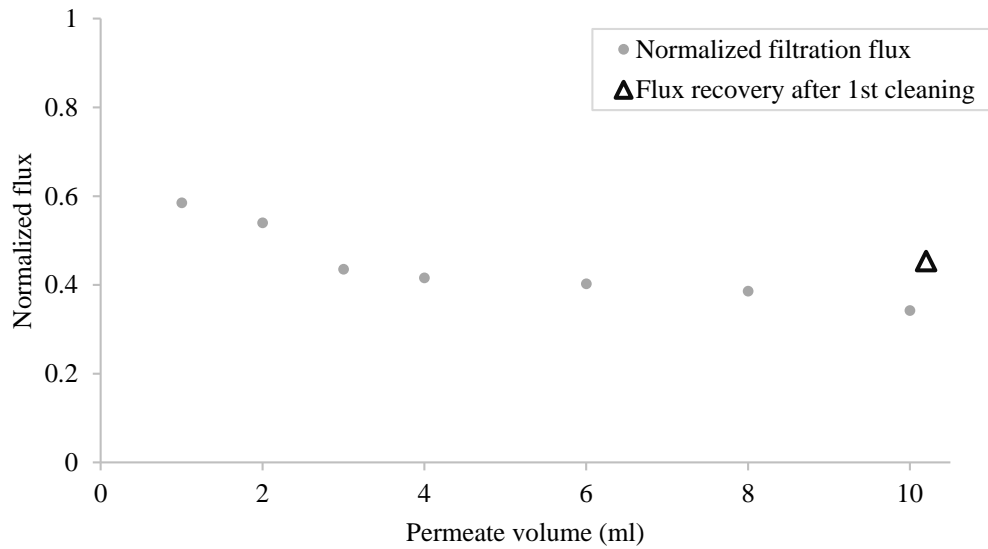


Figure 3.14 Normalized flux graph of HA and 0.1 g/L P(NIPAm) microgels filtrations at 35 °C with PES membranes and cleaning via cooling below LCST (procedure 1)

It was seen that HA brought a higher initial and final filtration flux during filtration compared to BSA for both microgel-free and microgel-added cases as shown in Figure 3.13 and Figure 3.14, respectively. This can be explained with its lower tendency to adsorb to PES surface than BSA. Also, microgel addition affected the initial flux decline negatively. Filtration flux ratio was around 70% of pure water flux for HA filtration while it declined to 60% with microgel.

Addition of P(NIPAm) microgels into humic acid feed neither resulted in higher filtration flux nor better flux recovery with *cooling below LCST for cleaning* procedure (Table 3.4). Also, their fouling and irreversible fouling resistances were seen as similar for microgel-added and microgel-free filtrations (Figure 3.15). It can be said that P(NIPAm) microgels addition does not improve cleaning efficiency of humic acid from PES membrane surface like in BSA filtrations. When compared to BSA filtrations with procedure 1, it is seen that HA ends up with less flux decline and fouling resistance.

Table 3.4 Filtration flux ratios and flux recoveries of HA and HA + 0.1 g/L P(NIPAm) microgels filtrations at room temperature with PES membranes cleaning via heating

Filt.	HA		HA + P(NIPAm)	
	FFR %	FR %	FFR %	FR %
1	54.9	57.6	34.5	45.7
2	38.1	39.3		
Avg	46.5 ± 8.4	48.5 ± 9.1		

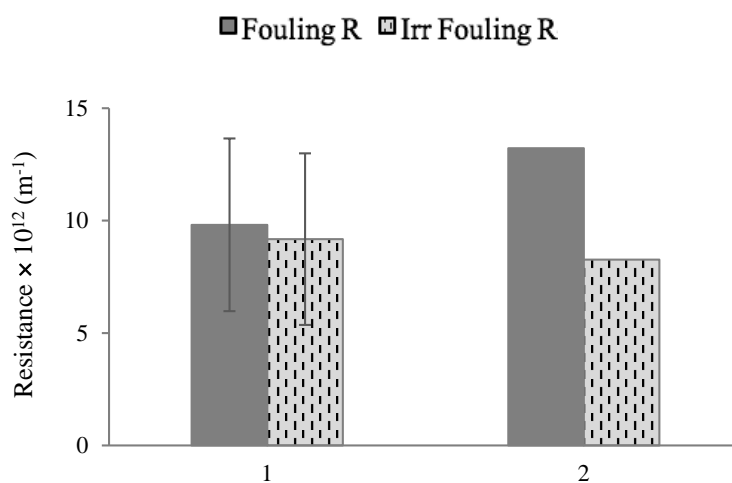


Figure 3.15 Resistances of (1) HA and (2) HA + 0.1 g/L P(NIPAm) microgels filtrations at room temperature with PES membranes cleaning via cooling below LCST (procedure 1)

3.3.3 Effect of P(NIPAm-co-SBMA) Microgels Addition into Humic Acid Solution on Fouling Removal from PES membrane

HA feed solutions were used with PES-25 for understanding how P(NIPAm-co-SBMA) microgels affect fouling removal. Experiments were only performed with procedure 2 (*heating above LCST*) where microgels were hydrophilic during filtrations. For P(NIPAm), there was not an obvious difference in results between two procedures in terms of flux recovery; then, procedure 2 was preferred in P(NIPAm-co-SBMA) experiments since it was more practical owing to room temperature-filtration. It was aimed to use denser membrane in order to get higher rejections. Then, they were obtained to be around 78 and 80 % without and with microgels, respectively (Appendix C). P(NIPAm-co-SBMA) microgels were used in 0.01 g/L concentration.

Filtrations were performed in series in this set of experiments. The same membrane was used four times after cleaning for each case which are microgel-free and microgel added (Figure 3.16). Additionally, an extra cleaning, which is described in Section 2.7, was applied beginning from the second cycle to see the effect of further cyclic exposure of stimuli (temperature) change and mixing on fouling removal. It was done just after the PWP*, which is the pure water permeance after the first cleaning, was measured. After that, PWP**, which is the pure water permeance after extra cleaning, was checked again to compare it with initial (PWP) and the second (PWP*) values.

Addition of p(NIPAm-co-SBMA) microgels enabled more efficient cleaning compared to microgel-free case. Flux declined more at the end of the first cycle with microgel addition than microgel-free filtration. Flux ratios were similar for each cycle of filtrations with microgel whereas there was a continuous decline in HA filtration, i.e. increasing number of filtrations brought lower flux ratio. Then, it reached the value of microgel added filtration set. Applying the first and extra cleaning steps did not provide complete cleaning for HA experiments. After that, membrane was used in the next cycle with some amount of fouling left on it. With microgels; on the other

hand, it was seen that membranes were cleaned and reached almost the initial pure water flux after one filtration-cleaning cycle; and then, it was fouled again until the similar Filtration flux ratios around 45%. In other words, there was no irreversible fouling left from one to another cycle in a series filtration of the feed which contained HA and p(NIPAm-co-SBMA) microgels together (Figure 3.16).

Resistance data (Figure 3.17) provide supportive information to normalized flux graphs as expected. It was seen that better cleaning was achieved with presence of p(NIPAm-co-SBMA) microgels although it was observed that fouling resistances were higher compared to only HA case. On the other hand, fouling and irreversible fouling resistances in HA filtrations increased after each cycle. Since it could not be removed completely, it accumulated on the membrane surface more and more with further filtrations and fouling resistance was getting closer and closer to the case with the microgels.

In Table 3.5, it is also seen that flux declined until 59% of the initial flux at the end of the 1st cycle in HA filtration, whereas it was 44% with microgel addition. However, filtration flux ratio at the end of HA filtration cycles was 46% of initial flux after the fourth filtration set while it is still 44% for microgel-added case. Furthermore, 63 and 98% of the initial fluxes were recovered for HA and HA with p(NIPAm-co-SBMA) microgels, respectively, at the end. As a result, fouling can be removed almost completely with the addition of p(NIPAm-co-SBMA) microgels into HA feed while about half of it was irreversible for HA feed without these microgels.

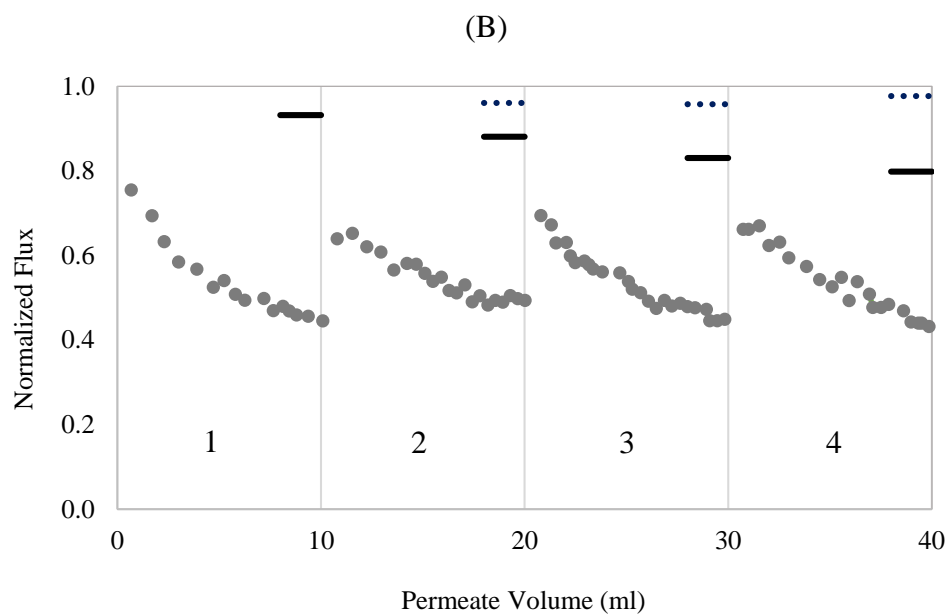
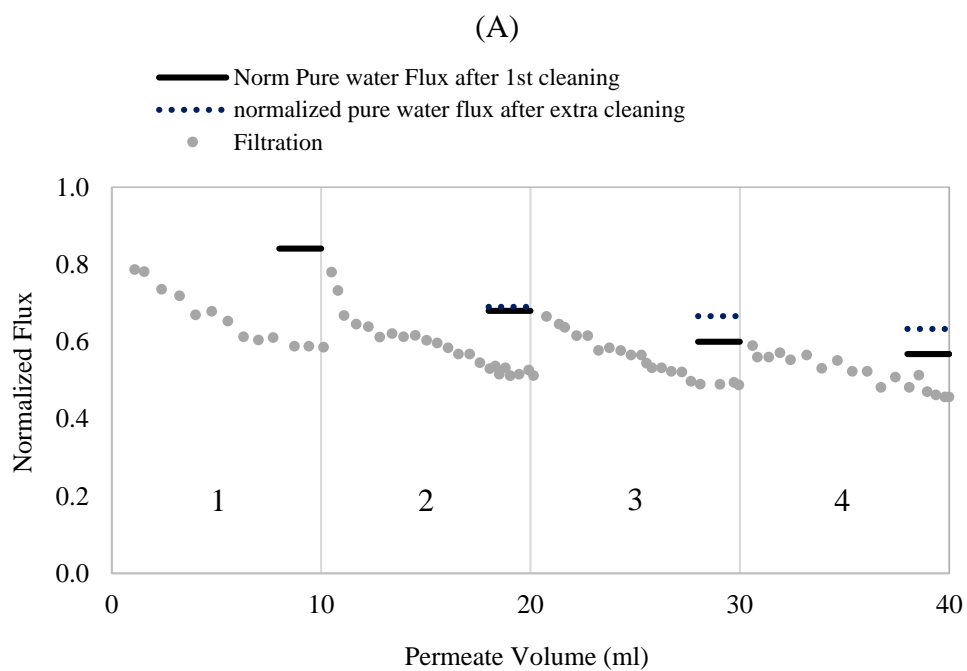


Figure 3.16 Normalized flux graphs of HA (A) and HA + 0.01 g/L P(NIPAm-co-SBMA) (B) series filtrations with PES membrane at room temperature and cleaning via heating above LCST (procedure 2)

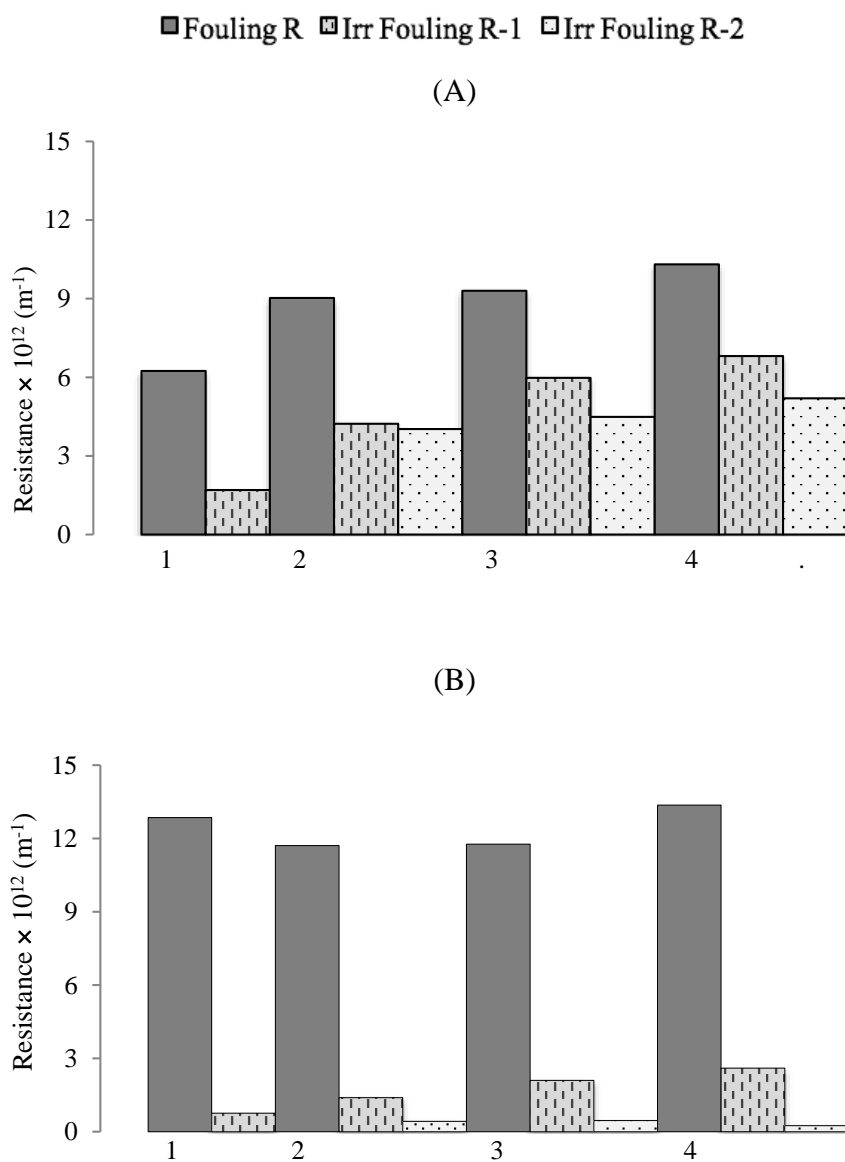


Figure 3.17 Resistance graphs of HA (A) and HA + 0.01 g/L P(NIPAm-co-SBMA) (B) series filtrations with PES membrane at room temperature and cleaning via heating above LCST (procedure 2)

Table 3.5 Filtration flux ratios and flux recoveries of HA and HA + 0.01 g/L P(NIPAm-co-SBMA) series filtrations with PES membrane at room temperature and cleaning via heating above LCST (procedure 2)

Filt	HA			HA + P(NIPAm-co-SBMA)		
	FFR %	FR – 1 %	FR – 2 %	FFR %	FR – 1 %	FR – 2 %
1	59	84	–	44	93	–
2	50	68	69	47	88	96
3	49	60	67	47	83	96
4	46	57	63	44	80	98

Below, membrane photographs of both filtrations which were taken after 1st and extra cleaning steps (Figure 3.18) summarize the effect of microgel addition on fouling removal clearly.

It can be said that the presence of p(NIPAm-co-SBMA) microgels in the feed may help reduce and/or break membrane-foulant and foulant-foulant interaction due to its hydrophilic interaction with water. Its presence in HA feed brought an additional fouling resistance with PES membrane. Still, better cleaning performance was observed than the feed with only HA at the end. As a result, it can be said that p(NIPAm-co-SBMA) microgels usage can definitely be preferable due to their positive fouling removal effect.

	HA		HA P(NIPAm-co-SBMA)	
	After 1 st cleaning	After extra cleaning	After 1 st cleaning	After extra cleaning
1		x		x
2				
3				
4				

Figure 3.18 PES membrane photographs after 1st and extra cleaning of HA and HA + 0.01 g/L P(NIPAm-co-SBMA) microgels series filtrations with PES membrane at room temperature and cleaning via heating above LCST (procedure 2)

3.3.4 Effect of P(NIPAm) Microgels Addition into Humic Acid Solution on Fouling Removal from PES/PVP Blend Membrane

In this set, p(NIPAm) microgels were added into humic acid feed but filtrations were performed with PES/PVP blend membranes by applying procedure 2 (*heating above LCST*). It was mentioned that PVP addition into PES membrane is widely used since it makes membrane more hydrophilic and accordingly decreases adsorptive fouling. Rejections were found in between 82 – 84 and 84 – 89 % with the absence and presence of microgels, respectively (Appendix C). P(NIPAm) microgels were used in 0.01 and 0.1 g/L concentrations. Membranes, here, were used for once so filtrations were performed and repeated separately, i.e. experiments were not done in series. Also, extra cleaning was applied to these.

Initial pure water fluxes could not be achieved after HA filtrations at room temperature with PES/PVP blend membrane in absence of microgels via cleaning with temperature increase (Figure 3.19 and Table 3.6). Also, fouling resistance graphs showed that fouling was highly irreversible (Figure 3.20).

Firstly, P(NIPAm) microgels were added to the HA feed solution in a weight ratio of 1:100 (0.01 g/L) which is the same ratio with the previous section, i.e. the ones with PES membrane. In these experiments, very close results to microgel-free ones were obtained in terms average Filtration flux ratios and flux recoveries (Figure 3.21 and Table 3.7). Also, both of them had similar fouling and irreversible fouling resistances (Figure 3.22). Actually, in the 3rd repetition of this set, it was seen an increase in fouling resistance after 1st cleaning. This might be because the microgels gained a denser or more resistive structure with the foulant in the case it could not be removed at all.

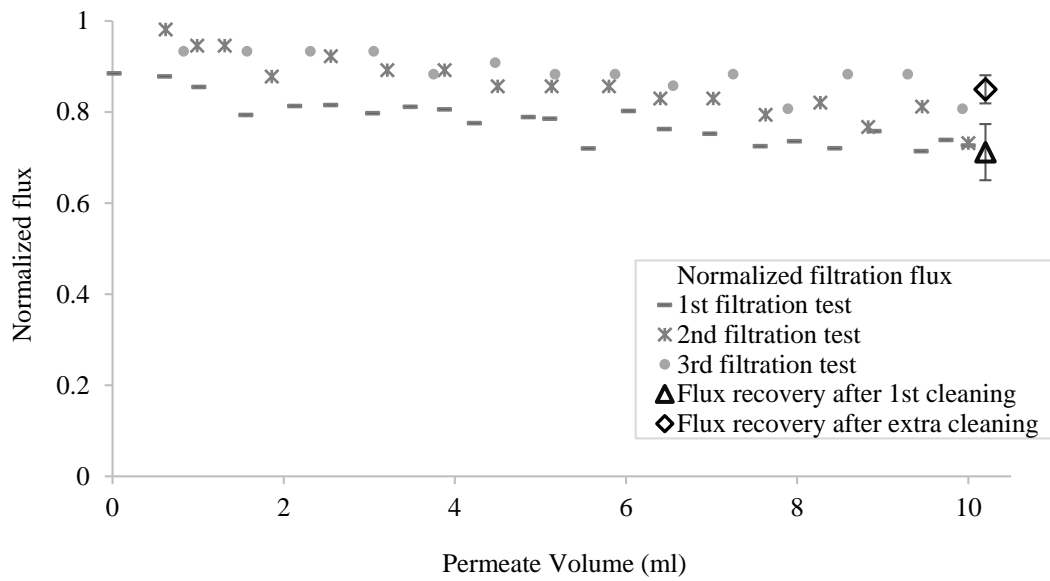


Figure 3.19 Normalized flux graphs of three HA filtrations with PES/PVP blend membranes at room temperature and their average flux recoveries after cleaning via heating above LCST (procedure 2)

Table 3.6 Filtration flux ratios and flux recoveries of HA filtrations with PES/PVP blend membrane at room temperature and cleaning via heating above LCST (procedure 2)

Filt	FFR %	FR – 1 %	FR – 2 %
1	73	68	69
2	75	81	85
3	70	85	91
Avg	73 ± 2	78 ± 7	82 ± 9

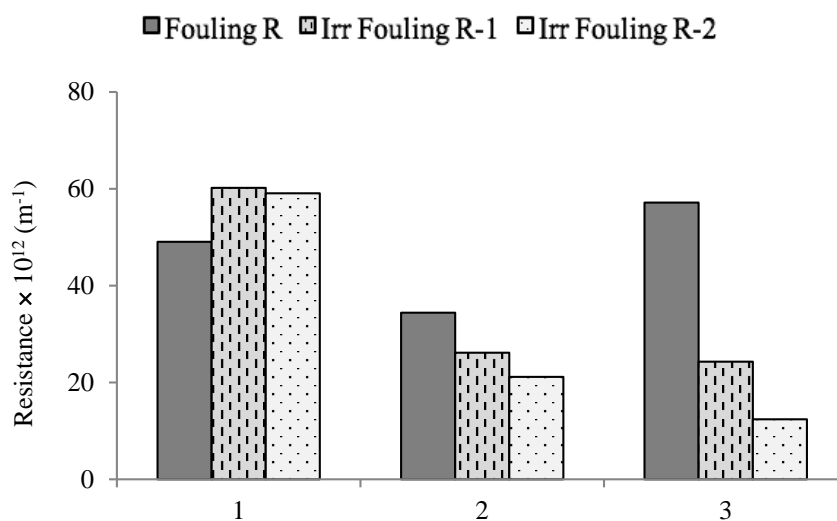


Figure 3.20 Resistances of HA filtrations at room temperature with PES/PVP blend membrane and cleaning via heating above LCST (procedure 2)

Then, P(NIPAm) microgels were used in 0.1 g/L concentration. However, they could not give a different result from the one with the concentration of 0.01 g/L microgels. From normalized flux graphs (Figure 3.23), filtration flux ratio and flux recovery table (Table 3.8), and resistance graphs (Figure 3.24), it is seen that increasing P(NIPAm) microgels concentration from 0.01 g/L to 0.1 g/L does not bring additional fouling or better recovery. At the end, all these three cases ended up with non-cleaned membranes.

It can be understood that P(NIPAm) behaves like species an inert into HA feed in terms of the fouling removal from PES/PVP blend membranes.

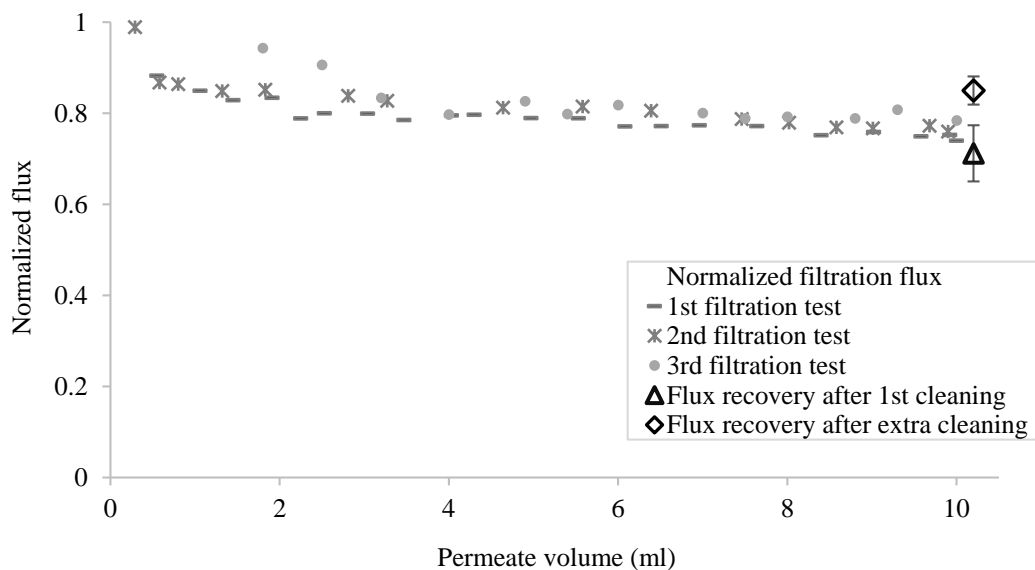


Figure 3.21 Normalized flux graphs of three HA and 0.01 g/L p(NIPAm) filtrations with PES/PVP blend membranes at room temperature and their average flux recoveries after cleaning via heating above LCST (procedure 2)

Table 3.7 Filtration flux ratio and flux recovery of HA and 0.01 g/L P(NIPAm) microgels filtration with PES/PVP blend membrane at room temperature and cleaning via heating above LCST (procedure 2)

Filt	FFR %	FR – 1 %	FR – 2 %
1	74	72	86
2	74	78	87
3	79	63	81
Avg	76 ± 2	71 ± 6	85 ± 3

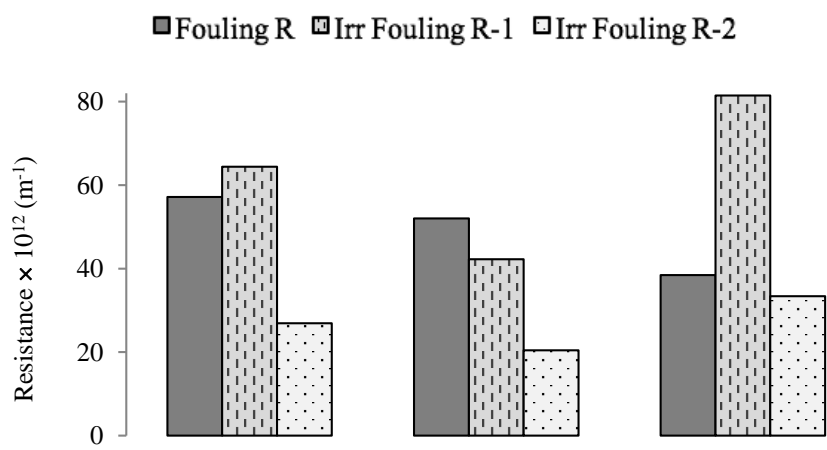


Figure 3.22 Resistances of HA and 0.01 g/L P(NIPAm) filtrations at room temperature with PES/PVP blend membrane and cleaning via heating above LCST (procedure 2)

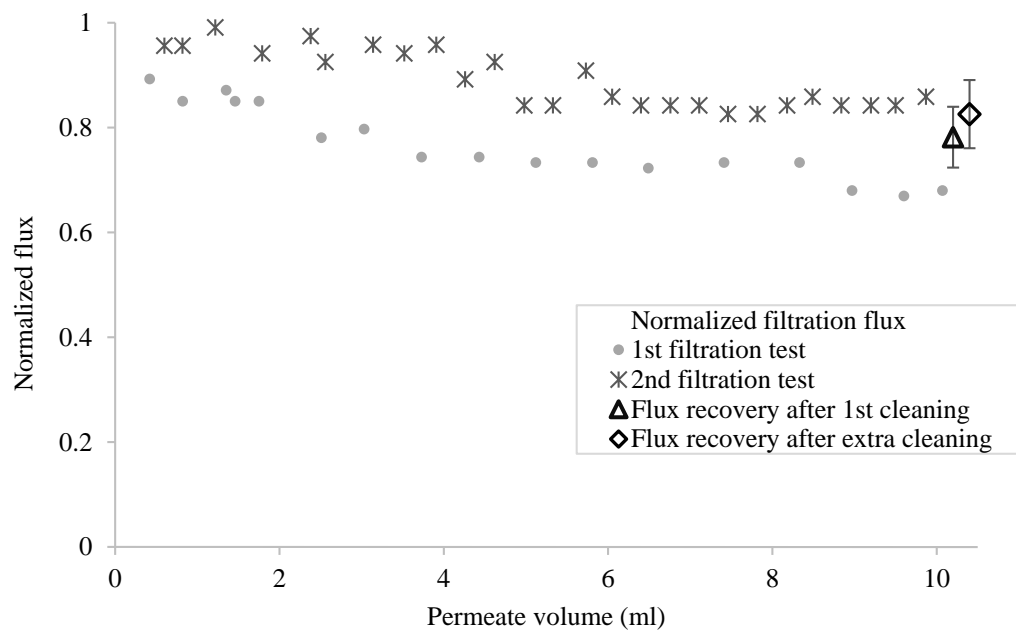


Figure 3.23 Normalized flux graphs of two HA and 0.1 g/L p(NIPAm) filtrations with PES/PVP blend membranes at room temperature and average flux recovery after cleaning via heating above LCST (procedure 2)

Table 3.8 Filtration flux ratio and flux recovery of HA and 0.1 g/L P(NIPAm) microgels filtration with PES/PVP blend membrane at room temperature and cleaning via heating above LCST (procedure 2)

Filt	FFR %	FR – 1 %	FR – 2 %
1	67	72	76
2	80	84	89
Avg	74 ± 7	78 ± 6	83 ± 7

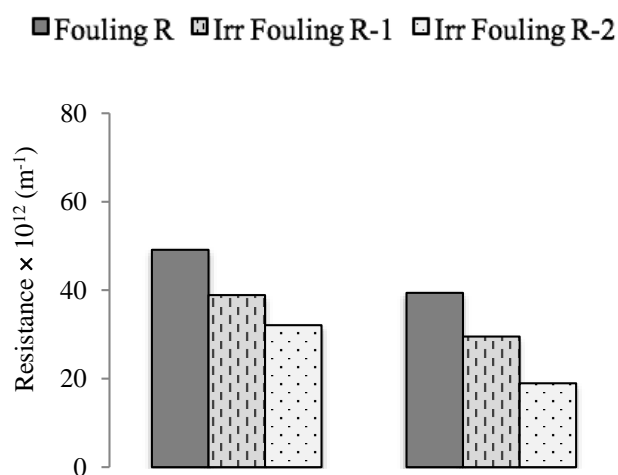


Figure 3.24 Resistances of HA and 0.1 g/L P(NIPAm) filtrations at room temperature with PES/PVP blend membrane and cleaning via heating above LCST (procedure 2)

Additionally, HA filtration was performed at room temperature and no temperature change applied for cleaning, i.e. cleaning was done at room temperature with only stirring to clean membrane surface at room temperature. It was seen that fouling was removed by a very little amount and initial pure water flux was not achieved by just mixing without any temperature change (Figure 3.25 and Table 3.9). It gave very similar results with the filtrations of HA that were cleaned via heating above LCST

despite the extra cleaning there. As a result, it can be said that heating does not have any effect on fouling removal for HA filtration with PES/PVP blend membrane.

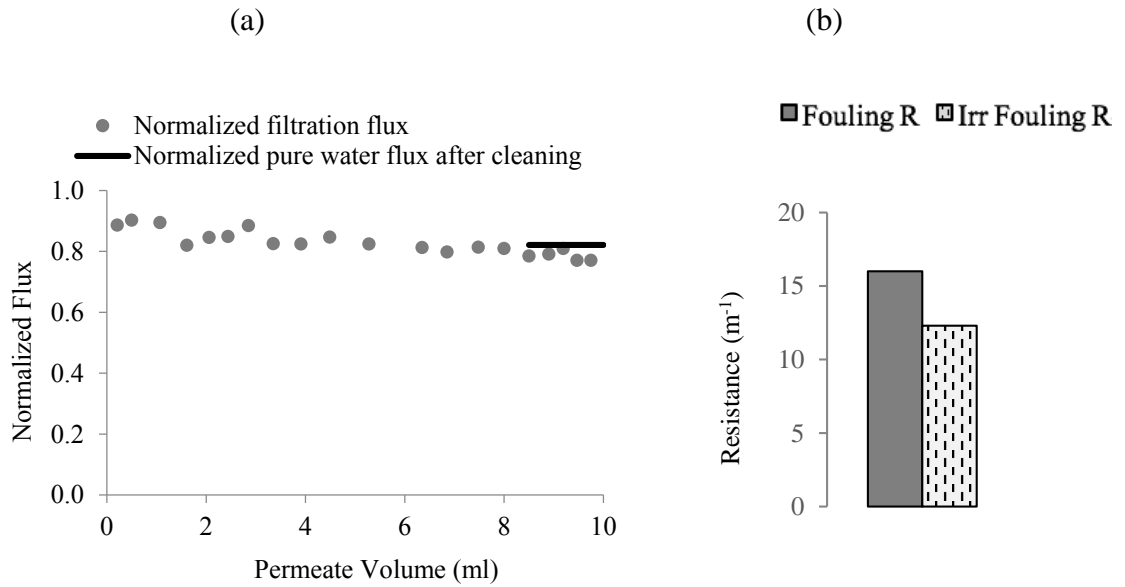


Figure 3.25 Normalized flux (a) and resistance (b) graphs of HA filtration with PES/PVP blend membrane at room temperature and cleaning at room temperature

Table 3.9 Filtration flux ratio and flux recovery of HA filtration with PES/PVP blend membrane at room temperature and cleaning at room temperature

FFR %	FR %
78	83

3.3.5 Effect of P(NIPAm-co-SBMA) Microgels Addition into Humic Acid Solution on Fouling Removal from PES/PVP Membrane

P(NIPAm-co-SBMA) microgels were added into HA feed, series filtrations were performed with PES/PVP blend membranes at room temperature where microgels are swollen, and cleanings were done via heating above LCST (procedure 2). Also, a set of series experiment was done without any change in temperature stimuli in order to see the effect of exposure to changing stimulus intensity on fouling removal. For HA feed, the same procedure was not repeated since it has been already seen that temperature had no effect on fouling removal of HA from PES/PVP blend membranes in previous section. Rejections of HA and HA with P(NIPAm-co-SBMA) were around 83 and 86 % (Appendix C). Concentration of P(NIPAm-co-SBMA) microgels were 0.01 g/L.

Filtration flux ratio was observed as only 90% with microgels whereas flux decreased to 79% of initial pure water flux with only HA at the end of filtration (Figure 3.26). It is possibly because of antifouling effect of the microgels due to zwitterions in the structure. They create hydration layer around them and cause low resistant cake layer with their existence in it. Also, fouling resistances were seen as similar for both cases (Figure 3.27). Yet, filtrations with HA feed ended in rising reversible and irreversible fouling during continuous filtration cycles like in the experiments with PES membrane since it could not be cleaned at all and accumulated on the membrane surface with further filtrations. At the end of series filtrations, flux recoveries were found as 99 and 91% with and without microgels, respectively, when procedure 2 was applied but it was 96% for microgel added filtration when cleaning was performed at room temperature (Figure 3.26 and Table 3.10). Fouling could not be removed without temperature stimulus in presence of P(NIPAm-co-SBMA) after 1st cleaning. After that, applying extra cleaning (again by just mixing without temperature increase), more efficient cleaning was achieved than HA experiment but cleaning via changing temperature stimulus had still higher efficiency than this case.

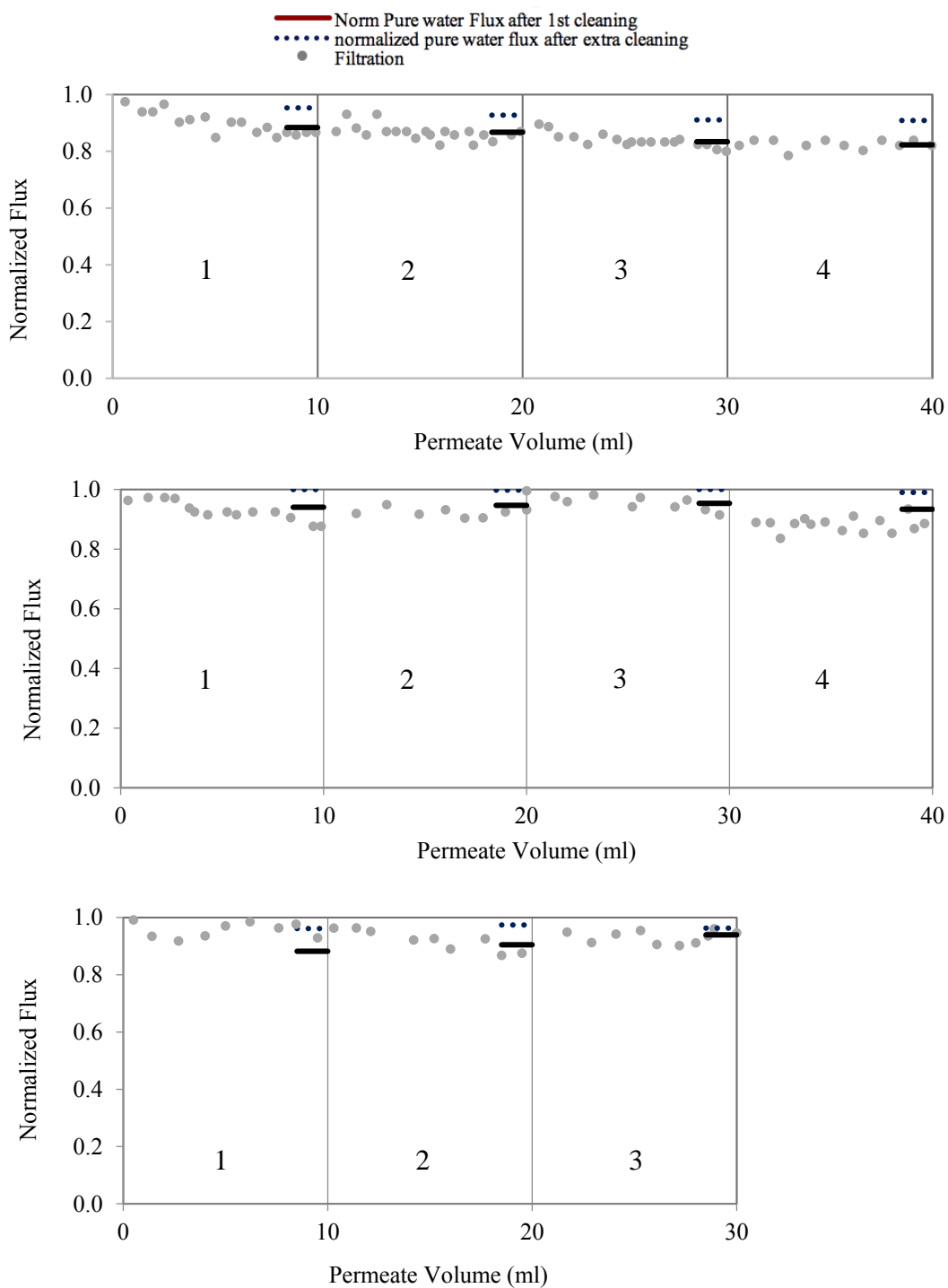


Figure 3.26 Normalized flux graphs of the series filtrations with PES/PVP blend membranes from top to bottom: HA filtration at room T and cleaning via heating above LCST (procedure 2), HA and 0.01 g/L p(NIPAm) microgels filtration at room T and cleaning via heating above LCST (procedure 2), and HA and 0.01 g/L p(NIPAm) microgels filtration at room T and cleaning at room T

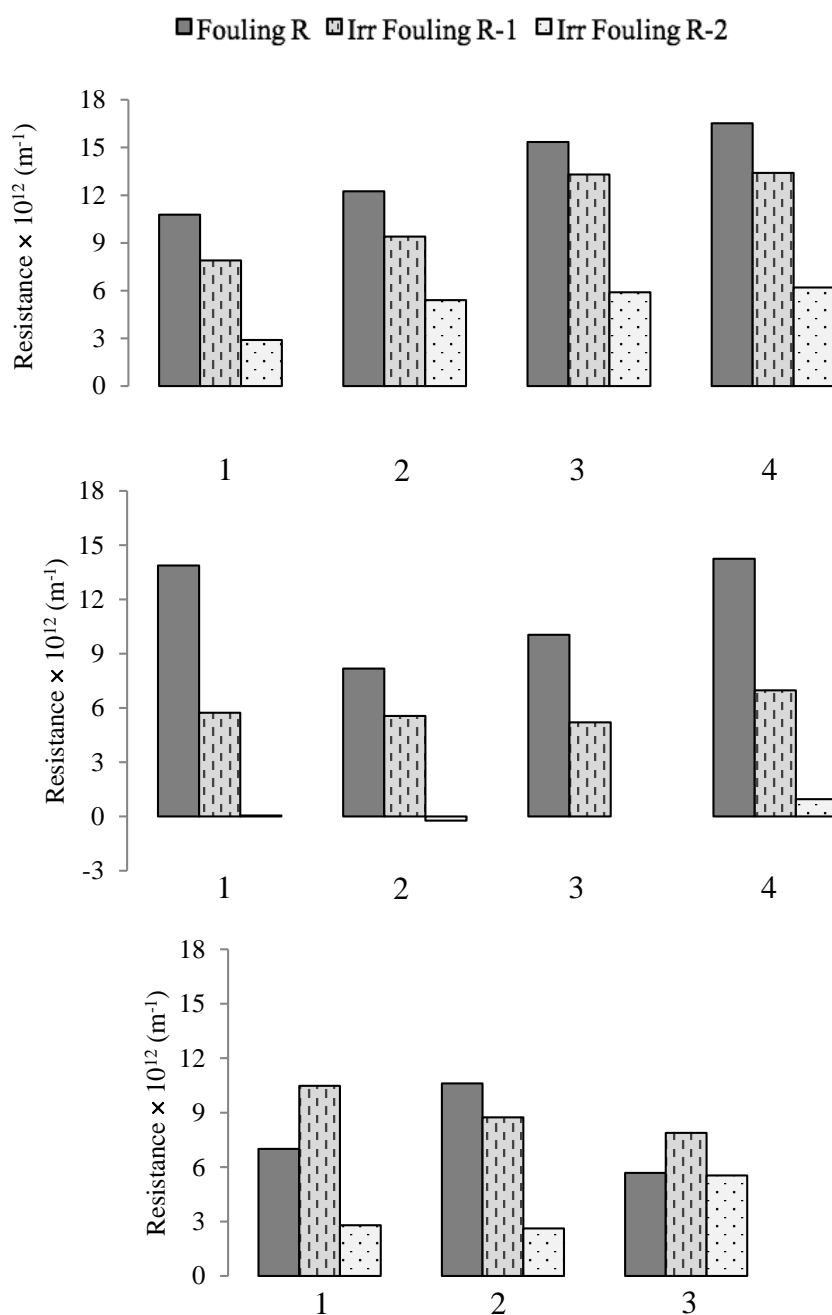


Figure 3.27 Fouling resistances of filtrations in pure water with PES/PVP membrane: HA solution and cleaning with temperature stimulus (top); HA and P(NIPAm-co-SBMA) microgels solution and cleaning with temperature stimulus (middle); HA and P(NIPAm-co-SBMA) microgels solution and cleaning without response (bottom)

Table 3.10 Filtration flux ratios and flux recoveries of HA with and without 0.01 g/L P(NIPAm-co-SBMA) microgels filtration at room T with PES/PVP blend membrane and cleaning via heating above LCST (procedure 2) and cleaning at room T

HA (Heating above LCST)			
Filt.	FFR %	FR – 1 %	FR – 2 %
1	85	89	93
2	84	87	92
3	80	82	91
4	79	82	91

HA + P(NIPAm-co-SBMA) (Heating above LCST)			
Filt.	FFR %	FR – 1 %	FR – 2 %
1	87	94	100
2	92	95	100
3	91	95	100
4	88	93	99

HA + P(NIPAm-co-SBMA) (Cleaning at room temperature)			
Filt.	FFR %	FR – 1 %	FR – 2 %
1	91	87	95
2	89	91	98
3	96	94	96

PES/PVP membrane photographs after 1st and extra cleaning also support the filtration data in terms of positive effect of microgel addition (Figure 3.28). In presence of microgel, cake formation was also seen to appear. However, lower and fouling resistance occurred since P(NIPAm-co-SBMA) microgels possibly weaken the hydrophobic interactions between foulants.

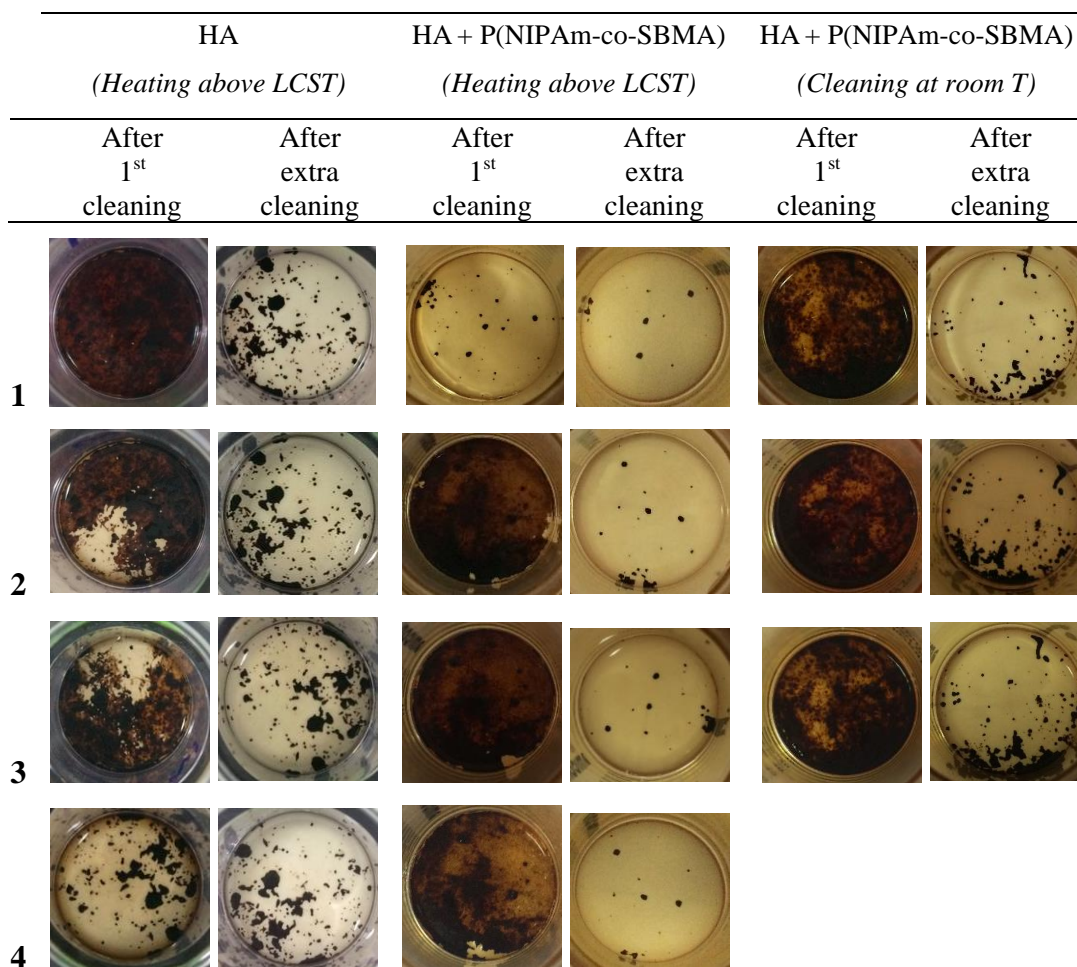


Figure 3.28 PES/PVP membrane photographs after 1st and extra cleaning of HA solution filtration with and without 0.01 g/L P(NIPAm-co-SBMA) microgels, cleaning via heating above LCST (procedure 2) and cleaning at room T

Also, more hydrophilic structure of PES/PVP membrane compared to PES membrane brought less and better recovery in general.

To sum up, addition of P(NIPAm-co-SBMA) microgels into HA feed solution provided less during filtration. These microgels enabled almost complete fouling removal by cleaning with temperature stimulus for PES/PVP membrane. Moreover, presence of P(NIPAM-co-SBMA) in the feed solution ensured less during filtration and higher flux recovery after cleaning compared to presence of the same amount of P(NIPAM) microgels in the feed. Therefore, PES/PVP membranes can be used more and more times with P(NIPAm-co-SBMA) microgels by applying temperature stimulus for cleaning.

3.3.6 Effect of P(NIPAm-co-SBMA) Microgels Addition into Humic Acid Solution on Fouling Removal from PES/PVP Membrane in 0.5 M NaCl Solution

In this set of experiments, filtrations were performed at room temperature in 0.5 M NaCl medium, while cleaning was done in pure water at 38°C (procedure 2). Only 1st cleaning was applied here. Rejections were calculated in between 70 – 75 and 75 – 80 % for the filtrations of HA alone and HA with P(NIPAm-co-SBMA), respectively (Appendix C). Fluxes decreased more than in pure water for both feeds. However, the difference in flux recoveries between microgel-free and microgel-added cases were more apparent in 0.5 M NaCl than in pure water. (Figure 3.29). Filtration flux ratio was around 68% for HA feed at the end while flux recovery did not exceed 80%. On the other hand, flux declined to 77% of initial pure water flux and better flux recovery was achieved than only HA filtration but complete flux recovery was not achieved with microgels like in pure water (Table 3.11). It can be seen from

Figure 3.30 that higher amount of fouling could be removed in the presence of microgels whereas most of the fouling was remained as irreversible after cleaning in only HA filtration.

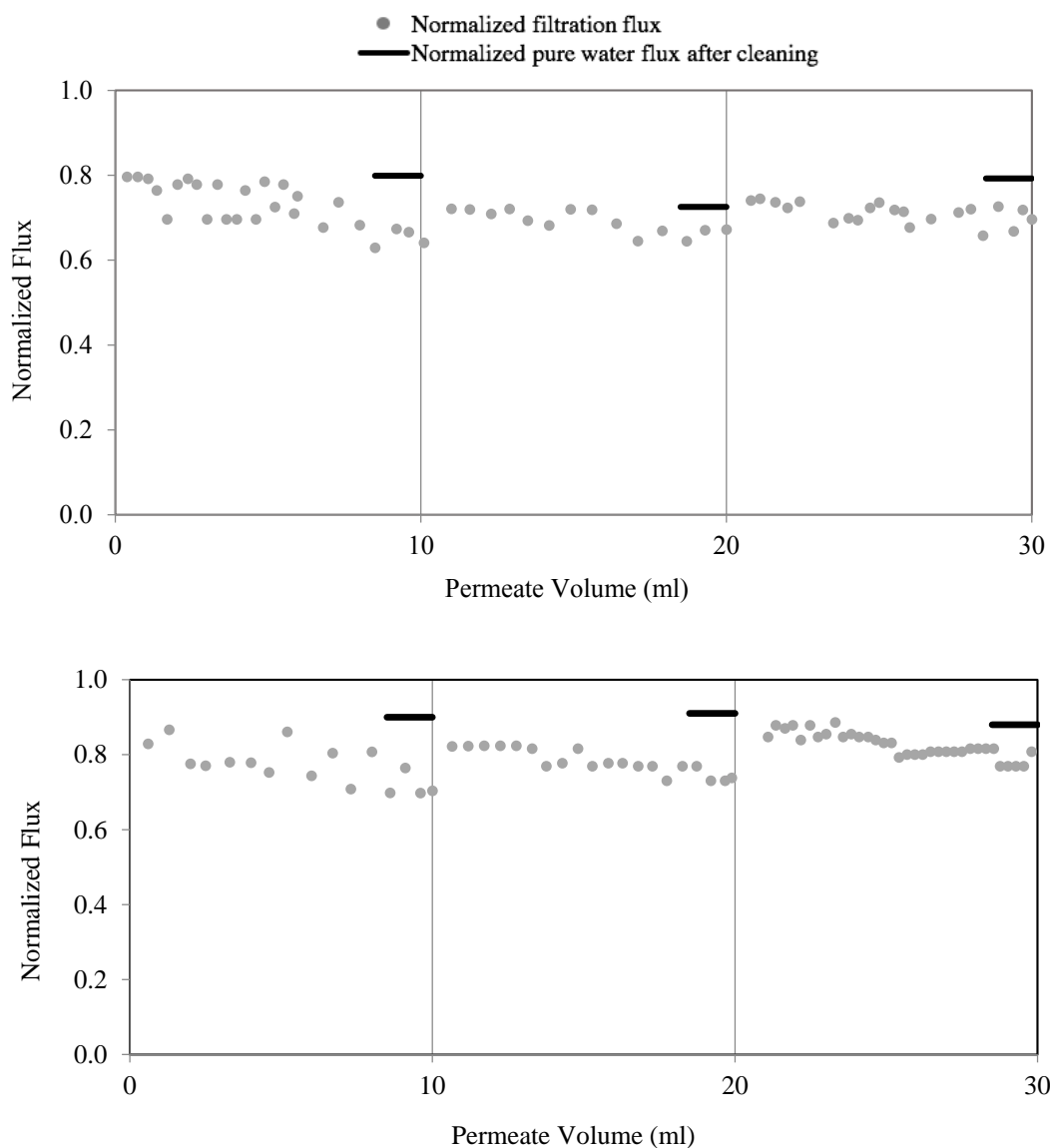


Figure 3.29 Normalized flux graphs of HA (top) and HA with P(NIPAm-co-SBMA) microgels (bottom) filtrations in 0.5 M NaCl with PES/PVP blend membranes at room T and cleaning via heating above LCST (procedure 2)

In addition to these results, comparison of microgel usage in pure water and 0.5 M NaCl solution showed that filtration flux ratio and cleaning efficiency was higher in pure water experiments. This is most probably due to reduced hydration at high ionic strength which results in loss of antifouling properties of the microgels. Still, it can

be a useful information to know better fouling removal effect of P(NIPAm-co-SBMA) microgels in 0.5 M NaCl solution where HA gelation became more serious for membrane operation with increasing amount of salt.

Table 3.11 Filtration flux ratios and flux recoveries of HA and HA with P(NIPAm-co-SBMA) microgels filtrations in 0.5 M NaCl with PES/PVP blend membranes at room T and cleaning via heating above LCST (procedure 2)

Filt.	HA		HA + P(NIPAm-co-SBMA)	
	FFR %	FR %	FFR %	FR %
1	65	80	70	90
2	65	73	73	91
3	68	79	77	88

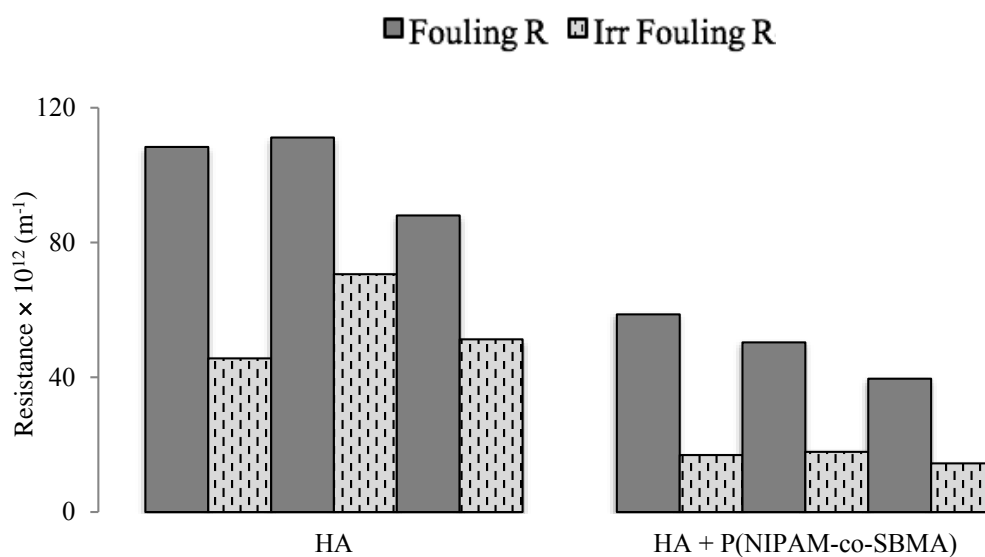


Figure 3.30 Fouling and irreversible fouling resistances of HA with P(NIPAm-co-SBMA) microgels (left) and HA (right) filtrations in 0.5 M NaCl with PES/PVP blend membranes at room T and cleaning via heating above LCST (procedure 2)

3.3.7 Cleaning of similar fouling resistances

Humic acid filtrations ended up with different fouling resistances in microgel free and microgel added cases for the same amount of permeate. Presence of P(NIPAM-co-SBMA) microgels brought less fouling resistance with PES/PVP membrane due to its antifouling properties that lowers the membrane-foulant and foulant-foulant interactions during filtrations. Then, filtrations were performed until the fouling resistances reached similar values in order to see how much fouling removal can be obtained for the same fouling resistance. Here, procedure 2 was applied.

Filtration of HA with P(NIPAm-co-SBMA) was continued until its fouling resistance reached a similar value with the standard (std) HA experiments as shown in Figure 3.31(a). Then, that experiment was named as *high resistance (high R)* since it had higher fouling resistance than its own standard experiments. On the other hand, filtration of HA was stopped when fouling resistance of standard filtration of HA with P(NIPAm-co-SBMA) was reached as shown in Figure 3.31(b). Then, it was called as *low resistance (low R)* due to the same reasoning. To sum up, two separate fouling resistance values were analyzed in these experiments around 20×10^{12} and 36×10^{12} m^{-1} for *low* and *high resistance* filtrations, respectively.

Fouling resistance was completely removed after extra cleaning and 70 % of it was cleaned just after 1st cleaning in the standard experiment with HA feed containing P(NIPAm-co-SBMA) microgels while only 45 % of fouling resistance could be removed after extra cleaning for the *low R* experiment of HA filtration. It showed that use of the microgels provided more efficient cleaning. On the other hand, only 70 % of fouling resistance was removed with addition of P(NIPAm-co-SBMA) microgels in the *high R* experiment. Still, it had better cleaning performance when compared to the standard HA filtration which had the same fouling resistance with the *high R*. Also, it was observed that applying only 1st cleaning did not work to remove fouling but cyclic cleaning was needed for efficient cleaning with P(NIPAm-co-SBMA) microgels in *high R* case.

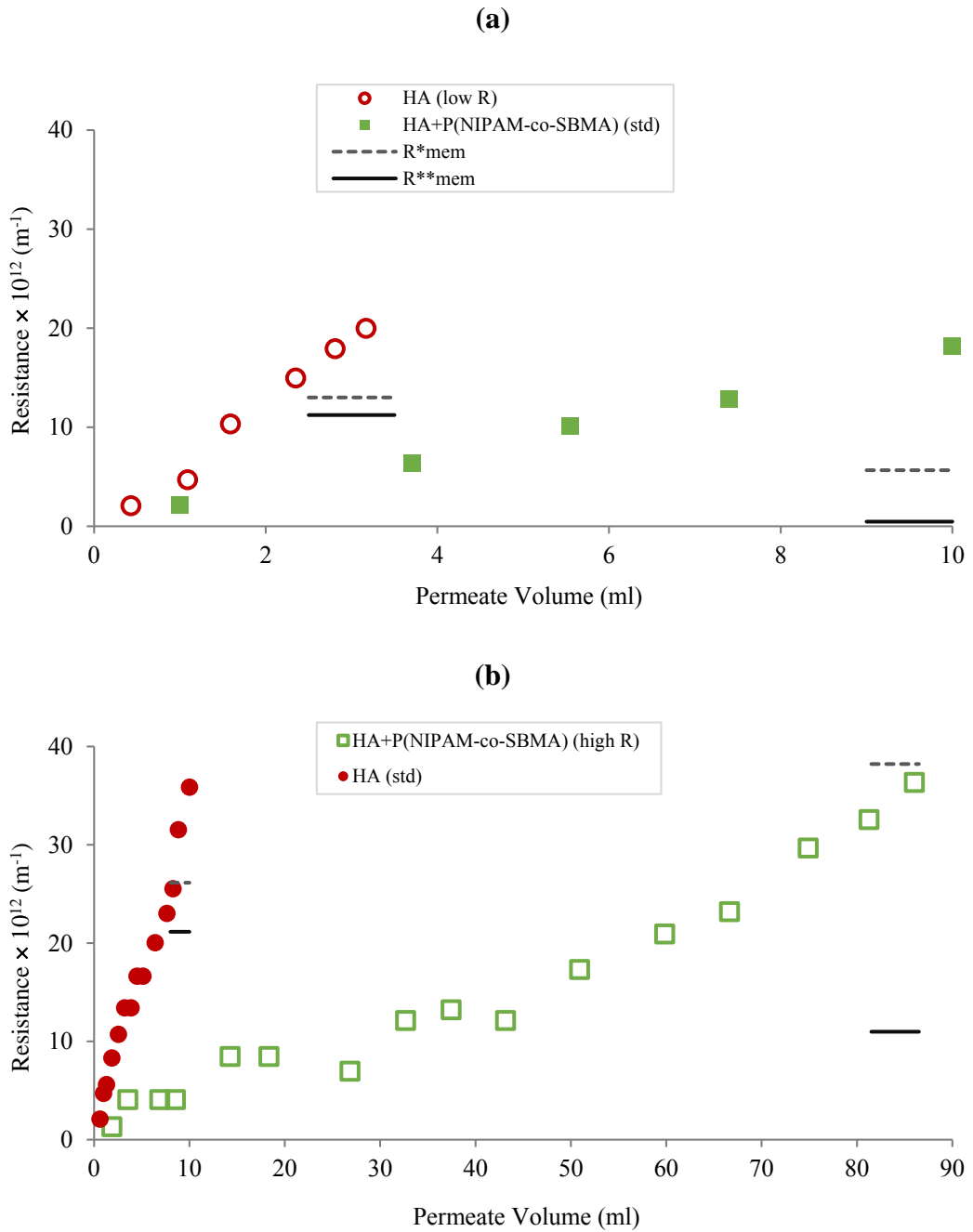


Figure 3.31 Comparison of fouling and irreversible fouling resistances graphs of (a) standard (std) HA + P(NIPAM-co-SBMA) microgels filtration and low R filtration of HA filtrations and (b) std HA filtration and high R HA + P(NIPAM-co-SBMA) microgels filtrations with procedure 2

When the cleaning performances were compared for the same feed but different fouling resistances, it was seen that lower deposition brought higher cleaning efficiency for both feed in terms of fouling resistances. Additionally, their rejections were seen as similar with the other cases and each other. They were found as 80 and 81 % for *low R* and *high R*, respectively (Appendix C).

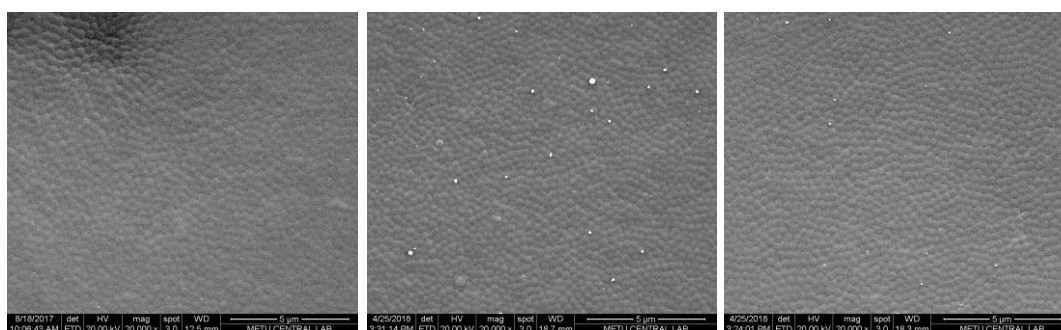
3.3.8 SEM Results of microgel depositions

P(NIPAm) and P(NIPAm-co-SBMA) microgels were deposited on PES and PES/PVP blend membranes at room temperature. And, cleaning via heating above LCST and cleaning at room temperature were applied separately to microgel deposited membranes. SEM images of these experiments are given in Figure 3.32 to gain insight on microgels-membrane interactions.

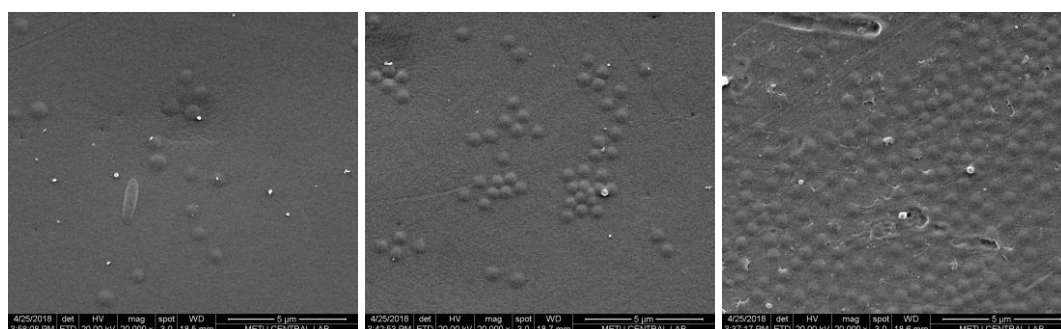
Both microgels were deposited and seen to be present on the membrane surfaces for each case. They were seen on the membrane surface after cleaning without any stimulus as monolayer in Figure 3.32 (bottom). P(NIPAm-co-SBMA) microgels hold on to both surface but then they were removed more from PES/PVP blend membrane than PES by giving stimuli change. Also, P(NIPAm) and P(NIPAm-co-SBMA) microgels gave similar images to each other for both cleaning at room temperature and cleaning via heating above LCST. However, it was observed that P(NIPAm-co-SBMA) microgels made a positive contribution to Filtration flux ratios and flux recoveries while P(NIPAm) did not, despite the higher volume change with temperature change. It may be explained as the microgel-foulant (HA) interaction is stronger with P(NIPAm) and weaker with P(NIPAm-co-SBMA) such that despite the higher volume change and similar microgel-membrane interaction, P(NIPAm) microgels increase fouling and do not make it more reversible. Besides that, presence of P(NIPAm-co-SBMA) in the cake layer among HA also may prevent humic acid gelation.

P(NIPAm)	P(NIPAm-co-SBMA)	
PES/PVP	PES/PVP	PES

Deposition of microgels



Cleaning via heating above LCST



Cleaning at room T

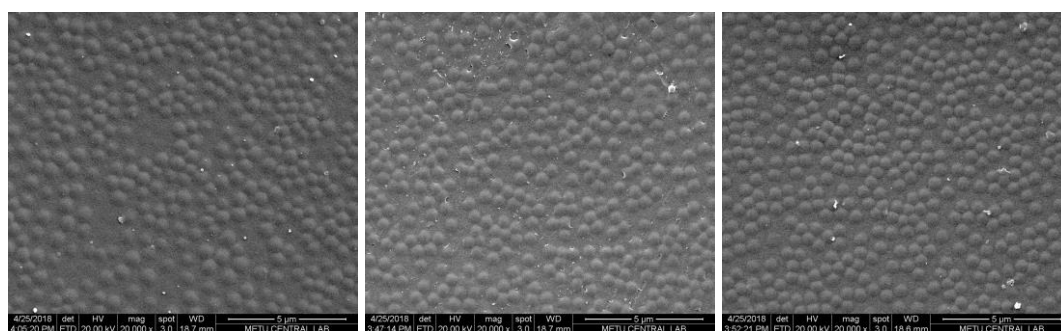


Figure 3.32 SEM images of PES and PES/PVP blend membranes with the microgels after deposition, cleaning via heating above LCST and cleaning at room temperature

3.4 Adsorption Tests

Adsorption experiments were performed in order to explain the contribution of adsorption on membrane fouling and to understand the interactions of foulant-membrane, foulant-microgel and microgel-membrane. It was important because accumulation on the surface is the target fouling for adding microgels into the feed rather than adsorptive fouling.

From Table 3.12, it was observed that PES membrane adsorbs more HA ($26.9 \pm 5.2 \mu\text{g}/\text{cm}^2$) than PES/PVP blend one ($3.3 \pm 2.6 \mu\text{g}/\text{cm}^2$) as expected since it is a more hydrophobic membrane and prone to adsorb solutes more. These results support less flux declines and fouling resistances with PES/PVP membranes. Also, it was seen that there was a sharp decline in flux of PES membrane at the beginning of the filtration whereas the filtration flux of PES/PVP membrane started to decrease slowly from the pure water flux by looking at normalized flux versus permeate volume graphs (Figure 3.33). That sharp decline points at adsorptive fouling on PES membrane.

From Table 3.13, it is seen that PES membrane adsorbs BSA ($69.8 \pm 17.9 \mu\text{g}/\text{cm}^2$) more as compared to PES/PVP blend membrane ($8.6 \pm 2.3 \mu\text{g}/\text{cm}^2$) as similar to HA results. It is again because the blend one is more hydrophilic. PES membrane adsorbs similar amount of BSA in presence of P(NIPAM) microgels in the solution ($68.6 \pm 11.0 \mu\text{g}/\text{cm}^2$). In BSA tests, PES membrane whose surface was covered with P(NIPAm) microgels adsorbs higher amount of BSA on its surface than neat PES membrane ($107.9 \pm 7.7 \mu\text{g}/\text{cm}^2$). Then, it can be inferred that foulant-microgel interaction is more powerful than foulant-membrane interaction in the cake layer.

Adsorption of BSA was not affected by presence of P(NIPAm) microgels in the medium. In these adsorption experiments with P(NIPAm) microgels, BSA was separated from the microgels by syringe filter to measure its concentration. However, adsorption experiments were not performed with BSA-P(NIPAm-co-SBMA), HA-P(NIPAm), and HA-P(NIPAm-co-SBMA) couples because 1st one was not used

together in performance tests and HA could not be separated from the microgels by syringe filter for the other two couple due to its poly-disperse structure.

Table 3.12 Adsorption of Humic Acid on PES and PES/PVP blend membranes

Adsorption of H on	$\mu\text{g}/\text{cm}^2$
PES membrane	26.9 ± 5.2
PES/PVP membrane	3.3 ± 2.6

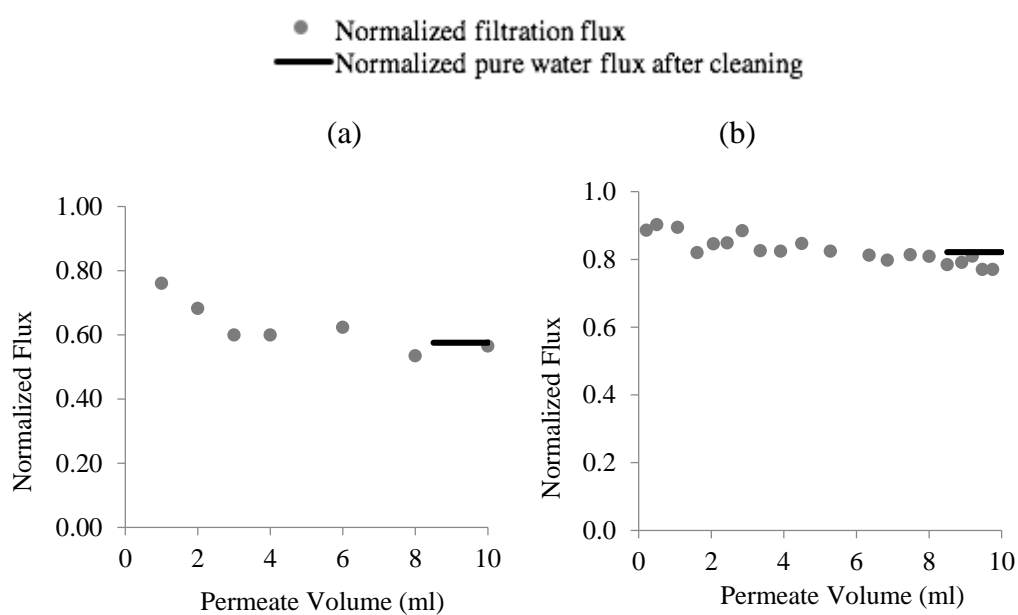


Figure 3.33 Humic acid filtrations with (a) PES and (b) PES/PVP membrane

The results of adsorption experiments are consistent with the filtration data of BSA, too. Figure 3.34 (a) and (b) are the sample graphs that show the filtrations of BSA with PES membrane and PES/PVP blend membranes, respectively. It is seen that flux decreases rapidly at the very beginning of the filtration with PES membrane while

there is a little decline in flux with PES/PVP blend membrane for the same permeate volume. Hence, it can be said that PES/PVP membranes adsorbs humic acid and BSA less than PES membranes in general.

Table 3.13 Adsorption of BSA on PES membrane with and without P(NIPAM) microgels, and on PES/PVP membrane

Adsorption of BSA on	$\mu\text{g}/\text{cm}^2$
PES membrane	69.8 ± 17.9
PES membrane in presence of P(NIPAM) microgels	68.6 ± 11.0
PES membrane with P(NIPAM) microgels deposited	107.9 ± 7.7
PES/PVP membrane	8.6 ± 2.3

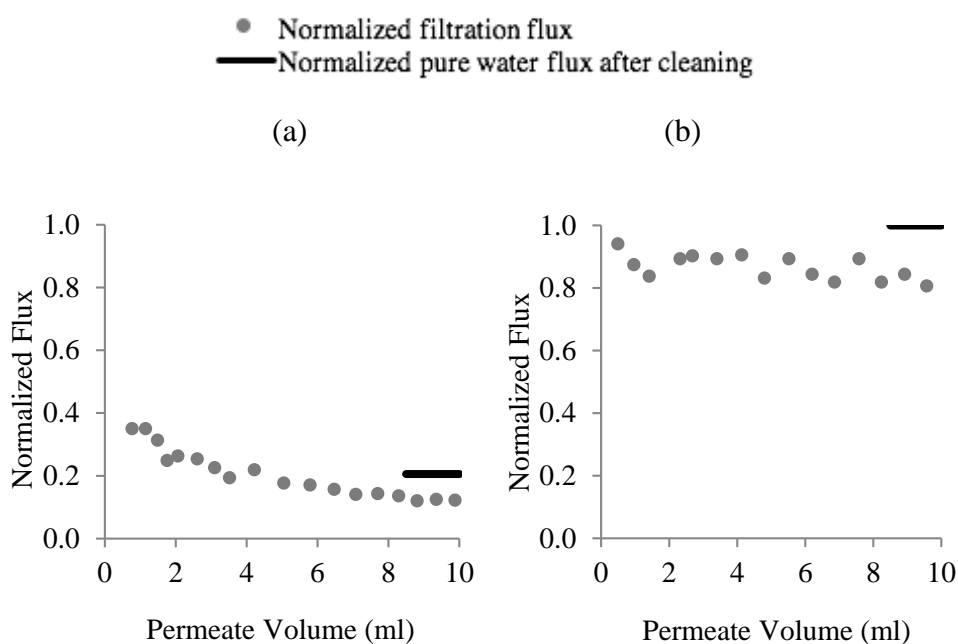


Figure 3.34 BSA filtration with (a) PES and (b) PVP- PES membrane

Adsorption of P(NIPAm) microgels on PES and PES/PVP blend membranes were found similar to each other (Table 3.14). It means that membrane-microgel interaction are not different for these two membranes with P(NIPAm).

Table 3.14 Adsorption of P(NIPAm) on PES and PES/PVP blend membranes

Adsorption of P(NIPAm) on	$\mu\text{g}/\text{cm}^2$
PES membrane	9.4 ± 15.9
PES/PVP membrane	11.5 ± 8.8

CHAPTER 4

CONCLUSION

This study focused on fouling removal via addition of temperature and ionic-strength responsive polymeric microgels into feed solutions during membrane filtrations. They were deposited into fouling layer in swollen or collapsed phase and cleaning was performed in collapsed or swollen phase, respectively, with the help of changing appropriate stimuli. Effect of responsive microgels on fouling removal was studied recently in literature with addition of responsive polymers into membrane matrix or grafting membrane surface with these microgels generally. It was reported that these approaches made membrane antifouling and/or rendered fouling more cleanable with changing hydrophilic interactions, pore sizes or moving surface. In this study, however, it was suggested that the microgels freely be located in all over the cake layer by adding them into feed and then to make it easily removable by the help of volume change of the microgels under favor of an appropriate stimuli. By this way, it could weaken and/or break fouling layer and accordingly increase the cleaning efficiency. This approach is applicable to exiting membrane systems and it could be an effective way to clean the fouling layer distant from the membrane surface.

Synthesized microgels swelling ratio were calculated as 2.9 and 2.1 and LCST were observed as 32 and 29°C for p(NIPAm) and p(NIPAm-co-SBMA), respectively. Comparison of performance tests showed that p(NIPAm-co-SBMA) microgels addition provided higher efficiency for fouling removal for HA filtration with both PES and PES/PVP blend membranes while p(NIPAm) did not affect flux recovery in any way at all for BSA and HA with the same membranes. In the presence of p(NIPAm-co-SBMA) microgels with PES/PVP blend membranes, HA fouling could be removed totally from membrane surface in pure water but around 90% of flux was recovered in presence of 0.5 M NaCl. On the other hand, only 60, 92 and 80% of

fluxes were recovered in filtrations with PES membrane in pure water. For similar fouling resistances with PES/PVP membranes, better fouling removal was achieved.

To conclude, use of p(NIPAm-co-SBMA) microgels into feed brought lower flux decline, higher flux recovery and more efficient fouling removal than only HA filtration in pure water with both PES and PES/PVP blend membranes. In the presence of salt, cleaning performance was good but filtration flux ratio was similar to the only HA filtration. As a major result, it can be said that P(NIPAm-co-SBMA) addition provides a promising cleaning method for fouling removal and this gives an opportunity to use the same membrane more and more times. Accordingly, we expected to bring lower operating cost and longer membrane lifetime with its anti-fouling nature.

REFERENCES

- Arkhangelsky, E., Kuzmenko, D., & Gitis, V. (2007). Impact of chemical cleaning on properties and functioning of polyethersulfone membranes. *Journal of Membrane Science*, 305(1-2), 176-184.
- Arndt, K., Schmidt, T., & Reichelt, R. (2001). Thermo-sensitive poly(methyl vinyl ether) micro-gel formed by high energy radiation. *Polymer*, 42(16), 6785-6791.
- Baker, R. (2004). *Membranes and Modules. Membrane Technology and Applications* (2nd ed., pp. 89-155). Chichester: J. Wiley.
- Basri, H., Ismail, A., & Aziz, M. (2011). Polyethersulfone (PES)–silver composite UF membrane: Effect of silver loading and PVP molecular weight on membrane morphology and antibacterial activity. *Desalination*, 273(1), 72-80.
- Burmistrova, A., Richter, M., Eisele, M., Üzüüm, C., & Klitzing, R. V. (2011). The Effect of Co-Monomer Content on the Swelling/Shrinking and Mechanical Behaviour of Individually Adsorbed PNIPAM Microgel Particles. *Polymers*, 3(4), 1575-1590.
- Burmistrova, A., Richter, M., Uzum, C., & Klitzing, R. V. (2011). Effect of cross-linker density of P(NIPAM-co-AAc) microgels at solid surfaces on the swelling/shrinking behaviour and the Young's modulus. *Colloid and Polymer Science*, 289(5-6), 613-624.
- Byeongmoon, J., & Anna, G. (2002). Lessons from nature: Stimuli-responsive polymers and their biomedical applications. *Trends in Biotechnology*, 20(8), 360.
- Chede, S., & Escobar, I. C. (2015). Fouling Control Using Temperature Responsive N-isopropylacrylamide (NIPAAm) Membranes. *Environmental Progress & Sustainable Energy*, 35, 416-427.

- Chen, J., Kim, S., & Ting, Y. (2003). Optimization of membrane physical and chemical cleaning by a statistically designed approach. *Journal of Membrane Science*, 219 (1-2), 27-45.
- Chen, T., Ferris, R., Zhang, J., Ducker, R., Zauscher, S. 2010. "Stimulus-responsive polymer brushes on surfaces: Transduction mechanisms and applications", *Progress in Polymer Science (Oxford)*, 35 (1-2), 94-112.
- Chen, Y., Xie, R., & Chu, L. (2013). Stimuli-responsive gating membranes responding to temperature, pH, salt concentration and anion species. *Journal of Membrane Science*, 442, 206-215.
- Das, M., Kumacheva, E., & Sanson, N. (2008). Zwitterionic Poly(betaine-N-isopropylacrylamide) Microgels: Properties and Applications. *Chemistry of Materials*, 20, 7157-7163.
- Das, M., Kumacheva, E., & Sanson, N. (2008). Zwitterionic Poly(betaine-N-isopropylacrylamide) Microgels: Properties and Applications. *Chemistry of Materials*, 20, 7157-7163.
- Du, C., Deng, D., Shan, L., Wan, S., Cao, J., Tian, J., Achilefu, S., Gu, Y. (2013). A pH-sensitive doxorubicin prodrug based on folate-conjugated BSA for tumor-targeted drug delivery. *Biomaterials*, 34(12), 3087-3097.
- Fröhlich, Holger, et al. "Membrane Technology in Bioprocess Science." *Chemie Ingenieur Technik*, Mar. 2012.
- Gandhi, A., Paul, A., Sen, S. O., & Sen, K. K. (2015). Studies on thermoresponsive polymers: Phase behaviour, drug delivery and biomedical applications. *Asian Journal of Pharmaceutical Sciences*, 10(2), 99-107.
- Gençal, Y., Durmaz, E.N., Çulfaz-Emecen, P.Z. (2014). "Preparation of patterned microfiltration membranes and their performance in crossflow yeast filtration", *Journal of Membrane Science*, 476, 224-233.

- Goosen, M.F., Sasblani, S.S., Al-Hinai, H., Al-Obeidani, S., Al-Belushi, R., & Jackson, D. (2004). Fouling of Reverse Osmosis and Ultrafiltration Membranes: A Critical Review. *Separation Science and Technology*, 39, 2261-2297.
- Gorey, C. & Escobar, I. C. (2011). N-isopropylacrylamide (NIPAAM) modified cellulose acetate ultrafiltration membranes. *Journal of Membrane Science*, 383, 272-279.
- Han, Z., Cheng, C., Zhang, L., Luo, C., Nie, C., Deng, J., Zhao, C. (2014). Toward robust pH-responsive and anti-fouling composite membranes via one-pot in-situ cross-linked copolymerization. *Desalination*, 349, 80-93.
- Huisman, I. H., Prádanos, P., & Hernández, A. (2000). The effect of protein–protein and protein–membrane interactions on membrane fouling in ultrafiltration. *Journal of Membrane Science*, 179(1-2), 79-90.
- Jönsson, C., & Jönsson, A. (1995). Influence of the membrane material on the adsorptive fouling of ultrafiltration membranes. *Journal of Membrane Science*, 108(1-2), 79-87.
- Kaner, P., Rubakh, E., Kim, D. H., & Asatekin, A. (2017). Zwitterion-containing polymer additives for fouling resistant ultrafiltration membranes. *Journal of Membrane Science*, 533, 141-159.
- Lee, N., Amy, G., Croué, J., & Buisson, H. (2004). Identification and understanding of fouling in low-pressure membrane (MF/UF) filtration by natural organic matter (NOM). *Water Research*, 38(20), 4511-4523.
- Li, J., Wang, T., Wu, D., Zhang, X., Yan, J., Du, S., Guo, Y., Wang, J., Zhang, A. (2008). Stimuli-Responsive Zwitterionic Block Copolypeptides: Poly(N-isopropylacrylamide)-block-poly(lysine-co-glutamicacid). *Biomacromolecules*, 9(10), 2670-2676.

- Li, D., Zhang, X., Yao, J., Simon, G. P., & Wang, H. (2011). Stimuli-responsive polymer hydrogels as a new class of draw agent for forward osmosis desalination. *Chemical Communications*, 47(6), 1710.
- Liang, X., Liu, F., Kozlovskaya, V., Palchak, Z., & Kharlampieva, E. (2015). Thermoresponsive Micelles from Double LCST-Poly(3-methyl-N-vinylcaprolactam) Block Copolymers for Cancer Therapy. *ACS Macro Letters*, 4(3), 308-311.
- M.M. Dal-Cin, C.N. Striez, T.A. Tweddle, C.E. Capes, F. McLellan and H. Buisson, Effect of adsorptive fouling on membrane performance: case study with a pulp mill effluent, *Desalination*, 101 (1995) 155-167.
- Madaeni, S. S., Mohamamdi, T., & Moghadam, M. K. (2001). Chemical cleaning of reverse osmosis membranes. *Desalination*, 134(1-3), 77-82.
- Majorek, K. A., Porebski, P. J., Dayal, A., Zimmerman, M. D., Jablonska, K., Stewart, A. J., Chruszcz, M., Minor, W. (2012). Structural and immunologic characterization of bovine, horse, and rabbit serum albumins. *Molecular Immunology*, 52(3-4), 174-182.
- Marselina, Y., Le-Clech, P., Stuetz, R., Chen, V. 2008. "Detailed characterisation of fouling deposition and removal on a hollow fibre membrane by direct observation technique", *Desalination*, 231 (1-3), 3-11.
- Meng, J., Cao, Z., Ni, L., Zhang, Y., Wang, X., Zhang, X., & Liu, E. (2014). A novel salt-responsive TFC RO membrane having superior antifouling and easy-cleaning properties. *Journal of Membrane Science*, 461, 123-129.
- Na, J., & Y. Z. (2011). The Effect of Humic Acid on Ultrafiltration Membrane Fouling. *Energy Procedia*, 11, 4821-4829.
- Nyström, M., Ruohomäki, K., & Kaipia, L. (1996). Humic acid as a fouling agent in filtration. *Desalination*, 106(1-3), 79-87.

- Obiweluozor, F. O., Ghavaminejad, A., Hashmi, S., Vatankhah-Varnoosfaderani, M., & Stadler, F. J. (2014). A NIPAM-Zwitterion Copolymer: Rheological Interpretation of the Specific Ion Effect on the LCST. *Macromolecular Chemistry and Physics*, 215(21), 2125-2125.
- Paolis, F. D., & Kukkonen, J. (1997). Binding of organic pollutants to humic and fulvic acids: Influence of pH and the structure of humic material. *Chemosphere*, 34(8), 1693-1704.
- Pelton, R. 2000. "Temperature-sensitive aqueous microgels", *Advances in Colloid and Interface Science*, 85 (1), 1-33.
- Qiu, Y., Park, K. 2012. "Environment-sensitive hydrogels for drug delivery", *Advanced Drug Delivery Reviews*, 64 (SUPPL.), 49-60.
- Razi, F., Sawada, I., Ohmukai, Y., Maruyama, T., & Matsuyama, H. (2012). The improvement of antibiofouling efficiency of polyethersulfone membrane by functionalization with zwitterionic monomers. *Journal of Membrane Science*, 401-402, 292-299.
- Reis, R. V., & Zydney, A. "Bioprocess Membrane Technology." *Journal of Membrane Science*, vol. 297, no. 1-2, May 2007, pp. 16–50.
- Roche, M., Rondeau, P., Singh, N. R., Tarnus, E., & Bourdon, E. (2008). The antioxidant properties of serum albumin. *FEBS Letters*, 582(13), 1783-1787.
- Roy, D., Brooks, W. L., & Sumerlin, B. S. (2013). New directions in thermoresponsive polymers. *Chemical Society Reviews*, 42(17), 7214.
- Rubio-Retama, J., Zafeiropoulos, N. E., Frick, B., Seydel, T., & López-Cabarcos, E. (2010). Investigation of the Relationship between Hydrogen Bonds and Macroscopic Properties in Hybrid Core–Shell γ -Fe₂O₃–P(NIPAM-AAS) Microgels. *Langmuir*, 26(10), 7101-7106.

- Salgın, S., Takaç, S., & Özdamar, T. H. (2006). Adsorption of bovine serum albumin on polyether sulfone ultrafiltration membranes: Determination of interfacial interaction energy and effective diffusion coefficient. *Journal of Membrane Science*, 278(1-2), 251-260.
- Schmaljohann, D. (2006). Thermo- and pH-responsive polymers in drug delivery. *Advanced Drug Delivery Reviews*, 58(15), 1655-1670.
- Sutton, R., & Sposito, G. (2005). Molecular Structure in Soil Humic Substances: The New View. *Environmental Science & Technology*, 39(23), 9009-9015.
- van de Ven, W. J. C. (2008). *Towards optimal saving in membrane operation*
Enschede
- Wang, H., Yu, T., Zhao, C., & Du, Q. (2008). Improvement of hydrophilicity and blood compatibility on polyethersulfone membrane by adding polyvinylpyrrolidone. *Fibers and Polymers*, 10(1), 1-5.
- Wang, Z., Ma, J., Tang, C., Kimura, K., Wang, Q., & Han, X. (2014). Membrane cleaning in membrane bioreactors: A review. *Journal of Membrane Science*, 468, 276-307.
- Wavhal, D. S., & Fisher, E. R. (2002). Hydrophilic modification of polyethersulfone membranes by low temperature plasma-induced graft polymerization. *Journal of Membrane Science*, 209(1), 255-269.
- Werber, Jay R., et al. "Materials for next-Generation Desalination and Water Purification Membranes." *Nature Reviews Materials*, 2016.
- Wienk, I., Boom, R., Beerlage, M., Bulte, A., Smolders, C., & Strathmann, H. (1996). Recent advances in the formation of phase inversion membranes made from amorphous or semi-crystalline polymers. *Journal of Membrane Science*, 113(2), 361-371.

- Yu, S., Chen, Z., Liu, J., Yao, G., Liu, M., & Gao, C. (2011). Intensified cleaning of organic-fouled reverse osmosis membranes by thermo-responsive polymer. *Journal of Membrane Science*, 392, 181-191.
- Yu, S., Liu, X., Liu, J., Wu, D., Liu, M., & Gao, C. (2010). Surface modification of thin-film composite polyamide reverse osmosis membranes with thermo-responsive polymer (TRP) for improved fouling resistance and cleaning efficiency. *Separation and Purification Technology*, 76, 283-291.
- Yuan, W., & Zydney, A. L. (2000). Humic Acid Fouling during Ultrafiltration. *Environmental Science & Technology*, 34(23), 5043-5050.
- Yuan, Z., & Dan-Li, X. (2008). Porous PVDF/TPU blends asymmetric hollow fiber membranes prepared with the use of hydrophilic additive PVP (K30). *Desalination*, 223(1-3), 438-447.
- Zhao, Y., Bai, T., Shao, Q., Jiang, S., & Shen, A. Q. (2015). Thermoresponsive self-assembled NiPAm-zwitterion copolymers. *Polymer Chemistry*, 6(7), 1066-1077.
- Zhu, L., Zhao, Y., & Zhang, P. (2016). Electrolyte-responsive polyethersulfone membranes with zwitterionic polyethersulfone-based copolymers as additive. *Journal of Membrane Science*, 510, 306-313.
- Zondervan, E., & Roffel, B. (2007). Evaluation of different cleaning agents used for cleaning ultrafiltration membranes fouled by surface water. *Journal of Membrane Science*, 304(1-2), 40-49.
- Zularisam, A., Ismail, A., & Salim, R. (2006). Behaviours of natural organic matter in membrane filtration for surface water treatment — a review. *Desalination*, 194(1-3), 211-231.

APPENDICES

APPENDIX A ADSORPTION TESTS

Prepared and measured solution concentrations are given for each test. Also, membrane areas, solution volumes which membranes were put into, concentrations of solutions measured after 1 day and estimated adsorbed amounts of solutes are given at the related tables below.

HA adsorption on PES Membrane

- Solution prepared : 0.5 g/L HA
- Concentration measured : 0.405 g/L HA

Table A.1 Adsorption of HA on PES membrane

Membrane Area (cm ²)	Solution Volume (ml)	Concentration after 1 day (g/L)	Adsorbed amount (mg)	Adsorbed amount (µg/cm ²)
22.5	13	0.355	0.65	29.0
27	15	0.361	0.67	24.7
9	12	0.378	0.32	35.9
9	12	0.391	0.17	18.5
19.5	12	0.362	0.51	26.1
19.5	12	0.361	0.53	27.1

Average = 26.9 ± 5.2

HA adsorption on PES/PVP blend Membrane

- Solution prepared : 0.5 g/L HA
- Concentration measured : 0.458 g/L HA

Table A.2 Adsorption of HA on PES/PVP blend membrane

Membrane Area (cm ²)	Solution Volume (ml)	Concentration after 1 day (g/L)	Adsorbed amount (mg)	Adsorbed amount (µg/cm ²)
30	18	0.456	0.03	1.0
28	15	0.448	0.14	4.9
20	15	0.449	0.13	6.5
20	15	0.449	0.12	6.1
20	15	0.458	0.00	-0.1
12	12	0.456	0.01	1.2

Average = 3.3 ± 2.6

BSA adsorption on PES Membrane

- Solution prepared : 0.5 g/L BSA
- Concentration measured : 0.480 g/L BSA

Table A.3 Adsorption of BSA on PES membrane

Membrane Area (cm ²)	Solution Volume (ml)	Concentration after 1 day (g/L)	Adsorbed amount (mg)	Adsorbed amount (µg/cm ²)
25	20	0.378	2.04	81.7
25	20	0.389	1.81	72.5
16	20	0.399	1.62	101.1
16	20	0.435	0.90	56.2
16	15	0.415	0.97	60.5

Average = 69.8 ± 17.9

BSA adsorption with presence of P(NIPAm) microgels on PES Membrane

- Solution prepared : 0.5 g/L BSA
- Concentration measured : 0.506 g/L BSA

Table A.4 Adsorption of BSA on PES membrane with presence of P(NIPAm) microgels in the solution

Membrane Area (cm ²)	Solution Volume (ml)	Concentration after 1 day (g/L)	Adsorbed amount (mg)	Adsorbed amount (μg/cm ²)
25	18	0.396	1.51	60.6
25	18	0.386	1.69	67.6
20	15	0.378	1.53	76.6
20	15	0.362	1.78	88.8
16	15	0.419	0.92	57.4
16	15	0.415	0.97	60.5

Average = 68.6 ± 11.0

BSA adsorption on P(NIPAm) microgels deposited PES Membrane

- Solution prepared : 0.5 g/L BSA
- Concentration measured : 0.489 g/L BSA

Table A.5 Adsorption of BSA on P(NIPAm) microgels deposited PES membrane

Membrane Area (cm ²)	Solution Volume (ml)	Concentration after 1 day (g/L)	Adsorbed amount (mg)	Adsorbed amount (µg/cm ²)
15.9	20	0.402	1.75	109.9
15.9	20	0.397	1.85	116.1
15.9	20	0.411	1.55	97.6

Average = 107.9 ± 7.7

BSA adsorption on PES/PVP blend Membrane

- Solution prepared : 0.5 g/L BSA
- Concentration measured : 0.496 g/L BSA

Table A.6 Adsorption of BSA on PES/PVP blend membrane

Membrane Area (cm ²)	Solution Volume (ml)	Concentration after 1 day (g/L)	Adsorbed amount (mg)	Adsorbed amount (μg/cm ²)
30	18	0.481	0.26	8.8
28	15	0.485	0.16	5.7
20	15	0.485	0.16	8.0
20	15	0.478	0.26	12.9
20	15	0.482	0.20	9.8
12	12	0.489	0.08	6.5

Average = 8.6 ± 2.3

P(NIPAm) adsorption on PES and PES/PVP blend membranes

- Solution prepared : 0.2 g/L P(NIPAm)
- Concentration measured : 0.224 g/L P(NIPAm)

Table A.7 Adsorption of P(NIPAm) microgels on PES membrane

Membrane Area (cm ²)	Solution Volume (ml)	Concentration after 1 day (g/L)	Adsorbed amount (mg)	Adsorbed amount (µg/cm ²)
28	15	0.214	0.15	5.4
28	15	0.197	0.41	14.7
20	15	0.182	0.63	31.4
16.5	12	0.249	-0.29	-17.6
18.24	15	0.209	0.23	12.9
28	15	0.214	0.15	5.4
Average =				9.4 ± 15.9

Table A.8 Adsorption of P(NIPAm) microgels on PES/PVP blend membrane

Membrane Area (cm ²)	Solution Volume (ml)	Concentration after 1 day (g/L)	Adsorbed amount (mg)	Adsorbed amount (µg/cm ²)
15	12	0.216	0.10	6.4
20	15	0.209	0.23	11.3
20	15	0.186	0.57	28.5
20	15	0.219	0.08	4.0
18	15	0.215	0.13	7.4
Average =				11.5 ± 8.8

APPENDIX B CALIBRATIONS

B.1 Bovine Serum Albumin (BSA) Calibration

Wavelength: 280 nm

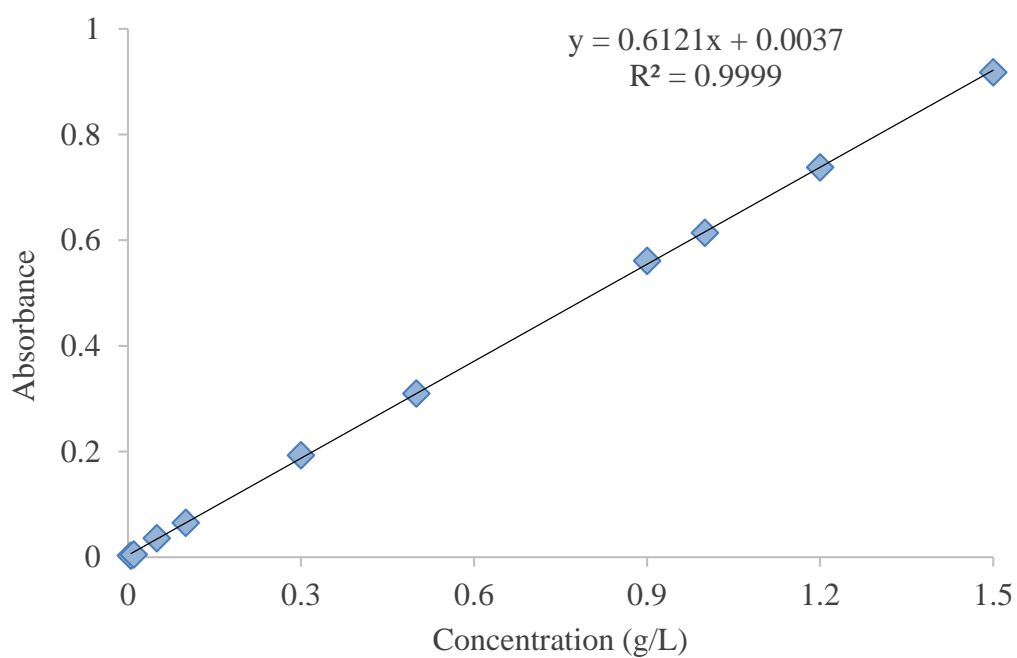


Figure B.1 BSA calibration in UV/Visible Spectroscopy at 280 nm

$$\text{Concentration (g/L)} = \frac{\text{Absorbance} - 0.0037}{0.6121}$$

B.2 Humic Acid Calibration

Wavelength: 254 nm

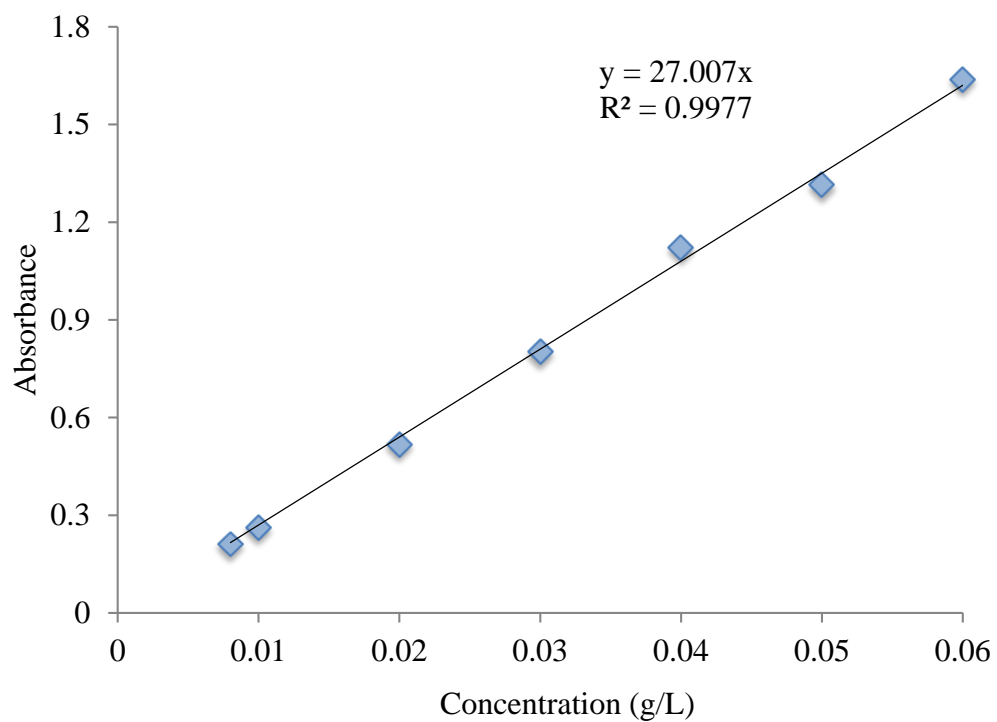


Figure B.2 Humic acid calibration in UV/Visible Spectroscopy at 254 nm

$$\text{Concentration (g/L)} = \frac{\text{Absorbance}}{27.007}$$

B.3 P(NIPAm) Microgels Calibration

Wavelength: 239 nm

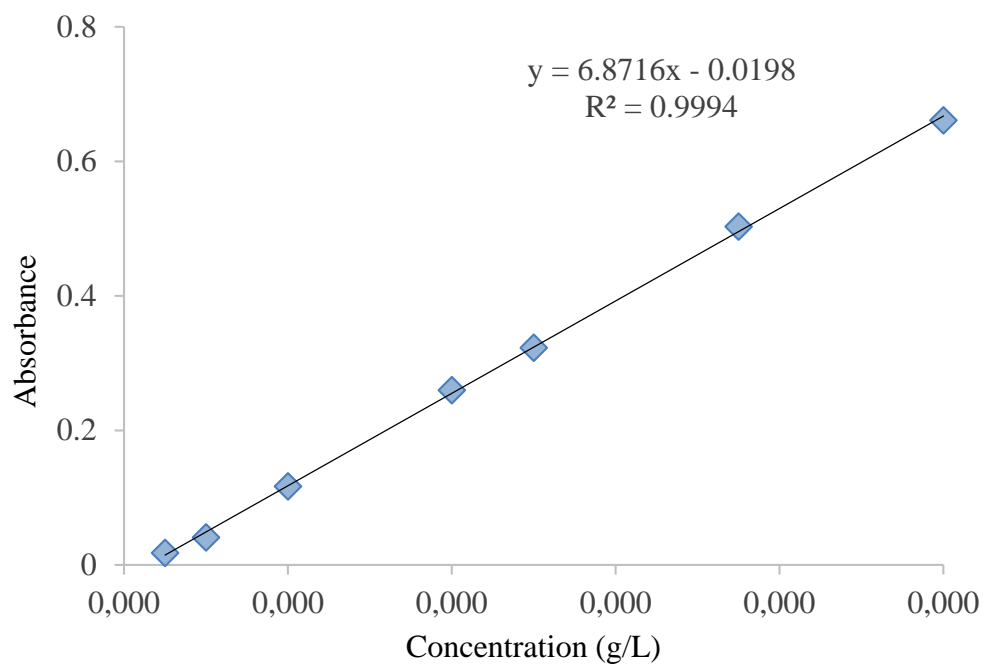


Figure B.3 P(NIPAm) microgels calibration in UV/Visible Spectroscopy at 239 nm

$$\text{Concentration (g/L)} = \frac{\text{Absorbance} + 0.0198}{6.8716}$$

APPENDIX C FILTRATION DATA

Abbreviations are given in nomenclature part but the related ones in table are represented again below to follow tables easily. In the tables, permeate volume was 10 ml from 40 ml feed and filtration pressure was 2 bar and no stirring was applied during filtrations. For yeast, different conditions are given at the table.

BSA	1 g/L Bovine serum albumin
C, SC	Cooling, slow cooling
CL	Cleaning condition
FP	Filtration permeance, L/hm ² bar
H, SH	Heating, slow heating
HA	1 g/L Humic acid + 2 mM CaCl ₂
PWP	Pure water permeance, L/hm ² bar
R _i	Resistance of I where i is used for membrane, fouling, irreversible fouling, m ⁻¹ x10 ¹²
RT	Cleaning at room temperature without stimuli
T	Temperature, C
TMP	Trans membrane pressure (during filtration)
Y	1 g/L Yeast
* and **	means after 1 st and extra cleaning, respectively
0.01 PN	0.01 g/L P(NIPAm) microgels
0.01 PNcS	0.01 g/L P(NIPAm-co-SBMA) microgels
0.1 PN	0.1 g/L P(NIPAm) microgels

Table C.1 Yeast filtrations by stirring feed solutions for 40 ml permeate volume at given pressures and temperatures using PES membrane

Filt #	Feed	Cl. Pr.	TMP	T (°C)				PWP	FP	PWP*
				PWP	FP	PWP*	CL			
1			4	20	20	20	50	216	40	111
2	Yeast	SH	2	20	20	20	50	57	15	40
3				23	23	23		72	15	34
4			4	20	20	20	50	193	4	17
5	Yeast 0.1 PN	SH	2	20	20	20	50	53	8	23
6				23	23	23		74	6	10
7			4	20	50	20	20	194	12	64
8	Yeast	SC	2	23	50	23	20	92	9	7
9				24	50	24		82	8	33
10			4	20	50	20	20	155	4	7
11	Yeast 0.1 PN	SC	2	23	50	23	20	42	5	6
12				24	50	24		95	5	10

Table C.1 (Continued)

Filt #	R_{mem}	R_{foul}	R*_{mem}	R_{irr}	R_{irr} / R_{foul}	FFR %	FR %	R_i%
1	1.7	7.3	3.2	1.6	21	19	51	100
2	6.3	17.6	8.9	2.7	15	26	70	100
3	5.4	19.9	11.5	6.1	31	21.2	46.8	100
4	1.9	87.6	21.1	19.2	22	2	9	100
5	6.8	44.7	38.0	15.6	29.2	8.8	23	100
6	5.2	60.8	38.4	33.2	55	8	14	100
7	1.8	51.9	5.6	3.7	7	3	33	100
8	4.2	67.4	54.9	50.7	75	6	8	100
9	4.8	78.9	12.1	7.3	9	6	40	100
10	2.3	158.8	51.1	48.8	31	1	5	100
11	9.1	118.8	67.4	58.3	49	7	13	100
12	4.1	129.6	40.1	35.9	28	3	10	100

Table C.2 BSA and HA filtrations using P(NIPAm) microgels with PES membrane

Filt #	Feed	Cl. Pr.	T (°C)				PWP	FP	PWP*
			PWP	FP	PWP*	CL			
13			20.5	35	20	20	28.8	4.5	5.0
14	BSA	C	20	35	19.5	20	67.6	5.5	9.8
15			18	35	19	20	53.5	5.6	10.5
16			21.5	35	22	20	26.1	5.0	7.6
17	BSA 0.1 PN	C	20.5	35	21.5	20	34.0	4.0	8.7
18			17.5	35	18	20	48.6	5.9	10.3
19	BSA	H	19	19	19	35	83.6	5.4	16.7
20	BSA 0.1 PN	H	19	19	19	35	86.3	3.5	13.4
21			19	19	19	35	82.4	3.6	18.3
22	HA	C	25	35	25	20	55.2	37.3	31.8
23			24	35	24	20	46.7	22.4	18.4
24	HA 0.1 PN	C	25	35	25	20	57.8	24.5	26.4

Table C.2 (Continued)

Filt #	R_{mem}	R_{foul}	R*_{mem}	R_{irr}	R_{irr} / R_{foul}	FFR %	FR %	R_i%
13	12.6	97.2	72.2	59.6	61	11.5	17.4	99.2
14	5.3	84.6	36.1	30.8	36	5.9	14.7	99.5
15	6.4	81.9	33.3	26.9	33	7.2	19.1	99.4
16	14.2	83.8	49.5	35.0	42	14.5	28.7	100
17	10.7	112.9	42.6	32.0	28	8.6	25.0	99.7
18	6.9	76.8	33.1	26.2	34	8.3	20.9	99.3
19	4.2	60.5	20.9	16.8	28	6.5	20.0	99.0
20	4.0	95.8	26.1	22.0	23	4.1	15.5	99.6
21	4.2	92.8	19.1	14.9	16	4.4	22.1	99.5
22	7.3	6.0	12.6	5.4	90	54.9	57.6	74
23	8.4	13.7	21.4	13.0	95	38.1	39.3	72
24	6.9	13.2	15.2	8.3	63	34.5	45.7	77

Table C.3 HA filtrations using P(NIPAm) microgels with PES/PVP blend membrane

Filt #	Feed	Cl. Pr.	T (°C)				PWP	FP	PWP* PWP**
			PWP	FP	PWP* PWP**	CL			
25	BSA	RT	25	25	26	25	3.0	2.3	3.1
26	HA	RT	26	26	26	26	7.0	5.5	5.8
27	HA 0.1 PN	H	27	27	27	38	2.0	1.7	1.6
28			26	26	26	38	3.2	2.3	2.2
					26				2.2
29	HA	H	28	28	29	38	4.2	3.1	3.4
					29				3.5
30			23.5	23.5	23.5	38	3.0	2.1	2.5
					23.5				2.7
31			26	26	26	38	2.5	1.9	1.8
					26				2.2
32	HA 0.01 PN	H	27.5	27	27	38	2.7	2.0	2.1
					27				2.4
33			23.5	23.5	23.5	38	2.7	2.2	1.7
					23.5				2.2
35			20	20	20	38	3.5	2.4	2.5
					20				2.7
36	HA 0.1 PN	H	19	19	19	38	2.3	1.8	1.9
					19				2.0

Table C.3 (Continued)

Filt #	R_{mem}	R_{foul}	$\frac{R_{mem}^*}{R_{mem}^{**}}$	$\frac{R_{irr} - 1}{R_{irr} - ex}$	R_{irr} / R_{foul}	FFR %	FR % FR%-ex	$R_i\%$
25	134	43	132	-1	76	76	101	99.5
26	58	16	71	12	77	78	83	82
27	211	30	267	56	186	87	79	85
28	130	49	191	60	123	73	68	84
			189	59	121		69	
29	103	34	129	26	76	75	81	83
			124	21	62		85	
30	131	57	156	24	43	70	84	84
			144	12	23		91	
31	162	57	227	64	112	74	72	84
			189	27	47		86	
32	155	52	197	42	81	74	78	89
			175	20	40		84	
33	141	38	222	81	212	79	63	87
			175	33	87		81	
35	102	49	141	39	79	67	72	89
			134	32	65		76	
36	155	39	184	30	75	80	84	88
			174	19	48		89	

Table C.4 Series filtrations of HA using P(NIPAm-co-SBMA) microgels with PES/PVP blend membrane

Filt #	Feed	Cl. Pr.	T (°C)				PWP	FP	PWP* PWP**
			PWP	FP	PWP* PWP**	CL			
37 -1	HA	H	21.5	23.1	23.5	38	6.0	5.3	5.5
					22.5				
37 -2			22.5	22.9	22.7	38	5.8	5.1	5.3
					24				
37 -3			24	23.4	24	38	5.8	5.0	5.2
					23.5				
37 -4			23.5	23.4	24	38	5.7	4.9	5.2
					23.8				
38 -1	0.01 PNcS	H	19.2	19.2	19.7	38	3.9	3.4	3.7
					20.2				
38 -2			15.8	16.2	16.2	38	3.3	3.0	3.1
					17.8				
38 -3			14.2	15.8	17.3	38	3.0	2.9	3.1
					19				
38 -4			18	16	17		3.4	2.9	3.2
					17.8				
39 -1	HA 0.01 PNcS	RT	16.3	16.8	17.2	20	4.4	4.0	3.9
					17.2				
39 -2			14.2	15.3	16.3	20	4.0	3.7	3.9
					16.8				
39 -3			16.8	16.8	17.8	20	4.3	4.1	4.0
					17.8				

Table C.4 (Continued)

Filt #	R_{mem}	R_{foul}	R_{mem}[*] R_{mem}^{**}	R_{irr} -1 R_{irr} -ex	R_{irr} / R_{foul}	FFR %	FR % FR%-ex	IR_i %
37 -1	62.2	10.8	70.1	7.9	74	85	89	84
			66.5	4.4	40		93	
37 -2	66.5	12.2	71.5	9.4	76	84	87	83
			67.5	5.4	44		92	
37 -3	67.5	15.3	75.5	13.3	87	80	82	83
			68.0	5.9	38		91	
37 -4	68.0	16.5	75.6	13.4	81	79	82	82
			68.4	6.2	38		91	
38 -1	91	13.9	96	5.7	41	87	94	88
			91	0.1	0		100	
38 -2	99	8.2	105	5.6	68	92	95	86
			99	-0.2	-3		100	
38 -3	102	10.0	107	5.2	51	91	95	85
			102	0	0		100	
38 -4	99	14.2	105	5.7	40	87	95	85
			100	0.5	3		100	
39 -1	75	7.5	86	11.6	155	91	87	87
			79	3.8	51		95	
39 -2	76	9.2	84	7.4	80	89	91	87
			78	1.3	14		98	
39 -3	78	4.3	84	7.6	175	96	92	85
			81	4.2	97		96	

Table C.5 Series filtrations of HA using P(NIPAm-co-SBMA) microgels with PES membrane

Filt #	Feed	Cl. Pr.	T (°C)				PWP	FP	PWP* PWP**
			PWP	FP	PWP* PWP**	CL			
40 -1			19	19.2	20.1 -	38	39.0	23.1	33.7 -
40 -2	HA	H	20.1	20.2	21.5 21.5	38	33.7	20.0	28.1 28.6
40 -3			21.5	20.2	21.5 21.6	38	28.5	19.7	24.8 27.6
40 -4			21.5	20.5	21.8 21.7	38	27.6	18.8	23.7 26.4
41 -1			17.5	17.8	18.5 -	38	32.7	14.7	31.2 -
41 -2	HA	H	18.5	18.8	19.8 20.5	38	31.2	15.8	30.5 33.8
41 -3	0.01 PNcS		20.5	20.2	22 22	38	33.8	16.3	30.3 34.9
41 -4			22	20.2	22.8 22.8	38	34.9	15.2	29.6 36.3

Table C.5 (Continued)

Filt #	R_{mem}	R_{foul}	R_{mem}[*] R_{mem}^{**}	R_{irr -1} R_{irr -ex}	R_{irr} / R_{foul}	FFR %	FR % FR%-ex	R_i%
40 -1	9.0	6.2	10.6	1.7	27	59	84	78
			-	-	-		-	
40 -2	10.6	9.0	13.2	4.2	47	50	68	78
			13.0	4.0	45		69	
40 -3	13.0	9.3	14.9	6.0	64	49	60	77
			13.4	4.5	48		67	
40 -4	13.4	10.3	15.8	6.8	66	46	57	77
			14.1	5.2	50		63	
41 -1	10.3	12.9	11.1	0.8	6	44	93	82
			-	-	-		-	
41 -2	11.1	11.7	11.7	1.4	6	47	88	80
			10.7	0.4	-3		96	
41 -3	10.7	11.8	12.4	2.1	15	47	83	79
			10.8	0.5	0		96	
41 -4	10.8	13.4	12.9	2.6	17	44	80	80
			10.5	0.2	-2		98	

Table C.6 Series filtrations of HA using P(NIPAm-co-SBMA) microgels with PES/PVP blend membrane in 0.5 M NaCl

Filt #	Feed	Cl. Pr.	T (°C)				PWP	FP	PWP*
			PWP	FP	PWP*	CL			
42 -1			20	19	18.5	38	1.6	1.1	1.3
42 -2	HA	H	20	19	19	38	1.3	1.1	1.2
42 -3			19	19	19	38	1.4	1.1	1.3
43 -1	HA		20	19	19	38	2.4	1.7	2.1
43 -2	0.01 PNCs	H	20	19	18.5	38	2.4	1.8	2.1
43 -3			19	19	19	38	2.4	1.9	2.1

Table C.6 (Continued)

Filt #	R _{mem}	R _{foul}	R* _{mem}	R _{irr}	R _{irr} / R _{foul}	FFR %	FR %	R _i %
42 -1	218.4	108.4	264.0	45.6	42	65	83	75
42 -2	277.4	111.1	289.0	70.6	64	82	96	71
42 -3	246.6	88.0	269.7	51.3	58	80	91	70
43 -1	149.3	58.7	166.2	16.9	29	70	90	80
43 -2	152.6	47.0	167.1	14.5	31	75	91	78
43 -3	143.5	45.3	163.7	20.2	45	76	88	75

Table C.7 HA filtrations for *low resistance* and *high resistance* analysis using P(NIPAm-co-SBMA) microgels with PES/PVP blend membrane

Filt #	Feed	Cl. Pr.	T (°C)				PWP	FP	PWP*
			PWP	FP	PWP*	CL			
44	HA (<i>low R</i>)	H	16.5	17.5	18 19.1	38	3.0	2.7	2.9 3.0
45	HA 0.01 PNcS (<i>high R</i>)	H	18	17.5	16.5 17.8	38	3.2	2.3	2.2 2.8

Table C.7 (Continued)

Filt #	R_{mem}	R_{foul}	$\frac{R_{mem}^*}{R_{mem}^{**}}$	$\frac{R_{irr} - 1}{R_{irr} - ex}$	R_{irr} / R_{foul}	FFR %	FR %	R_i %
44	108.7	16.4	118.4 116.6	9.6 7.9	59 48	87	92 93	80
45	105.4	38.5	146.9 119.7	41.6 14.3	108 37	73.2	72 88	81

APPENDIX D ADDITIONAL FILTRATION

PES membranes were highly fouled by BSA and a rapid flux decline at the beginning of the filtration showed that adsorption was an important part of fouling in these conditions. However, the main target among fouling types was cake or gel layer on the membrane surface for the proof of the claim. In order to decrease adsorptive fouling and work with irreversible cake layer, with the addition of PVP, more hydrophilic PES/PVP blend membranes were prepared compared to PES membranes. BSA filtration were also performed with PES/PVP blend membrane. It was done at room temperature and also tried to clean at room temperature to see how it fouled and how it could be removed from that membrane without temperature dependence. As a result, it was observed that it slightly fouled PES/PVP membrane and it could be removed totally at the end (Figure D.1). Then, PES/PVP membrane was not used in BSA filtrations.

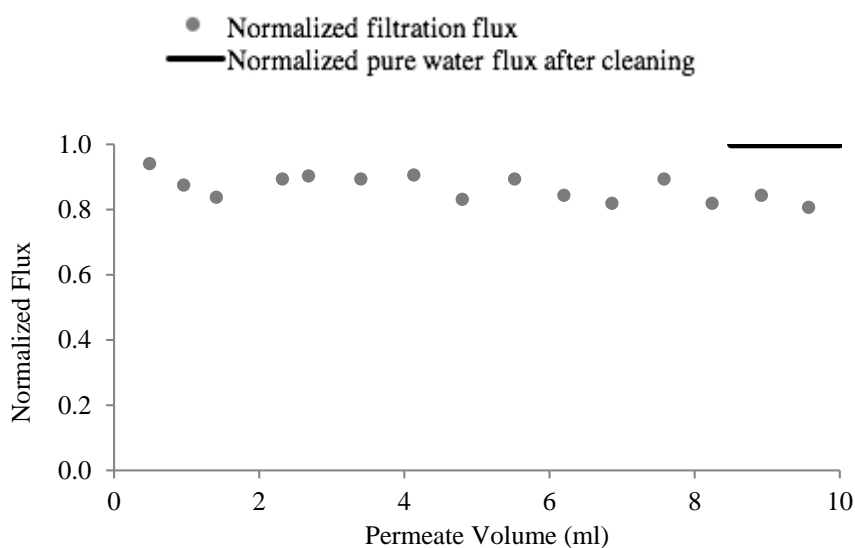


Figure D.1 Normalized flux graph of BSA filtrations at room temperature with PES/PVP membranes and cleaning at room temperature

APPENDIX E MICROGEL RECOVERY

After efficient cleaning of membrane is achieved with responsive microgels, a question immediately comes to mind: how will these microgels be recovered from retentate stream in order to avoid continuous input of material to the process? This is the following part of the study. It is planned to make responsive particles magnetic with iron oxide incorporated in order to recover them from retentate using a magnetic field and reuse them in next filtrations more and more times. Schematic view of the complete process is represented in Figure E.1.

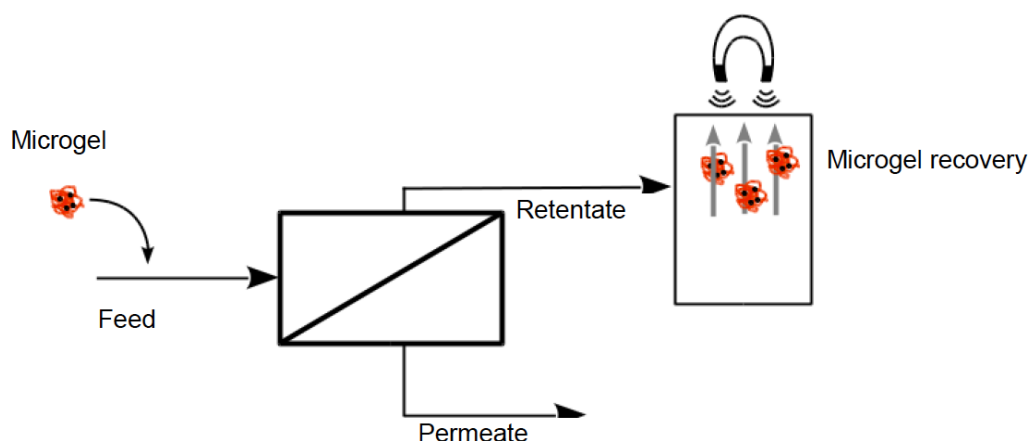


Figure E.1 Schematic representation of microgel recovery

Preliminary work was done with P(SBMA) to obtain magnetic particles. In iron decoration, big particles that could be seen with naked eye were formed during preparation. After filtration of those particles with 1 micron syringe filter, all particles with orange color were rejected by it at 60 °C where they were collapsed. Then, it was thought that experience that iron oxide might be formed as big iron particles somewhere else from the nanogels or around nanogels. Then, different procedures were noted in order to try later in the study. Synthesized particles

can be seen in Figure E.2 where particles were attracted by a magnet. Procedure that was followed is given below:

1. Dissolve 1 g NaOH in 250 ml water to prepare aqueous solution in 0.1 M concentration.
2. Disperse 0.1 g of p(SBMA) microparticles in 50 ml of 0.1 M NaOH aqueous solution.
3. Dissolve 0.865 g HCl in 250 ml water to prepare aqueous solution in 0.1 M concentration.
4. Dissolve 0.036 g (0.27 mmol) of $\text{FeCl}_2 \cdot 4\text{H}_2\text{O}$ and 0.0975 g (0.54 mmol) of $\text{FeCl}_3 \cdot 6\text{H}_2\text{O}$ in 50 ml of 0.1 M aqueous HCl solution
5. Add the solution in Step 4 drop wise to the microparticle dispersion prepared in Step 2 under continuous stirring. The milky microparticle dispersion should turn to red-orange, indicating iron oxide formation.

Here it is important to add the solution in Step 4 very slowly into the solution in Step 2 by stirring it very fast.

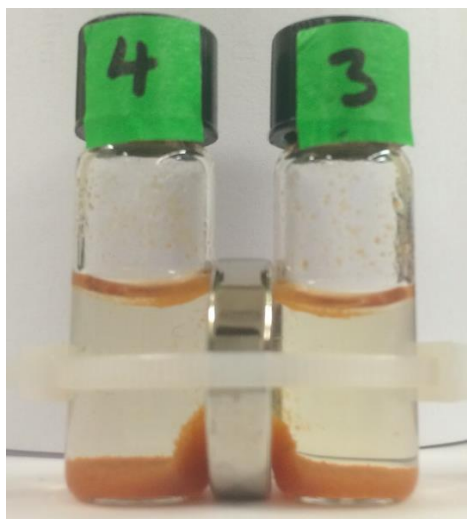


Figure E.2 Iron decorated P(SBMA) microgels

6. Leave solution to settle for an hour then pour away the supernatant solution and wash the iron-microparticles with DI water.
7. leave it overnight for drying.